SYNTHESIS OF NEW GOLD (III) COMPLEXES WITH ALKYLDIAMINE AND CYANIDE LIGANDS AND THEIR INTERACTION WITH SOME BIOLOGICALLY IMPORTANT LIGANDS

BY

BASSEM ABDULLATIF AL MAYTHALONY

A Dissertation Presented to the

DEANSHIP OF GRADUATE STUDIES

KING FAHD UNIVERSITY OF PETROLEUM & MINERALS

DHAHRAN, SAUDI ARABIA

In Partial Fulfillment of the
Requirements for the Degree of

DOCTOR OF PHILOSOPHY

In

CHEMISTRY

MAY 2010

KING FAHD UNIVERSITY OF PETROLEUM & MINERALS

DHAHRAN 3126, SAUDI ARABIA

DEANSHIP OF GRADUATE STUDIES

This dissertation, written by BASSEM ABDULLATIF AL MAYTHALONY under the direction of his advisor and approved by his thesis committee, has been presented to and accepted by the Dean of Graduate Studies, in partial fulfillment of the requirements for the degree of DOCTOR OF PHILOSOPHY in CHEMISTRY.

Dissertation Committee

Professor Anvarhusein A. Isab

(Dissertation advisor)

Professor Mohammed Wazeer

(Co-advisor)

Dr. Mohammad Fettouhi

(Member)

Dr. Mazen Khaled

(Member)

Professor Akhtar A. Naqvi

(Member)

Dr. A. J. Hamdan

(Department Chairman)

Dr. Salam A. Zummo (Dean of Graduate Studies)

Date 11/6/10

بسم الله الرحمن الرحيم

THIS WORK DEDICATED TO

ALLAH

TO HIS PROPHET MOHAMMAD SALLA ALLAH ALIHE W SALLAM.

TO MY FATHER ABDULLATIF MAHMOUD AL MAYTHALONY, MY MOTHER NADA AHMAD GHANAM.

TO MY BROTHERS MUNEER, NIDAL, MOHAMMAD, AHMAD, AND SISTERS RANA AND ARWA.

TO MY WIFE DIANA HASSAN MOHAMMAD AND MY KIDS OMAR, NOOR AND MOHAMMAD.

TO EVERY PALESTINIAN AND TO GHAZA PEOPLE.

ACKNOWLEDGEMENT

Acknowledgment is due to the King Fahd University of Petroleum & Minerals for supporting this research.

I wish to express my appreciation to my advisor Dr. Anvarhusein A. Isab and for co-advisor Dr. Mohammad I. M. Wazeer for their cooperation and continuous guidance throughout this work I also wish to thank the other members of my dissertation committee Dr. M.Fettouhi, Mohammed, Dr. Mazen M. Khaled and Dr. Akhtar A. Naqvi, for their appreciated cooperation, help and support, for chairman Dr Abdullah Hamdan, for other faculty members Prof. Abdullah Abu Alkebash, Prof. Bassam Al Ali (Academic advisor), Dr. Musa Musa, Dr Ibdah, Dr. Osama Bjeremi Dr. Amer Albata.

My appreciation is also due to all my colleagues Dr. Basem Moosa, Dr. Rami Samara, Dr. Abdulazeez Amro, Dr. Atif Fazel. Dr. Khaizar Hayat, Dr. Nidal Abu Thabit, Dr. Ahsan Shamsi, Dr. Abdullah Manda'a, Dr. Tawfeeq Saleh, Dr. Mahboub and future Dr. Mohie Eldeen Haffar, Dr. Khalid Arafeh, Dr. Hatem Dfa'a Allah, Dr. Abdulnaser Alshara, and form other departments to Dr. Esam Amro, Dr. Ahmad Dweik, Dr. Mohammad Ali Hassan Dr. Bassel Al Saeed, Dr. Mohammad Jarrar, Dr. Mohammad Dergham and all friends from Al-Khaleel others who I didn't mention. My thanks also to chemistry staff, particularly, Mr. Arab, Mr. Haydar, Mr. Mazhar, Mr. Ayman, Mr. Shahed, Mr. Saleem, Mr. Inayat, Mr. Nooh, Mr Hussain, Mr. Arif Baba Mr. Mohammad Elseba'a and others in chemistry department who I didn't mentioned.

Finally, I would like to express my special thanks to my father Abdullatif Al Maythalony and my mother Nada Ahmad Ghanam, my brothers Muneer, Nidal, Mohammad, Ahmad, Rana and Arwa, my wife Diana and sons, Omar, Noor and Mohammad.

TABLE OF CONTENTS

LIST OF SCHEMES

LIST OF FIGURES

LIST OF TABLES

ABSTRACT

NAME: BASSEM ABDULLATIF AL-MAYTHALONY

TITLE OF STUDY: SYNTHESIS OF NEW GOLD(III) COMPLEXES WITH ALKYLDIAMINE AND CYANIDE LIGANDS AND THEIR INTERACTION WITH SOME BIOLOGICALLY IMPORTANT LIGANDS**.**

MAJOR FIELD: CHEMISTRY

DATE OF DEGREE: May, 2010

A series of gold(III) metalacycle of five, six and seven membered ring was prepared by reacting Auric acid ($HAuCl_4 \bullet 3H_2O$) with one equivalent alkyldiamine, such as; *en*, *pn* and *bn* ligands and with some N-*en* as well as N,N'-*en* ligands. The general formula of these complexes is $[Au(alkyldiamine)Cl_2]Cl$, in addition to $[Au(CN)_4]^-$ complex. Synthesized complexes were characterized by melting point and EA. Structural analysis were done by UV-Vis, Far-IR, IR spectroscopy, ^1H and ^{13}C solution as well as ^{13}C and ^{15}N solid-state NMR.

Interaction of representative $[Au(\textit{alkyldiamine})Cl_2]Cl$ complexes were carried out and studied with several biologically important thiols e.g. L-cysteine, DL-pencillamine, thiomalic acid and glutathione, thiones e.g. ergothioneine, imidazolidien-2-thiones and its derivatives i.e. diazinane-2-thione and diazipan-2-thione, thioether and selenoether e. g. methionine and seleno-methionine in addition to imidazole and histidine ligands.

A series of aurocyanide and auricyanide complexes of phosphines, phosphine sulphides and phosphine selenides ligands were synthesized.

These reactions were monitored using UV-Vis, Far and med-IR, ^1H and ^{13}C NMR as well as solid state ^{13}C and ^{15}N NMR spectroscopy.

The results obtained from this work will provide better understanding of the gold(III) chemistry, which will help to design better medicinally important complex.

DOCTOR OF PHOLOSOPHY DEGREE

KING FAHD UNIVERSITY OF PETROLEUM & MINERALS

DHAHRAN, SAUDI ARABIA

الخلاصة

الأسم: باسم عبداللطيف الميثلوني

عنوان الدراسة: تحضير معقدات جديدة من الذهب(+ 3) مع مرتبطات الأكيل-ثنائي –الأمين و السيانيد و تفاعلاتها مع مرتبطات ذات أهمية بيولوجية.

المجال: الكيمياء

تاريخ الدرجة: مايو 2010 م

سلسلة من المركبات الحلقية الخماسية و السداسية و السباعية الغير المتجانسة للذهب (3+) تم تحضيرها عن طريق مفاعلة Auric acid ($HAuCl_4 \bullet 3H_2O$) مع مكافئها من المرتبطات ethylenediamine (*en*) و propylenediamine (*pn*) و butylenediamine (*bn*) بالاضافة لعدد من مركبات *en* و مشتقاتها أحادية و ثنائية الاستبدال على النيتروجين , اضافة الى مركب $[Au(CN)_4]^-$. لقد تم تشخيص المركبات المحضرة بإستخدام فحص درجة الانصهار وتحليل العناصر و لقد تم دراسة بنية المركبات المحضرة باستخدام التحليل الطيفي UV-Vis و Far-IR و IR و تحليل NMR لذرات ^1H و ^{13}C في الحالة السائلة بالاضافة الى ذرات ^{13}C و ^{15}N بالحالة الصلبة. صيغة مركبات.

لقد تم دراسة تفاعلاتها مع مركبات ثيول ذات أهمية بيولوجية مثل السيستين, البنسلمين, حمض الثيومماليك والجلوتاثيون ومركبات الثيو ن الارجوثيونين, 2,4-ثنائي الثيويوراسيل, ايميدازولدين- 2-ثيون و مشتقاتها, الديازينان- 2-ثيون مر كبات الثيوئ يثر و السيلينو يثر مثل الميثيونين و السيلينو ميثايونين و بالاضافة الى الايميدازول و الهستدين.

لقد تحضير سلسلة من معقدات الفوسفين و الفوسفين سلفايد و الفوسفين سيليند الأوروسيانيد والأوريسيانيد.

لقد تم متابعة التفاعلات باستخدام التحليل الطيفي مثل UV-Vis و Far-IR و IR و تحليل NMR لذرات ^1H و ^{13}C في السائلة بالاضافة الى ذرات ^{13}C و ^{15}N بالحالة الصلبة.

نتائج هذه الدراسة سوف تقدم فهم أفضل لكيمياء الذهب (+3) مما سيساعد في تصميم معقدات أفضل ذات أهمية طبيه.

درجة الدكتوراه في الفلسفة

جامعة الملك فهد للبترول و المعادن

الظهران-المملكة العربية السعودية

CHAPTER ONE

INTRODUCTION

Cis-platin was one of the first metal complexes used for cancer treatment with its anti-cancer activity discovered in the 1960s [1-3]. It is responsible for the cure of more than 90 % of testicular cancer cases and plays a vital role in the treatment of cancers such as ovarian, head & neck cancer, bladder cancer, cervical cancer, melanoma, and lymphomas [4].

Because platinum(II) complexes have exhibited such promising results against selected types of cancers, several families of non-platinum metal complexes have been studied intensely as potential cytotoxic and antitumor agents. Gold(III) is isoelectronic with platinum(II) and tetracoordinate gold(III) complexes have the same square-planar geometries as *cis*-platin [5]. They are known to have antimicrobial activity [6,7], therapeutic effect [8] and they are used in metal-based drugs [9,10]. Recently, gold(III) complexes of N-donor ligands showed anti-tumor effect at the preclinical results [11]. However, compared to the corresponding platinum(II) complexes, gold(III) complexes have not been well explored chemically possibly because few gold(III) complexes have been shown to be sufficiently stable in aqueous solution [12].

Gold complexes exist predominantly as gold(I) in-vivo [13-15]. Thioethers, peptide and L-methionine residues as well as disulfide bonds are able to reduce gold(III) to gold(I). Aurosomes (i.e., lysosomes of phagocytic, liver, and kidney cells with large accumulations of gold), isolated from gold(III)-treated rats as well as those treated with gold(I), contain predominantly gold(I). The bulk of gold *in-*

vivo is therefore likely to be gold(I). So gold(I) chemistry attracts most of the attention until recent decade because of its stability. Nonetheless, under biomimetic conditions, gold(I) can be oxidized to gold(III) in-vivo [16]. Recently, extensive work was published involving gold(III) chemistry which found application in anticancer drugs [16].

Ethylenediamine (en) ligand is a common chelating ligand, for which the chemistry and reactivity with gold metal have been studied since 1931 by Gibson *et al* [17], in addition to gold(III)-ethylenediamine complex, other gold(III) complexes with similar chelating ligands such as propylenediamine (pn) and butylenediamine (bn) ligands were prepared. The exchange and substitution reactions of these complexes with some bioligands were investigated, because of their similarities to *cis*-platin. These alkyldiamines are expected to cause blocking of the two *cis* positions of the square planar structure and make the other two positions available for coordination and bonding to bioligands, as for *cis*-platin. In addition, stabilization of gold(III) oxidation state and square planar structure is achieved using such chelating ligands. Synthesis and characterization of a range of Au(III) complexes and derivatives with various unsubstituted and N,N'-disubstituted alkyldiamine ligands (Schemes 1.1-3) are presented.

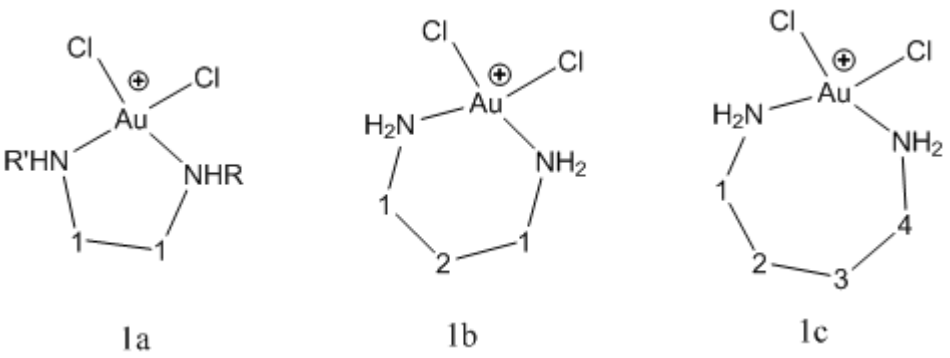

Scheme 1.1: [Au(alkyldiamine)Cl_2]$^+$ complexes, where R, R' could be H or alkyl groups such as Me, Et, 2-hydroxy-Et, Pr and *i*Pr.

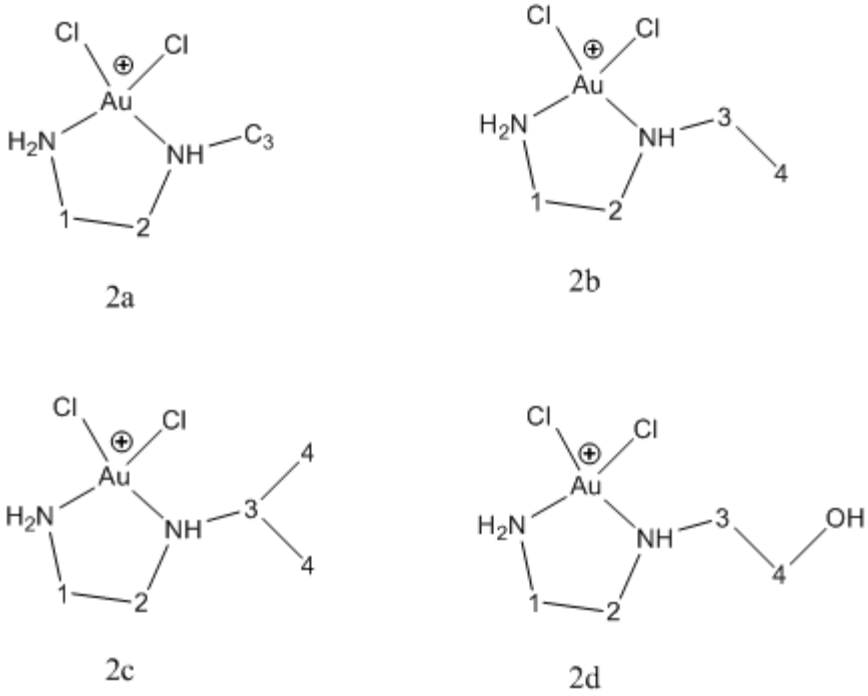

Scheme 1.2: [Au(N-substituted-*en*)Cl_2]$^+$ complexes.

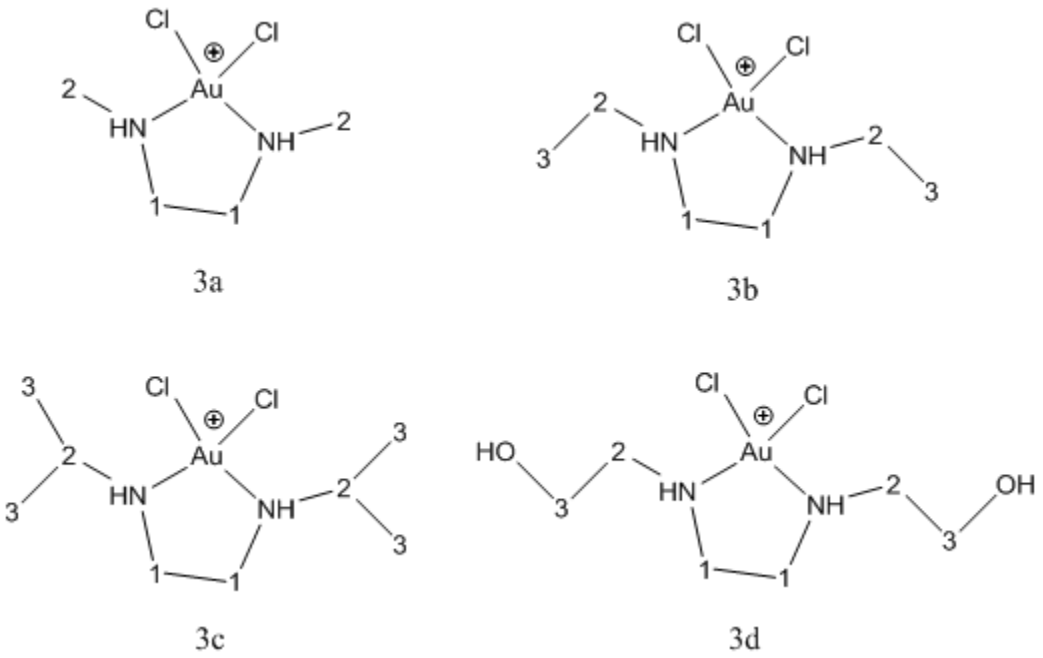

Scheme 1.3: [Au(N,N'-di-substituted-*en*)Cl_2]$^+$ complexes.

Gold applications in medicinal chemistry were found mainly for Au(I). Recently Au(II) was suggested to be stable while binding to hematoporphyrin [18], while Au(III) found very important applications in medicinal chemistry in spite of finding hindrance of improvement by the low stability in side tissues as reported by Ott [11].

Ethylenediamine-gold(III) complex [Au(en)Cl_2]Cl was prepared and characterized by Zhu and co-workers. Single crystal X-Ray structure was reported [5], which was found to have square-planar geometry around Au(III) metal center. Chloride atoms were shown to be located at two *cis* corners of the square planer base.

Tiekink [19] reported a full range of gold compounds currently being investigated for their potential anti-tumor activity. Gold(I) compounds related to the

anti-arthritic drug Auranofin continue to attract attention, especially those carrying biologically active molecules with anti-tumor activity.

Tetrahedrally coordinated gold(I) compounds, that possibly target mitochondria, are under development with a particular focus upon moderating their hydrophilicity. The interest in square-planar gold(III) compounds has increased in the last decade. A wide variety of species: mono- and di-nuclear, neutral and charged, coordination and organometallic, etc. are being developed. Many investigations and studies of mechanistic aspects of gold compounds where conducted but a clear understanding of the mechanism of action of these compounds has yet to be determined.

Gabbiani, *et al* [20] have recently reported the synthesis as well as cytotoxic studies of some ethylenediammine gold(III) complexes. They found that the mechanisms of action of cytotoxic gold(III) complexes seem to be innovative and substantially different from that of *cis*-platin. This as well as related other recent studies [21] lead us to synthesize series of unsubstituted ethylenediammine along with another group of N-mono-substituted as well as N,N'-disubstituted ethylenediamine ligands with $AuCl_4^-$. The ligands used here are ethylenediamine (en), propylene diamine (pn) and butylenediamine (bn) ligands, N-Me-en, N-Et-en, N-*i*Pr-en, N-hydroxy-Et-en and N,N'-di-substituted ethylenediamine ligands, such as N,N'-Me_2-en, N,N'-Et_2-en, N,N'-(iPr)$_2$-en and N,N'-(2-hydroxy-Et)$_2$-en. The general formula of these complexes is [Au(alkanediamine)Cl_2]Cl.

In [Au(*en*)Cl_2]Cl complex, gold(III) is blocked by *en* ligand from two coordination sites and only two Cl^- ligands are available for reaction. Therefore, it

will be of interest to see the difference in reactivity between two types of gold(III) complexes, with and without the *en* ligand.

Notable results for the appearance of new potential anti-tumor application of these gold(III) complexes reported in literature. They showed promising cytotoxic properties toward cancer cells, both *in-vitro* and *in-vivo* studies [22]. Several derivatives of multi-dentate ligands were used to build square planar gold(III) complexes [23,24].

Anticancer activities of any antitumor complex depend on its interaction with DNA [25], so its reaction with other molecules in biological fluid will prevent these compounds from reaching the targeted organs [26]. Several complexes with chelating ligands such as pyrazolyl on palladium(II), platinum(II) and gold(III) metal were prepared by Keter *et al* and found to be exchanged by cysteine [25], they also reported that gold(III) complexes targeted molecules other than DNA as also reported by Marcon *et al* [27], so these side interactions will decrease its activity as well as its efficiency.

Gold complexes were used as anti-arthritic drug such as auranofin and myocrisin [28-31]. Anti-rheumatic gold complexes are activated by their conversion into aurocyanide $[Au(CN)_2]^-$ [32], this stimulates investigation of aurocyanide complexes interaction with various bioligands, especially that contain sulfur because of the known gold-sulfur affinity [33,34]. While auricyanide $[Au(CN)_4]^-$ was considered previously as metabolic product of anti-arthritic gold(I) *in-vivo* [16], however, low stability of gold(III) complexes limited their medical

importance. Heavier chalcogens-gold chemistry is still an unexplored field of modern inorganic chemistry [35]; this could be attributed to their lower stability.

Inhalation of HCN from tobacco smoke raises $[Au(CN)_2]^-$ concentration in smokers blood who takes gold(I) anti-arthritic drug [36]. Large formation constant is believed to be responsible for generating $[Au(CN)_2]^-$, (log β = 36.6-39) [37-39]. Graham *et al* have reported aurothiomalate (Autm) activation through its interaction with cyanide ion [40], this interaction was found to increase red blood cells uptake of gold from gold(I)-thiomalate by 21.1% after incubation for 24 hours [39,40].

In a study of $[Au(CN)_4]^-$ reaction with GSH three potential mechanisms were suggested for auricyanide reduction into aurocyanide [16,41];(i) Reductive elimination of cyanogen, followed by nucleophilic attack of GSH on cyanogen leading to its reduction to cyanide [42]; (ii) Formation of hexacyanodiaurate(II), $[(NC)_3Au–Au(CN)_3]^{2-}$, probably by 2 one-electron transfers, followed by redox disproportionation [43,44] and (iii) cyanide ligand exchange by GSH followed by reductive elimination of GSSG.

The first generation injectable drugs solganal (gold thioglucose, AuSTg) and myochrysine (gold sodium thiomalate, AuSTm) followed by the second generation orally administered auranofin (2,3,4,6-tetra-O-acetyl-β-1-D-Thioglucopyranosato-S-(triethylphosphine))gold(I), ($Et_3PAuSATg$) [16] have been developed. Both Solganal and auranofin bind to albumin by exchange of its tetraactyl thioglucose ligand by L-cysteine [45]. Despite being used for over 70

years for rheumatoid arthritis treatment, gold complexes anti-cancer potential has been recently suggested [46].

Bio-ligands containing sulfur such cysteine, pencillamine, glutathione, methionine, thiones etc. have a strong gold(III) affinity so it is of great important to evaluate the proposed antitumor complexes according to their interaction with sulfur containing bioligands [47].

Gold-sulfur complexes are very important building blocks that are used in many important applications in medicine as in anti-arthritic drugs, such as auranofin. Thione ligands are simple sulfur containing ligands, their heterocyclic rings with various metal ions have received much attention [48,49]. A variety of gold-sulfur complexes has been prepared and utilized for many applications e.g. pharmacological, thin film, glass, and ceramic applications [50-52].

Thiols are known to be very reactive with gold complexes [53,54] e.g. AuS_2 coordination environment was reported to be formed by bridging thiolate (RS^-) ligands between two gold(I) ions forming oligomer [55], more thiol ligand added found to cause formation of simpler complexes as $[Au(SR)_2]^-$ [55].

It was reported by Shmidbaur that gold(III) reacts with glutathione in two steps. Gold(III) is first reduced to gold(I) then glutathione acts as a bridge between two gold(I) units through sulfur forming macro-clusters (Scheme 1.4). This structure is promoted by aurophilicity [56].

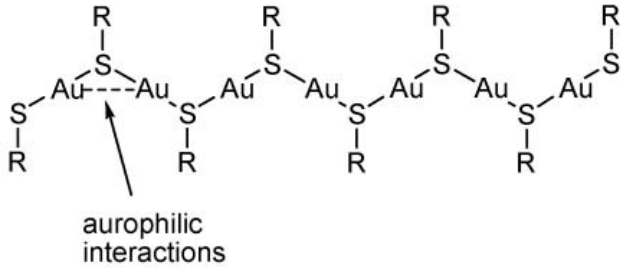

Scheme 1.4: Gold(I)–GS cluster.

Thiols were reported to be oxidized into the disulfides [57], while gold complexes were found to cause oxidative cleavage of proteins and peptides disulfide into sulphoinic acid; this reaction is reported to be responsible for gold toxicity [58-61].

Thiones like imidazolidine-2-thione (Imt), diazinane-2-thione (Diaz) and diazipane-2-thione (Diap) (Scheme 1.5) have different coordination sites (through S and N), these ligation sites can provide various coordination modes that can give different properties for complex, that can be useful for different applications [50].

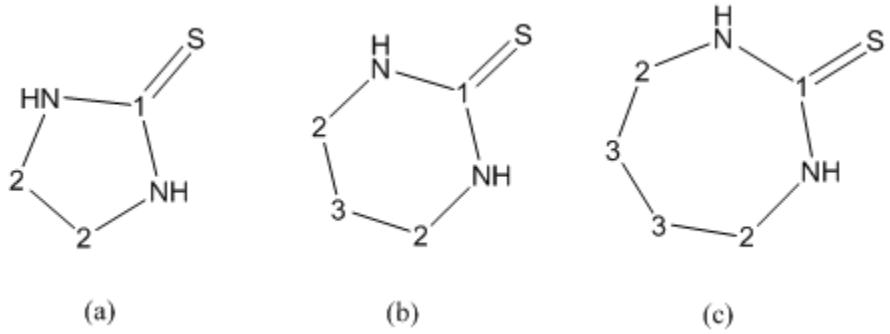

Scheme 1.5: (a) Imt, (b) diaz and (c) Diap.

Interaction of gold(I) with thiones have been explored well in literature [52,62,63], while less attention was given for gold(III) complexes. This may be due to lower stability of the gold(III) than the gold(I) complexes. This has lead to much scarce knowledge about Au(III) complexes interaction with biological ligands. However, gold(III) was found to be resilient *in vivo* by oxidative bursts [19] that can oxidize gold(I) to gold(III) by the help of the enzyme myeloperoxidase [19]. Gold(III)-tetracyanide was considered as a metabolic product of anti-arthritic and anti-rheumatic drugs [16], which found latter to increase cell uptake of drug [39,40].

Several researches were conducted concerning mechanistic aspects of gold complexes in-vivo [59]. Application and usage as anticancer drug where also discussed by several reports [1,59].

In order to determine the mechanism of action of the anti-arthritic gold complexes, it is necessary to understand the physiochemical properties of these complexes and their reactivity under physiological conditions.

By exploring the properties and reactivities of gold(III) complexes it is expected that this will provide a wider choice of drugs, which would avoid the severe side effects of *cis*-platin as well as trying to get higher activity toward tumor resistance [1].

CHAPTER TWO

OBJECTIVES

2.1 Synthesis and characterization.

1. Gold(III) mono-alkyldiamine complexes $[Au(L)Cl_2]Cl$ and $[Au(L)_2]Cl_3$ will be synthesized, L is ethylenediamine (*en*), propylenediamine (*pn*) and butylenediamine (*bn*). These complexes will be prepared as ^{15}N labeled and unlabeled ligands.

2. Complexes of nitrogen substituted ethylenediamine will be synthesized: $[Au(R,R'\text{-}en)Cl_2]Cl$. R and R' are Me, Et, n-Pr, i-Pr etc.

3. $[Au(^{13}C^{15}N)_4]^-$ will be synthesized by adding 4 equivalents of $^{13}C^{15}N^-$ to Au(III) halide.

4. The complexes will be characterized using melting point, elemental analysis, Mid-IR, Far-IR, UV-Vis, X-ray, solution and solid state NMR techniques.

2.2 Interactions of alkyldiamine gold(III) complexes with bioligands.

1. Interaction of these complexes with labeled L-cysteine-$^{13}C3$, glutathione, captopril, thiomalic acid, penicillamine etc. will be studied by ^1H and ^{13}C NMR.

2. Interactions of these complexes with L-methionine-$^{13}C5$, DL-seleno-methionine-$^{13}C5$) will be studied by ^1H and ^{13}C NMR.

3. Interactions of Au(III) complexes with ergothionine, imidazolidine-2-thione and its derivatives will be studied by ^1H and ^{13}C NMR.

4. Interactions of these complexes with imidazole and L-histidine will be studied by ^{1}H and ^{13}C NMR.

2.3 Interactions of $[Au(^{13}C^{15}N)_4]^-$ complex with bioligands.

1. Interaction of $[Au(^{13}C^{15}N)_4]^-$ with thiols such as L-cysteine, glutathione, captopril etc, and thioether such as L-methionine and DL-seleno-methionine will be studied by ^{1}H, and ^{13}C NMR.

2. Interaction of $[Au(^{13}C^{15}N)_4]^-$ with imidazolidine-2-thione (Imt) and its derivatives will be studied by ^{1}H and ^{13}C NMR.

3. Interaction of $[Au(^{13}C^{15}N)_4]^-$ with phosphines such as $(2\text{-CN-Et})_3P$, Cy_3P will be studied by ^{1}H, ^{13}C and ^{31}P NMR.

4. Interaction of $[Au(^{13}C^{15}N)_4]^-$ with phosphine sulfides such as Me_3PS, Et_3PS, Ph_3PS will be studied by ^{1}H, ^{13}C and ^{31}P NMR.

5. Interaction of $[Au(^{13}C^{15}N)_4]^-$ with phosphine selenides such as Me_3PSe, Ph_3PSe will be studied by ^{1}H, ^{13}C and ^{31}P NMR.

CHAPTER THREE

EXPERIMENTAL

3. 1 Chemicals

Reagents and solvents were used as received from commercial sources. The synthesized compounds were identified by melting point, elemental analysis, IR and NMR spectroscopy techniques.

$HAuCl_4.3H_2O$ was obtained from Strem Chemicals Co., while acetone, absolute ethanol, acetonitrile, D_2O and CD_3OD were obtained from Fluka Chemicals Co, ligands e.g. ethylenediamine (en), propylenediamine (pn), butylenediamine (bn), L-glutathione, L-captopril, thiomalic acid, DL-penicillamine, ergothionine, 2,4-dithiouracil, imidazolidine-2-thione (Imt), 1,3-Diazinane-2-thione (Diaz), 1,3-diazipane-2-thione (Diap), imidazole, L-histidine and L-glycine were obtained from Sigma-Aldrich, L-^{13}C3-cysteine, L- methionine-^{13}C5, DL-Se-methionine-^{13}C5 were obtained from Isotech, USA.

3.2. UV measurements

3.2.1 [Au(alkyldiamine)Cl_2]Cl

Electronic spectra where collected for the alkyldiamine gold(III) complexes using Lambda 200, Perkin-Elmer UV-Vis spectrometer.

3.2.2 [Au(alkyldiamine)Cl_2]Cl with L-histidine; Kinetic Measurements.

Buffer solution was prepared from 0.01 M H_3PO_4 solution adjusted at pH 2.9. This solution was used to prepare [Au(*en*)Cl_2]Cl and L-histidine stock solution as 3.0 mM of each, which were mixed at different ratios to give various concentrations as

3.00 mL total volume. Absorbance of the [Au(*en*)Cl_2]Cl at 305 nm was monitored during the course of the reaction at 25 ^{o}C.

Fitting of the first 5-10 % of the UV-Vis absorbance change to linear equation gives the slope as the initial rate (v_i, mol•L^{-1}•s^{-1}) for [Au(*en*)Cl_2]$^{+}$ complex and L-histidine interaction.

3.2.3 [Au($^{13}C^{15}N$)$_4$]$^{-}$ reaction with L-cysteine, glutathione, captopril, L-methionine and DL-Seleno-methionine.

UV spectra in the range 200 to 330 nm (2 nm step size) for components of 0.1 mM concentration in phosphate buffer (100 mM) at pH = 7.4 at 25 ^{o}C were measured on GBC Cintra 303 spectrophotometer.

3.3 Mid and Far-IR studies

The solid-state IR spectra of the ligands and their gold(III) complexes were recorded on a Perkin–Elmer FTIR 180 spectrophotometer using KBr pellets over the range 4000–400 cm^{-1}. Far-infrared spectra were recorded at 4 cm^{-1} resolution in the range 200-600 cm^{-1} at room temperature as Cesium Chloride disks on a Nicolet 6700 FT-IR with Far-IR beam splitter.

3.4 ^{1}H, ^{13}C and ^{15}N NMR Spectroscopy

3.4.1 NMR samples for [Au(alkyldiamine)Cl_2]Cl complexes.

NMR measurements were carried out on JEOL JNM-LA 500 MHz NMR spectrometer at 297 K using 0.10 M solution of the complexes in D_2O. ^{13}C NMR spectra were obtained at 125.65 MHz with ^{1}H broadband decoupling. The spectral conditions were: 32k data points, 0.967s acquisition time, 1.00 s pulse delay and 45^{o} pulse angle, while ^{13}C DEPT NMR spectra recorded at 135^{o} pulse angle.

3.4.2 NMR samples for [Au(alkyldiamine)Cl_2]Cl reaction with L-histidine and imidazole.

NMR measurements were carried out on JEOL JNM-LA 500 MHz NMR spectrometer at 297 K using 0.10 M solution of the complexes in D_2O. NMR samples were prepared by mixing 0.05 M of [Au(*en*)Cl_2]Cl complex in D_2O with 0.05M L-histidine solution, pD was adjusted by DCl and NaOD solutions in D_2O, pD raising of the $[Au(en)Cl_2]^+$ complex causes precipitation of hydrolysis products, such as metal hydroxide and oxides [10]. In order to avoid hydrolysis, pD was adjusted for L-histidine solution before mixing with $[Au(en)Cl_2]^+$ solution and measured again after mixing.

Similarly for imidazole, samples were prepared by mixing solutions of 0.05 M imidazole with 0.05 M [Au(*en*)Cl_2]Cl. DSS (2,2-dimethylsilapentane-5-sulphonate) was used as internal reference for the ^{1}H NMR.

3.4.3. NMR samples for [Au(*en*)Cl_2]Cl reaction with L-methionine and DL-seleno-methionine.

NMR measurements were carried out on JEOL JNM-LA 500 MHz NMR spectrometer at 297 K using 0.10 M solution of the complexes in D_2O. NMR samples were prepared by mixing D_2O solutions of [Au(*en*)Cl_2]Cl (0.05 M) and Met and Se-Met solution (0.05 M), pD were adjusted by DCl and NaOD solutions in D_2O to pD = 3.8.

3.4.4 NMR samples for $[Au(CN)_4]^-$ with thiols, L-methionine and DL-seleno-methionine.

NMR measurements were carried out on JEOL JNM-LA 500 MHz NMR spectrometer at 297 K using 0.10 M solution of the complexes in D_2O. All NMR measurements were carried out by mixing 140 mM concentrations of reactants in D_2O, reactants pD were adjusted to 7.4 before and after mixing. ^{13}C NMR spectra were obtained at 125.65 MHz with ^{1}H broadband decoupling. The spectral conditions were: 32 k data points, 0.967 s acquisition time, 1.00 s pulse delay, 45^o pulse angle and 135^o pulse angle for ^{13}C DEPT NMR experiments.

3.5 Solid State NMR Spectroscopy

Solid-state NMR showed more sensitivity to coordination geometry rather than solution NMR, which is expected from the removal of the solvent effects, fluxional processes and other averaging processes that may be present in the solution state. It has the added advantage that it provides the three principal components of the shielding tensor, rather than just the average value observed in solution spectra. These components can be calculated from the intensities of the spinning side bands in the solid-state spectra. Under the conditions of magic-angle spinning (MAS), the isotropic chemical shift δ_I, given by equation 1, is equivalent to the chemical shift observed in solution

$$\delta_I = 1/3\ (\delta_{11} + \delta_{22} + \delta_{33}) \qquad \text{Eq (1)}$$

For a nonsymmetrical environment, with $\delta_{11} < \delta_{22} < \delta_{33}$, the chemical shift anisotropy ($\Delta\delta$) is defined as

$$\Delta\delta = \delta_{33} - \tfrac{1}{2}\ (\delta_{11} + \delta_{22}) \qquad \text{Eq (2)}$$

For a symmetric tensor, where $\delta_{11} = \delta_{22} = \delta_{\perp}$, then $\delta_{33} = \delta_{//}$; for $\delta_{33} = \delta_{22} = \delta_{\perp}$, then $\delta_{11} = \delta_{//}$. For these cases the shift anisotropy is defined as

$$\Delta\delta = \delta_{//} - \delta_{\perp} \qquad \text{Eq 3}$$

Unlike solution chemical shifts, solid state NMR results can be correlated directly with crystallographic structure determinations when available, and structural predictions can be made in the absence of crystallographic data.

3.5.1 Solid-state ^{13}C NMR

The $^{13}C\{^{1}H\}$ solid-state NMR spectra were obtained on a JEOL LAMBDA 500 spectrometer operating at 125.65 MHz (11.74 T), at 25 ^{o}C. Samples were packed into 6 mm zirconium oxide rotors. Cross-polarization and high power decoupling were employed. Pulse delay of 7.0 s and a contact time of 5.0 ms were used in the CPMAS experiments. The magic angle spinning rates were from 2 kHz to 4 kHz. Carbon chemical shifts were referenced to TMS by setting the high frequency isotropic peak of solid adamantane to 38.56 ppm.

3.5.2 Solid-state ^{15}N NMR

Natural abundance ^{15}N spectra were also recorded on the above machine, using a contact time of 5 ms and a pulse delay of 10 s. The magic angle spinning rates were between 2000 Hz to 4000 Hz. All ^{15}N spectra were referenced to $^{15}NH_4NO_3$ peak (δ_{iso})= -358.63 ppm relative to CH_3NO_2, (δ_{iso}) = 0 ppm [64a]. Both the ^{15}N spectra and ^{13}C spectra, containing spinning side-band manifolds, were analyzed using a program HBA [64b] based on Maricq and Waugh [65] which developed at Dalhousie University, Canada, and University of Tübingen, Germany.

3.5.3 Solid-state ^{13}P NMR

Solid state cross-polarization magic-angle spinning CPMAS $^{31}P\{^{1}H\}$ NMR spectra were obtained at ambient temperature on the same spectrometer, operating at a frequency of 202.35 MHz. A contact time of 3 ms was used with a proton pulse width of 6 μs, with a recycle delay of 10 s. Chemical shifts were referenced using an external sample of solid PPh_3 (δ = 8.40 ppm from 85 % H_3PO_4).

Both ^{31}P and ^{13}C spectra, containing spinning side-band manifolds, were analyzed using a program HBA [64b] based on Maricq and Waugh [65] which were developed at Dalhousie University, Canada, and University of Tübingen, Germany.

3.6 Synthesis and Preperation

3.6.1 Synthesis of [Au($^{15}N_2$en)Cl_2]Cl, Au($^{15}N_2$pn)Cl_2]Cl , [Au($^{15}N_2$bn)Cl_2]Cl complexes and [Au(R or R_2en)Cl_2]Cl complexes, where R = Me, Et, n-Pr, i-Pr.

All the complexes were prepared by dissolving of 0.25 mmol trihydrated auric tetrachloride $HAuCl_4.3H_2O$ in minimum amount of absolute ethanol at ambient temperature. In a separate beaker, solution of 0.25 mmol of the alkyldiamine in least amount of absolute ethanol was prepared, both solutions were mixed (total of ~ 20 mL) and stirred for around 30 minutes until clear solution obtained, which was filtered and concentrated to 10 ml volume then left for crystallization in the refrigerator. The produced solid was dried under vacuum. The product was in the range of 51-67 % yield. Abbreviations for prepared complexes are given in table 3.1. Melting points and elemental analysis for complexes are presented in table 3.2.

Table 3.1: abbreviations used for the new complexes.

Complex	Abbreviations
[Au(en)Cl_2]Cl	1a
[Au(pn)Cl_2]Cl	1b
[Au(bn)Cl_2]Cl	1c
[Au(N-Me-en)Cl_2]Cl	2a
[Au(N-Et-en)Cl_2]Cl	2b
[Au(N-*i*Pr-en)Cl_2]Cl	2c
[Au(N-hydroxyl-Et-en)Cl_2]Cl	2d
[Au(N,N'-Me_2-en)Cl_2]Cl	3a
[Au(N,N'-Et_2-en)Cl_2]Cl	3b
[Au(N,N'-*i*Pr_2-en)Cl_2]Cl	3c
[Au(N,N'-2-di-hydroxy-Et-en)Cl_2]Cl	3d

Table 3.2. Elemental analysis and of the prepared complexes

		Found (Calc.) %		
Complex	**M. pt. (°C)**	**H**	**C**	**N**
1a.2H_2O	145-148	2.92(3.03)	6.22 (6.01)	6.79(7.01)
1b.2H_2O	190-193	3.50(3.42)	8.90(8.71)	6.90(6.78)
1c.2H_2O	Dcmps.>230	4.25(4.08)	11.40(11.24)	6.70(6.55)
2a.H_2O	139-141	2.98(3.06)	8.95(9.11)	6.85(7.08)
2b.2H_2O	116-118	3.99(4.12)	13.33(13.60)	6.16(6.35)
2d.2H_2O	105-110	3.83(3.64)	11.00(10.83)	6.52(6.32)
3a.H_2O	80-83	3.83(3.78)	11.35(11.24)	6.61 (6.55)
3b	106-109	3.95(3.85)	17.24(17.17)	6.84(6.68)

3.6.2 Synthesis of Au(III) complexes with thiones

0.6 mmol [Au(alkyldiamine)Cl_2]Cl was dissolved in 20 mL distilled H_2O (solution 1). 1.2 mmol of thione was dissolved in 40 mL methanol (solution 2). Both solutions were mixed in round bottom flask and refluxed at 60 ^oC for 4 hour. The resulting solution was filtered, concentrated and laid aside for crystallization. Products were characterized by m.pt and elemental analysis (Table 3.3).

Table 3.3: Elemental analysis of the prepared $[Au(alkyldiamine)Cl_2]^+$ with different substituted Imt, Diaz and Diap.

Complex	M.pt ^oC	Found (Calc.) %			
		C	H	N	S
$[(Imt)_2Au(en)]Cl_3$	199-202	17.24(16.92)	3.73(3.55)	14.77(14.80)	11.19(11.30)
$[(Imt)_2Au(pn)]Cl_3$	217-20	18.88(18.58)	4.16(3.81)	15.04(14.45)	11.04(11.02)
$[(Imt)_2Au(bn)]Cl_3$	170-3	20.60(20.16)	4.20(4.06)	14.19(14.11)	9.97(10.76)
$[(Diaz)_2Au(en)]Cl_3$	239-41	21.34(20.16)	4.70(4.06)	14.50(14.11)	9.91(10.76)
$[(Diaz)_2Au(pn)_2]Cl_3$	210-3	24.43(24.59)	5.06(5.31)	15.59(15.55)	10.30(9.38)
$[(Diaz)_2Au(bn)]Cl_3$	268-71	23.18(23.31)	4.92(4.52)	13.50(13.47)	9.95(10.28)
$[(Diap)_2Au(pn)_2]Cl$	170-3	30.01(29.98)	5.94(6.29)	17.04(17.48)	10.42(10.00)
[(Imt)Au(N,N'-Me-en)]Cl	190-1	19.83(19.89)	4.65(4.29)	12.88(13.25)	8.17(7.59)
$[(Diaz)_2$ Au(N,N'-Me-en)$]Cl_3$	Dcmps.>250	23.09(23.10)	5.04(4.52)	12.91(13.47)	10.20(10.28)
$[(Diap)_2$ Au(N,N'-Me-	Dcmps.>250	25.85(25.79)	5.37(4.95)	12.31(12.89)	8.99(9.84)
[(Imt)Au(N,N'-*i*Pr_2-en)]Cl	260-2	27.80(27.59)	6.05(5.47)	11.85(11.70)	7.16(6.70)
$[(Diaz)_2Au(N,N'$-*i*Pr_2-en$)]Cl_3$	238-9	29.01(28.26)	5.84(5.34)	12.87(12.36)	8.99(9.43)

3.6.3 $KAu(CN)_4$ complex preparation

Gold(III)-tetracyanide was prepared according to literature [16]. Two solutions were prepared separately; solution 1 consists of 2.00 g (5.33 mmol) auric acid dissolved in 5 mL distilled water, and solution 2, 1.73 g KCN (8% $K^{13}C^{15}N$ enriched) (26.62 mmol) dissolved in 5 mL distilled water. Solutions 1 and 2 were mixed while stirring (this reaction must be done in fume hood, since HCN gas will evolve from reaction vessel), a white precipitate was formed immediately, and when allowed to grow for 3 hours, produced a solid, which was separated by decantation and dried in open air area, 95 % yield was obtained. IR data showed $\upsilon_{(CN^-)}$ band at 2189 cm^{-1} corresponding to $[Au(CN)_4]^-$ that agrees with literature data [16].

3.6.4 $KAu(CN)_4$ reaction with phosphines

$KAu(CN)_4$ (~0.6 mmol) was dissolved in 15 mL acetone. Ligand (~ 1.2 mmol) was dissolved in 20 mL absolute ethanol, the two solutions were mixed in round bottom flask and refluxed for ~3 hours at 75 ^oC. The resulting solution was filtered and concentrated. Product was crystallized out from solution. Elemental analysis and melting point data for the synthesized complexes are given in table 3.4.

Table 3.4: Elemental analysis and melting point of the synthesized complexes.

Complex	m. pt. (^{o}C)	Found (Calc.) %			
		C	H	N	S
$[((2\text{-}CN\text{-}Et)_3P)_2Au(CN)]$	205-6	38.65(38.44)	4.05(3.97)	15.91(16.09)	
$[(Cy_3P)_2AuCN].KCN$	137-8	53.87(53.76)	7.55(7.84)	3.45(3.30)	
$[(Me_3PS)_2Au(CN)_3]$	Dcmps.	22.56(22.00)	3.70(3.69)	8.87(8.55)	12.59(13.05)
$[(Et_3PS)_3Au(CN)_3]$	94-6	34.19(34.76)	6.30(6.25)	5.61(5.79)	13.14(13.25)
$[(Ph_3PS)_2Au(CN)_3]$	160-1	54.65(54.23)	3.65(3.51)	4.62(4.87)	7.23(7.42)
$[(Me_3PSe)_2Au(CN)_3]$	150-2	18.14(18.47)	3.09(3.11)	6.97(7.18)	
$[(Ph_3PSe)Au(CN)_3].KCN$	181-3	38.06(38.77)	2.20(2.22)	8.03(8.22)	

3.7. Computational study

3.7.1 [Au(alkyldiamine)Cl_2]Cl complexes.

Geometry optimization was done for the built structures and optimized by Density Funactional Theory (DFT) level of theory with LanL2DZ (Los Alamos ECP plus double-zeta) [66,67] basis sets using Gaussian 03W program package [68].

3.7.2 [(His)Au(*en*)]Cl_3 complex.

Geometry optimization was done for the built structures and optimized by DFT (B3LYP) level of theory using GAUSSIAN03 program package [68] with the following basis set; SDD for the gold, 6-31G(d) for the carbon, oxygen, nitrogen, and hydrogen. The optimized geometry was confirmed as minimum by running vibrational frequency on the optimized geometry using the same basis set.

CHAPTER FOUR

RESULTS AND DISCUSSION

4.1 Synthesis and characterization of gold(III) complexes with unsubstituted, N-mono and N,N'-di-substituted alkyldiamine ligands.

4.1.1 Electronic spectra

The λ_{max} values for the complexes studies are given in table 4.1. Au(III) complexes show absorption in the region 250-350 nm (40,000-28,570 cm^{-1}) which correspond to LMCT transitions signal at ~300 nm that could be assigned to Cl→Au charge transfer by analogy to auric acid absorption spectra which give a band at 320 nm [69], where this transition of extinction coefficient can't be assigned to the symmetry forbidden d-d transition. According to crystal field theory for d^8 complexes the LUMO orbital is $d_{x^2-y^2}$, so ligand to metal charge transfer could be due to $p_\sigma \rightarrow d_{x^2-y^2}$ transition [70]. Six-membered ring complex shows the lowest wavelength absorption at 293.5 nm which indicate the relative stability of the six member ring over both five and seven member rings. However, substitution on alkyldiamine nitrogen increased the absorption wavelength > 300 nm. This is consistent with a destabilizing steric effect caused by the substituents as the complexes under study.

Table 4.1 : UV-Vis spectra λ_{max} for Au(III) complexes of alkyldiamine.

Complex	λ_{max} (nm)
$HAuCl_4$	320.0
1a	297.0
1b	293.5
1c	296.0
3a	307.0
3b	308.5
3c	311.5
3d	301.0

4.1.2 Infrared spectroscopy

Infrared spectra of the complexes (Table 4.3) show a shift to higher wavenumber of N-H stretching band compared to free ligand in the range of 200 cm^{-1}. This could be a result of the absence of hydrogen bond after complexation because the nitrogen electron's pairs are involved in Au-N bond. The C-N stretching bands also showed a slight shift to higher wavenumber indicating a shorter C-N bond in the complex than for the free ligand.

Assignments of the vibrational bands are based on the computationally obtained frequencies at the B3LYP level with LanL2DZ bases set.

Far-IR showed signals at 353 to 367 cm^{-1} for symmetric and asymmetric stretching of the Au-Cl, which is consistent with Au-Cl stretching mode *trans* to nitrogen [71,72], and another group of bands at 391 to 491 cm^{-1} for the symmetric and asymmetric stretching of the Au-N bond [73a]. The red shift of the alkyldiamine complexes with respect to the auric acid shows the weakening of the Au-Cl bond. The Au-N stretching bands of the six and seven member metalcycle gold(III) complexes shows higher wavenumber than five member ones, indicating the higher stability for the six and seven member metalacycle complexes with less strained bonds.

Table 4.2. IR frequencies, $\nu(cm^{-1})$ Au(III)-alkanediamine complexes

Complex	**υ(N-H)**	**υ_{shift}**	**υ(C-N)**	**υ_{shift}**
en	3393 w		1033 m	
1a	3422 br	29	1045 m	12
pn	3357 m, 3282 m		1093 w	
1b	3447 br	90	1178 s	85
bn	3356 br, 3290 br		1069 m	
1c	3422 m, 3330 w	66, 40	1148 m	79
N-Me-en	3282 w		1130 m	
2a	3424 br	142	1047 m	-83
N-Et-en	3276 br		1130 m	
2b	3612 w, 3537 w	336	1197 m	67
N-*i*Pr-en	3300 m, 3289 m		1174 m	
2c	3484 br	184	1122 m	-52
N-2-hydroxyl-Et-en	3280 br		1123 w, 1051 m	
2d	3424 br	144	1160 w	37
N,N'-Me_2-en	3288 br		1148 w,1103 m	
3a	3407 w	119	1172 w	24
N,N'-Et_2-en	3235 br		1125 s	
3b	3563 w, 3371 w	328	1111 w	-14
N,N'-*i*Pr_2-en	3249 br		1173 m	
3c	3525m, 3421m	276	1115 m	-58
N,N'-(2-hydroxy-$Et)_2$-en	3263 br		1058 m	
3d	3400 s, 3313 s	137	1066 s	8

Table 4.3: Far-IR data for 1a, 1b, and 1c complexes

Species	Au-Cl	Au-N
$HAuCl_4$	367	-
1a	353, 367	391,474
1b	358	491
1c	355	457, 499

Table 4.4: ^{13}C NMR chemical shifts of free ligands and Au(III)-alkanediamine complexes in D_2O.

Species	**C-1**	**C-2**	**C-3**	**C-4**
en	37.32			
1a	51.75			
pn	37.61	25.79		
1b	39.81	27.70		
bn	39.78	24.77		
1c	47.21	27.51	24.76	39.81
N-Me-en	36.26	46.37	34.18	
2a	48.93	61.83	42.45	
N-Et-en	36.41	44.40	44.37	11.42
2b	50.21	57.49	49.23	12.89
N-*i*Pr-en	36.58	42.27	52.58	19.07
2c	49.91	56.70	52.19	20.14
N-hydroxy-Et-en	57.48	50.64	44.99	36.41
2d	58.38	57.73	56.03	49.90
N,N'-Me_2-en	45.15	34.20		
3a	58.90	46.29		
N,N'-Et_2-en	44.36	43.24	11.25	
3b	56.83	51.14	11.52	

Table 4.4 shows the assignments of the various ^{13}C NMR resonances of ligands and complexes.

^{13}C NMR downfield shift was observed for complexes with respect to the free diamine ligands. This can be attributed to the σ-donation of nitrogen lone pair to the gold ion that causes de-shielding of the carbon(s) next to the bonding nitrogen. The shifts vary significantly from one ligand to another suggesting different degrees of σ-donation from the ligand to the metal (Table 4.4). For example, in the series 1a,1b and 1c (Scheme 1.1) as the complex ring size was changed, six-membered ring 1b shows least chemical shift difference, indicating least participation of the propylenediamine ligand carbons in the electron donation to the metal. Another observation is that ^{13}C NMR spectra of 1a and 1b show the same number of signals compared to free ligand, while butylenediamine complex (1c) shows four different carbon atom resonances, instead of two in the free ligand. This could be attributed to the 7-membered ring adopting a puckered conformation where the equivalence of the carbons is lost, probably due to the ring folding away from the [AuN_2] plane and the slow fluxional rate of the ring is on the NMR time scale.

In the complexes 2a, 2b, 2c and 2d (Scheme 1.2) C-1, C-2 and C-3 signals in the ^{13}C NMR (Table 4.4) show considerable chemical shift difference relative to the corresponding free ligand. Comparison of ligand and complex chemical shifts reveal that the C-2 is the most de-shielded atom while in complex 2d the largest

effect was on C-3. Another observation is the down field shift of C-3, this effect decreases with increasing the substituents volume as we go from methyl (8 ppm for 2a) to isopropyl (< 1 ppm in 2c), this means less involvement of C-3 in the bonding as observed for bulkier groups.

N,N'-di-substituted complexes of gold(III) are shown in Scheme 1.3, ^{13}C NMR shows two resonances for both carbons C-1 and C-2 next to nitrogen, suggesting symmetry of the two substituents with respect to each other, but this does not differentiate whether there two groups are *cis* or *trans* with respect to the complex plane.

^{1}H NMR for gold(III) complexes of alkyldiamine ligands showed very complicated spectra because of the strained structure and inequivalency of the hydrogen environments in the complexes.

Recently, Silve *et al* [73b] studied four new ligands derived from 1,3-propanediamine with different carbon chains lengths in an attempt to correlate this factor, which influences the lipophilicity of the compounds, with cytotoxic activity. The effect of the four complexes on the growth of two tumoral cell lines, and their cellular uptake were investigated. They reported that lipophilicity enhances the rate of cellular uptake and, consequently, the cytotoxic activity. In this study, we have also prepared several new complexes with different carbon chains. It will be of interest to study their cytotoxic activity in comparison with *cis*-Pt complex.

4.1.3 Solid-State NMR

At the spinning speeds employed in our experiments, we observe only the isotropic signals due to the carbons and nitrogens, with small anisotropies due to the sp^3 hybridizations of these atoms. Compared to solution chemical shifts, slight de-shielding in solid state is observed. Similar to solution NMR, four signals of carbon atoms appear for the complex $[Au(bn)Cl_2]Cl$ (1c), this supports the idea of the unequivalency of the four carbon atoms of the butylenediamine. The ^{15}N NMR for complexes 1a, 1b and 1c were also measured and presented in Table 4.5. Comparison of the shift for free ligand with bound, suggest the nitrogen atoms of the ethylenediamine complex were least affected by complexation while these of butylenediamine were the most affected. This is consisitent with the largest electron donation being for the butylenediamine ligand to the gold (III) ion. This could be interpreted by the steric strain in five-membered ring in ethylenediamine complex. The strength of lone pair donation from N atom to the gold(III) increases in the order en < pn < bn in consistence with Far-IR data.

Recently Messori *et al*. described the *in vitro* activity of a series of gold(III) complexes, $[Au(en)_2]Cl_3$, $[Au(dien)Cl]Cl_2$, $[Au(cyclam)](ClO_4)Cl_2$, $[Au(terpy)Cl]Cl_2$, and $[Au(phen)Cl_2]Cl$, against the A2780 ovarian cancer cell line and a *cis*-platin resistant variant [74,75]. The relative order of cytoxicity was Au(terpy) >> Au(phen) > Au(en), Au(dien) >> Au(cyclam). Interestingly the three most active compounds retained activity against the *cis*-platin-resistant cell line.

Table 4.5: Solid-state ^{13}C and ^{15}N-NMR Isotropic Chemical Shifts (δ_{iso}).

Complex	**^{15}N**	**C-1**	**C-2**	**C-3**	**C-4**
en•HCl (solid)	-342.68				
1a	-342.09	53.76			
pn•HCl (solid)	-343.12				
1b	-337.86	43.19	27.36		
bn•HCl (solid)	-343.36				
1c	-333.23	51.24	26.30	27.66	41.73
2a	-	46.58	63.74	37.36	
2b	-	46.29	58.62	41.54	15.42
2c	-		50.56	-	21.54
2d	-	59.98	53.28	47.94	38.04
3a	-	62.89	45.13	33.38	15.14

In this study, we have demonstrated that the chemical shift difference between free and bound ligand for the solid ^{15}N NMR decreases as bn > pn > en, indicating stronger Au-N bond for bn complex compared to pn and en. The UV-Vis studies show relative stability of the Au(III) complexes of unsubstituted ethylenediamine with respect to their N,N'-di-substituted analoges. It will be of interest to test these three complexes for their anti-cancer activity and compare them with *cis*-Pt complex.

4.1.4 Computational study

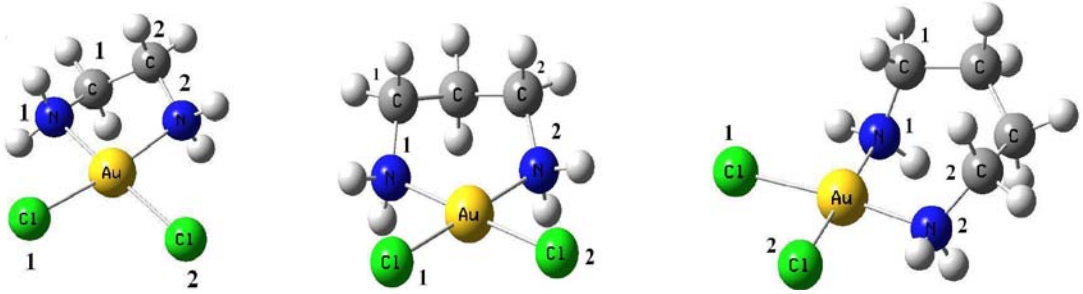

a b c

Scheme 4.1: Optimized geometries of 4.1a, 4.1b and 4.1c, obtained at the B3LYP/LanL2DZ level of theory using *Gaussian 03W*, *revision B04.*

B3LYP optimized structure was analyzed computationally for NMR spectra using B3LYP/LanL2DZ level of theory which shows acceptable error from the experimental values from the crystal structure of the gold(III) complex with ethylenediamine [5]. Selected bond lengths bond and torsion angles of the computationally optimized structure are presented in tables 4.6 and 4.7, respectively.

Table 4.6: Selected bond lengths for [Au(alkyldiamine)Cl_2]Cl for optimized structure using B3LYP\LanL2DZ.

	4a	4b	4c
Au-N(1)	2.133	2.129	2.135
Au-Cl(1)	2.379	2.389	2.392
Au-N(2)	2.133	2.129	2.131
Au-Cl(2)	2.379	2.389	2.391

Table 4.7: Selected bond and torsion Angles (°) for [Au(alkyldiamine)Cl_2]Cl for optimized structure using B3LYP/LanL2DZ.

	4a	4b	4c
N(1)-Au-Cl(1)	91.34	86.30	85.49
N(1)-Au-Cl(2)	175.04	179.37	179.09
Cl(1)-Au-Cl(2)	93.60	94.01	93.71
N(2)-Au-Cl(1)	175.04	179.17	179.03
N(2)-Au-Cl(2)	91.34	85.88	85.38
N(1)-Au-N(2)	83.72	93.80	95.43
N(2)-Au-N(1)-C(1)	13.97	40.66	67.74
Cl(1)-Au-N(1)-C(1)	-165.56	-138.52	112.59
Cl(2)-Au-N(1)-C(1)	18.76	-19.46	84.25
Au-N(1)-C(1)-C(2)	-39.45	-57.54	56.80
N(1)-Au-N(2)-C(2)	13.84	-40.66	82.24
Cl(1)-Au-N(2)-C(2)	19.27	56.39	-117.34
Cl(2)-Au-N(2)-C(2)	-165.75	138.79	-97.33

4.2 **Investigation of the interaction of gold(III)-alkyldiamine complexes with L-histidine and imidazole ligands.**

^{1}H NMR spectrum was studied and *en*-H signal was monitored in the free ligand and [Au(*en*)Cl_2]$^+$ complex at different pD's. Chemical shift of both *en* as free ligand and as [Au(*en*)Cl_2]$^+$ complex were directly increased in the range pD 1 to 2 as a result of *en*-nitrogen protonation. However, minor change of chemical shift was observed with pD in the range 2.0 to 6.0 (Figure 4.1). At pD higher than alkyldiamine pK_a value (7.0) [Au(*en*)Cl_2]$^+$ complex was found to be very stable because of better donation to the Au(III) metal center.

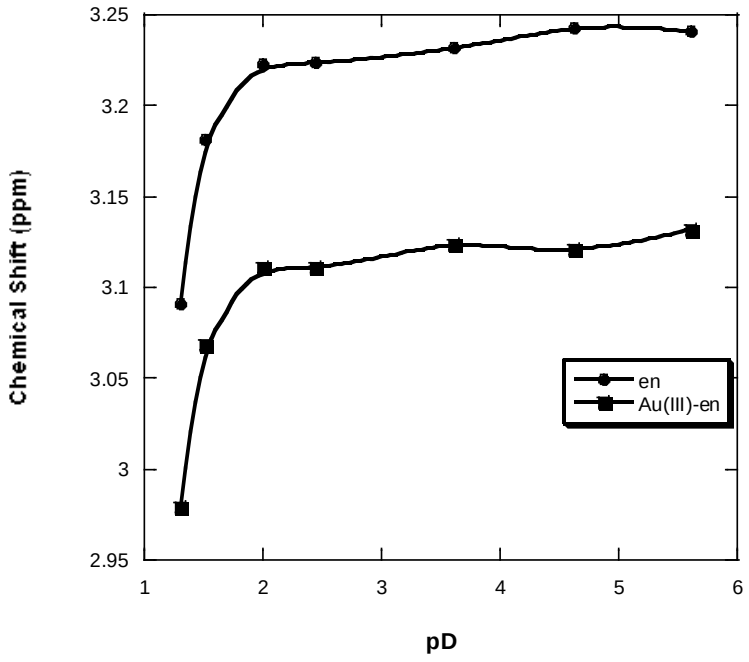

Figure 4.1: ^{1}H NMR chemical shift of free *en* (●) and *en* in $[Au(en)Cl_2]^+$ complex (■) as function of pD.

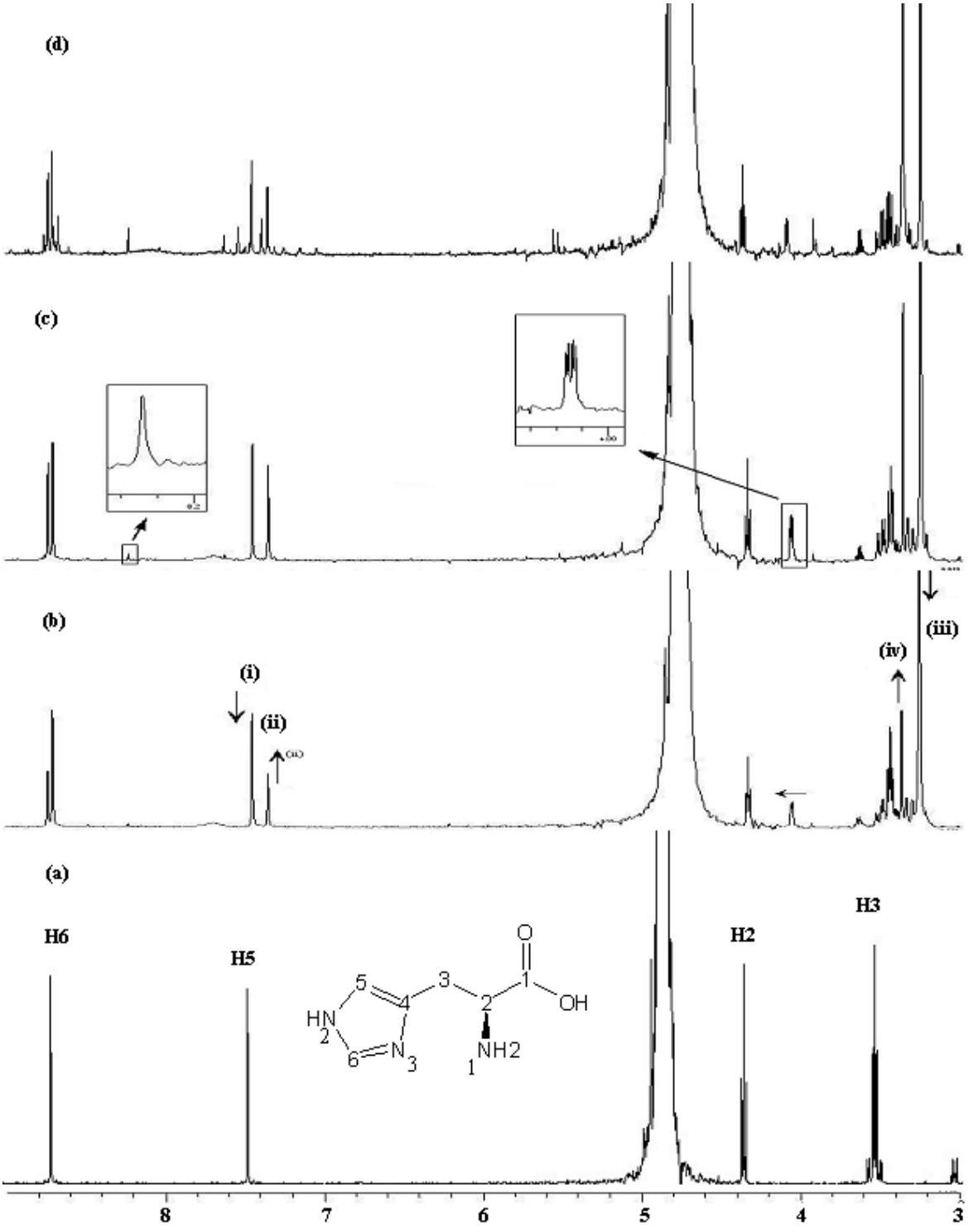

Figure 4.2: ^{1}H NMR spectra of L-histidine reaction with $[Au(en)Cl_2]^+$ vs. time at pD 1.6. (a) L-Histidine before mixing (pD=1.6), (b) 1hour after mixing (i) represents free L-histidine., (ii) represents L-histidine bound to Au(III) , (iii) represents *en* bound to Au(III) and (iv) represents free *en* (c) 4 hours after mixing and (d) 50 hours after mixing.

Spectrum of free L-histidine in solution at pD =1.6 is shown in Figure 4.2A. Signals at ~ 8.58, 7.20, 4.05 and 3.42 ppm (Figure 4.2) coresspond to position 6, 5, 2 and 3 protons of L-histidine, respectively. Study of ^{1}H NMR spectra of L-histidine vs. time (Figure 4.2) shows continuous intensity increase of signals corresponding to $[(His)Au(\textit{en})]^{3+}$ complex in solution (signal (ii)) along with decrease of signals correspond to free L-histidine. This shows that L-histidine and $[Au(\textit{en})Cl_2]^{+}$ reaction starts in solution right after mixing, while L-histidine oxidation products could be distinguished in by ^{1}H NMR in ~ 1 hour. L-histidine oxidation leads to the formation of 2-oxy-histidine and 2-hydroxy-histidine in equilibrium (Scheme 4.3) as shown by Zhao *et al* [76] along with gold(III) reduction which deposited on glass as Au(0).

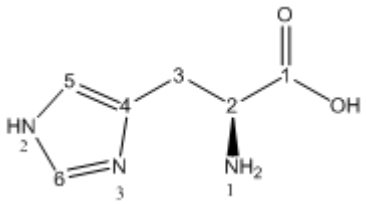

Scheme 4.2: L-Histidine atom numbering.

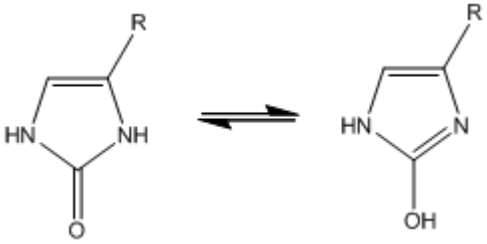

Scheme 4.3: 2-oxy and 2-hydroxy-histidine equilibrium**.**

Table 4.8: ^{1}H NMR chemical shifts of [Au(*en*)Cl_2]$^{+}$ complex with L-histidine and imidazole ligands at various pD's in aqueous solution.

	***en* / [(His)Au(*en*)]$^{3+}$**	**His / [(His)Au(*en*)]$^{3+}$**				**Others**
pD	**H-*en***	**H6**	**H5**	**H2**	**H3**	**HO-His.**
1.6	3.22/3.11	8.56/ 8.58	7.31/7.20	4.21/ 3.89	3.32/ 3.49	8.06
2.5	3.22/ 3.12	8.56/8.59	7.28/7.19	3.98/3.75	3.24/ 3.21	8.07
3.9	3.20/ 3.11	8.23/ 8.50	7.23/ 7.20	3.88/3.69	3.19/ 3.40	8.23
	***en*/[(Imi)$_2$Au(*en*)]Cl$_3$**	**Imi / [(Imi)$_2$Au(*en*)]Cl$_3$**				
	H-*en*	**H1**	**H2**			**HO-Imi.**
5.0	3.22 / 3.11	8.54/ 8.15	7.33/ 7.22			8.30
6.5	3.08/ 2.94	8.48/7.99, 8.04	7.24/ 7.07, 6.98			8.29

His. atom numbering refers to scheme 4.2.

Imi. atom numbering refers to scheme 4.12.

Table 4.9: ^{13}C NMR chemical shifts of the [Au(*en*)Cl_2]$^{+}$ complexes with L-histidine ligand at pD's 1.6 and 2.8.

			His / [(His)Au(*en*)]$^{3+}$						**Others**
	pD	**C-*en***	**C1**	**C2**	**C3**	**C4**	**C5**	**C6**	
***en* / [Au(*en*)Cl$_2$]$^{+}$**		37.30 / 51.77							
His.	1.6	-	171.22	52.84	25.89	127.34	11910	135.24	
[(His)Au(*en*)]$^{3+}$	1.6	51.80	177.02	51.82	28.75	127.30	117.29	137.14	
His.	2.8	-	173.13	54.21	26.49	128.10	118.60	134.83	
[(His)Au(*en*)]$^{3+}$	2.8	51.93	176.91	53.80	29.24	127.41	117.16	138.87	146.7, 151.0

His. atoms numbering refers to Scheme 4.2.

L-Histidine oxidation products such as 2-oxy-histidine and 2-hydroxy-histidine were detected by NMR. The ^{1}H signal at ~8.2 ppm corresponds to 2-hydroxy-histidine. The ^{13}C NMR, where signals at 151 and 146 ppm correspond to 2-oxy-hisidine and 2-hydroxy-histidine, respectively.

L-Histidine oxidation was carried out by hydrogen peroxide and the ^{1}H NMR spectra showed the formation of 2-hydroxy-histidine (δ = 8.2 ppm). The H5 and H6 signals were shifted downfield after oxidation due to the deshielding effect of oxygen. However, histidine reaction with gold complex shows upfield shift of H5 and downfield shift of H6, indication of ligation to metal through N3. Time dependent monitoring of signal at 8.2 ppm, correspond to 2-hydroxy-histidine, shows that redox reaction became more significant within ~ 4 hours (Figure 4.2C).

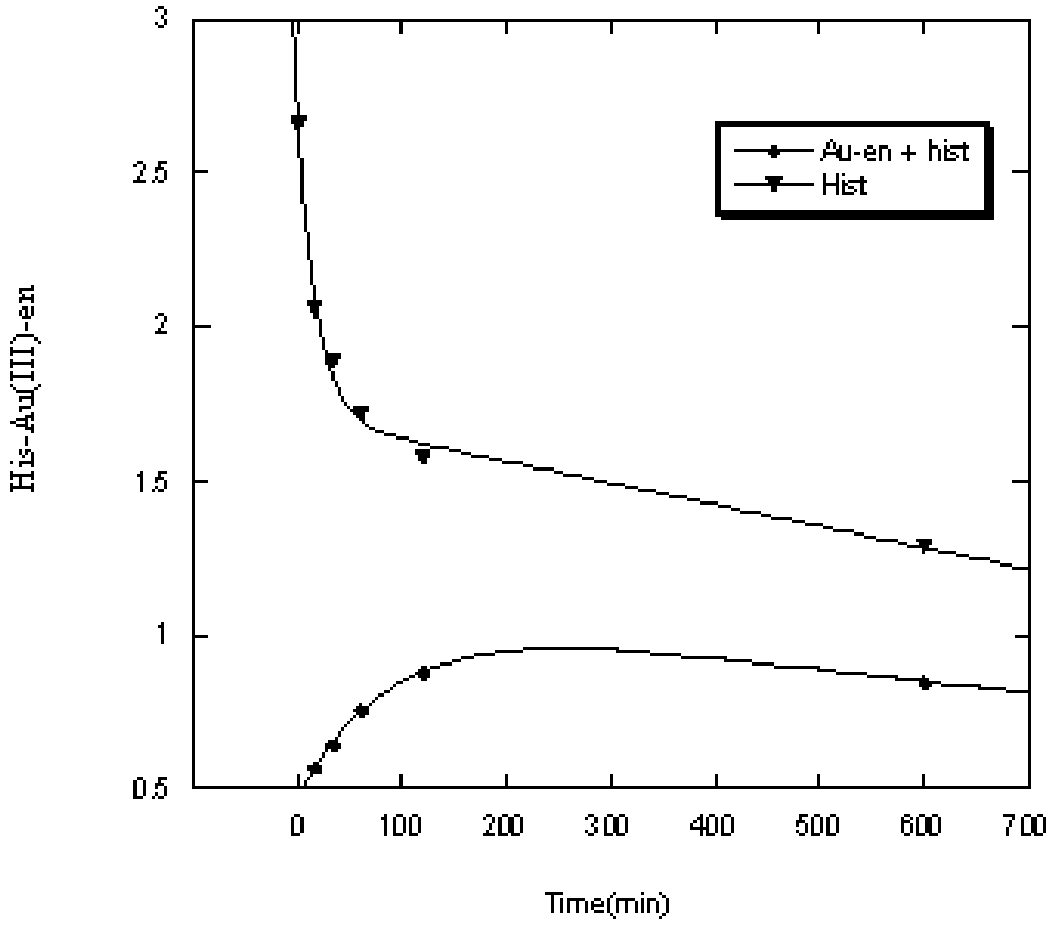

Figure 4.3: ^{1}H NMR monitoring of L-histidine-H5 signal intensity vs. time.▼() refers to free L-histidine and (●) refers to [(His)Au(*en*)]$^{3+}$ complex at 25 ^{o}C and pD = 1.6.

Figure 4.3 shows time dependant integration of signals corresponding to free L-histidine molecules and that bound to Au(III) metal ion in solution. Free and reacted L-histidine signals show decay in solution after ~ 200 min. This decay could be the result of L-histidine oxidation, which is consistent with the appearance of 2-hydroxy-histidine signal at 8.2 ppm (Figure 4.2).

Signal corresponding to *en* in the complex $[(His)Au(en)]^{3+}$ couldn't be followed by ^{1}H NMR because of overlapped resonances (region from 3.1 to 3.3 ppm). Sharp decay of ^{1}H NMR signal (ii) corresponds to *en* ligand bound to Au(III) (Figure 4.2) was observed along with increase of the *en* in solution (signal iv, Figure 4.2B-D).

Figure 4.4 shows released *en* ligand concentration vs. time, which was found to be linear through out the reaction time. Ligand (*en*) release could be an indication of the gold(III) reduction or *en* ligand exchange by L-histidine in solution. However gold(III) reduction seems to be more plausable, which is consistent with metallic gold deposition.

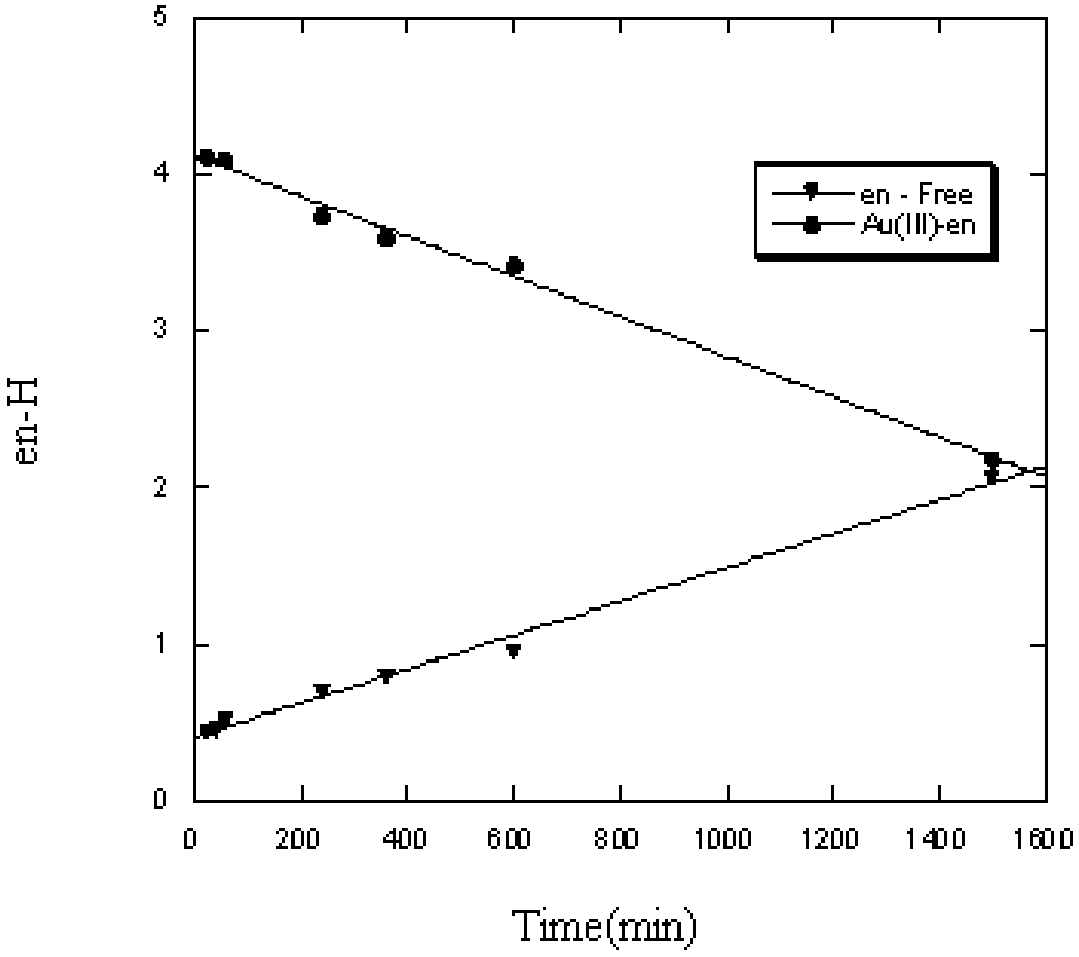

Figure 4.4: Intensity (a.u.) of the *en*-H ^{1}H NMR signal for L-histidine reaction with $[Au(en)Cl_2]^+$ complex vs. time. (●) Refers to *en*-H in $[Au(en)Cl_2]^+$ and (▼) refers to *en*-H as free ligand at 25 ^{o}C and pD = 1.6.

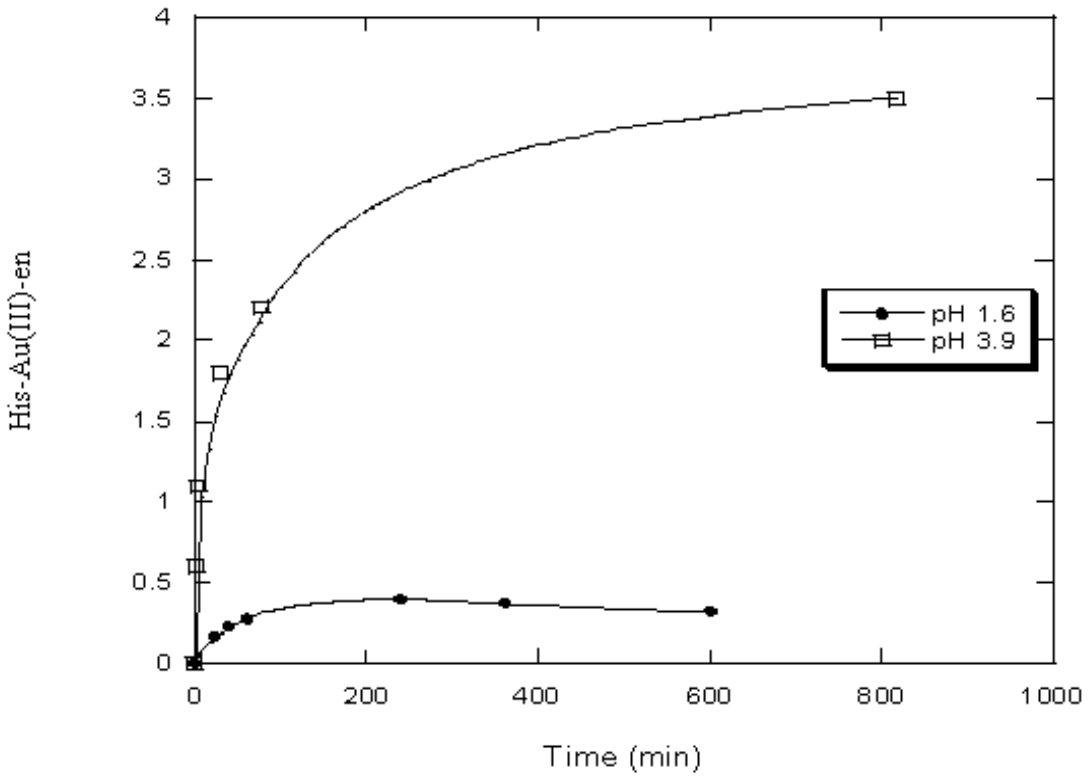

Figure 4.5: Intensity (a.u.) of the L-histidine-H3 ^{1}H NMR signal in $[(His)Au(en)]^{3+}$ vs. time for L-histidine reaction with $[Au(\textit{en})Cl_2]^{+}$ at pD 1.6 (●) and 3.9 (□).

L-Histidine has three pK_a's 1.82 (carboxylic acid), 6.04 (pyrrole NH) and 9.17 (ammonium NH) [77] hence ^{1}H NMR experiments were run at pD's ranges from 1.6 to 10.4. H3 signal (atom numbering refers to Scheme 4.2) was monitored and presented in Figure 4.5, which corresponds to $[(His)Au(\textit{en})]^{3+}$ formation in solution vs. time at pDs 1.6 and 3.9. It was found that L-histidine reaction rate with $[Au(\textit{en})Cl_2]^+$ complex was directly proportional to solution pD. At pD's 6.0 and 10.4 reactions were very fast and direct change of colour were observed immediately after mixing. ^{1}H NMR showed a remarkable increase of the signal corresponding to 2-HO-histidine, so we could conclude that immediate redox reaction takes place at high pDs. 2-HO-histidine signal change was monitored by ^{1}H NMR. A higher rate at pD 10.4 was found compared to pD's 6.5 and 3.9. The higher OH^- ion concentration in solution likely that promotes histidine oxidation.

L-Histidine has four expected binding sites; carboxylate-O, amine-N and two imidazole-Ns. Appleton *et al* [78] have studied the interaction of histidine with platinum(II) and palladium(II) complexes with diethylenetriamine (*dien*) ligand, which acts as a tri-dentate ligand leaving one available binding site. They have reported that carboxylate binding is thermodynamically unstable while amine-N binding is also not very stable, but it could presumably form pseudo-chelate binding with imidazole (Scheme 4.4). However, deprotonated imidazole-N binding was reported as thermodynamically preferred at pH 7.0.

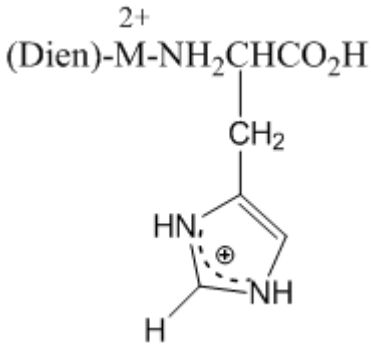

Scheme 4.4: $[(Dien)M(His)]^{2+}$, where M = Pt or Pd.

Zhu *et al* [5] have studied the interaction of ethylendiamine-gold(III) complex with guanosine 5'-monophosphate (5'-GMP). They concluded that 5'-GMP is bound to $[Au(en)Cl_2]^+$ by chelating through N(7) – O(6) or through N(7) – phosphate (Scheme 4.5) and that Au(III) undergoes hydrolysis reaction at pD > 2.5-3.0, and this report confirms the binding through oxygen at gold(III) complexes.

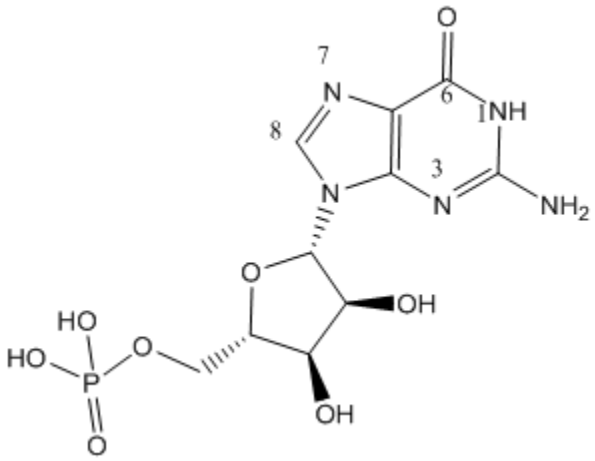

Scheme 4.5: 5'-Guanosine Mono Phosphate.

Table 4.9 shows ^{13}C NMR chemical shifts of free and Au(III) bound L-histidinein the presence of $[Au(en)Cl_2]^+$ complex in solutions at pD's 1.6 and 2.8. Higher change of chemical shift are observed at pD 2.8, this could be due to deprotonation of L-histidine carboxylic group so more electrons will be available for binding through carboxyl group. The signal corresponding to C1 in L-histidine shows the highest change in chemical shift (~ 5 ppm) at both pD's, because it has the lowest pK_a value. At pD 1.6, evidence of carboxylate-O binding of L-histidine C1 comes from the down-field shift of C1 signal (atoms numbering refers to scheme 4.2), while up-field shift of C5 signal and downfield shift of C6 signal minor up-field shift of C4 signal are indication of binding through imidazole ring. As pD is raised to 2.8, L-histidine structure will be in equilibrium (Scheme 4.6).

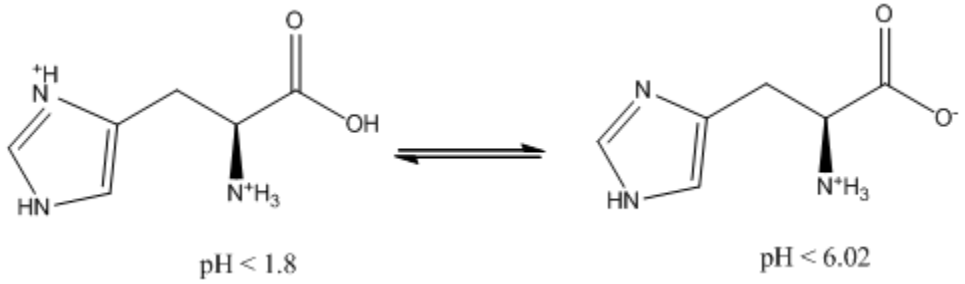

Scheme 4.6: L-Histidine pH dependant structure.

Similar shifts were observed at pD = 2.8 by ^{13}C NMR for $[(His)Au(en)]Cl_3$ complex as mentioned before at pD = 1.6 (Table 4.9) but with less shift for C1 signal indicating that legation through carboxylate group decreases, which could behave as counter ion rather than coordinationally binding ligand. C1 signal decreases within a periods of 4 days indicating histidine distribution into several

distinct species in solution and signals at 151 ppm and 146 ppm corresponding to 2-oxy and 2-hydroxy-histidine appear, respectively.

Our results have shown that gold(III) metal could be encapsulated by L-histidine by legation of imidazole-N and amine-N as well as carboxylate group that exchange the chloride counter ion in the presence of chelating en ligand. This mode of binding may illustrate the gold(III) histidine affinity (Scheme 4.7A), which has been reported by Iori *et al* [79] who have studied L-histidine-gold(III) interaction computationally, and concluded that imidazole side chain of histidine amino acid binds to Au(III) covalently through deprotonated imidazole, which they have reported as responsible for protein gold affinity.

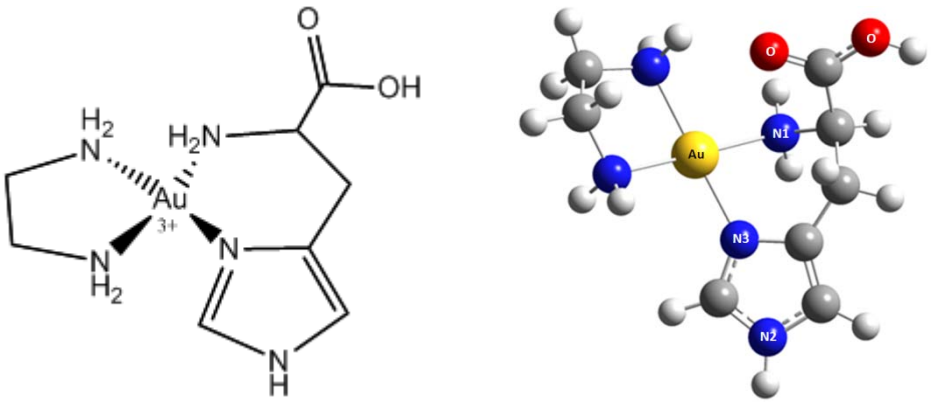

(A) **(B)**

Scheme 4.7: (A) Suggested $[(His)Au(en)]^{3+}$ structure and **(B)** $[(His)Au(en)]^{3+}$ structure optimized computationally at the B3LYP/SDD level of theory using GAUSSIAN03 W, Revision B.04.

Table 4.10: Selected bond lengths (Å) and bond angles (^{o}) for [(His)Au(*en*)]$^{3+}$ for optimized structure using B3LYP/SDD.

	Bond distances (Å)
Au-O	2.883
Au-N1	2.125
Au-N3	2.057
Au-N(*en*)$_{\text{trans-N3}}$	2.116
Au-N(*en*)$_{\text{trans-N1}}$	2.110
	Bond angles (^{o})
O-Au-N1	61.52
O-Au-N3	112.56
O-Au-N(*en*)$_{\text{trans-N3}}$	66.43
O-Au-N(*en*) $_{\text{trans-N1}}$	116.04

Prefered L-histidine ligation site was reported to be through N2 or N3 of the imidazole ring [78] (for atoms numbering refer to Scheme 4.2), at pD > 6.0, while carboxylate-O and amine-N binding were reported at low pH [78]. However, we are suggesting the binding to be initially through N3 (Scheme 4.7A) at low pD as evidenced by ^{1}H and ^{13}C NMR spectra, where de-shielding of C6 and shielding of C5 were observed for imidazole ring. This is followed by amine-N1 binding in a chelating mode, while the carboxylate group acts as a third binding site in a distorted square pyramid structure. The same structure was also obtained after computational optimization of the L-histidine interaction with [Au(*en*)Cl_2]Cl (Scheme 4.7B) in which carboxyl group rearrange itself at the top of the square planar structure in a distorted square pyramidal shape. This chelating mode, in addition to carboxylate presence as counter ion, stabilizes this structure as well as enhances the oxidation of imidazole ring and decarboxylation reaction of L-histidine by gold(III) complex to produce histamine. Positive charge at the imidazole ring can stimulate the imidazole oxidation by enhancing nucleophilic attack at C6 carbon. This illustrates oxidation preference at C6 and also the increased rate of gold reduction by L-histidine at elevated solution pHs. Decay of C1 signal may be a result of histidine decarboxylation reaction by [Au(*en*)Cl_2]$^{+}$ complex, which produces CO_2 and histamine (Scheme 4.8), this suggestion is supported by previous reports about metal catalyzed decarboxylation of amino acids, particularly histidine [80,81].

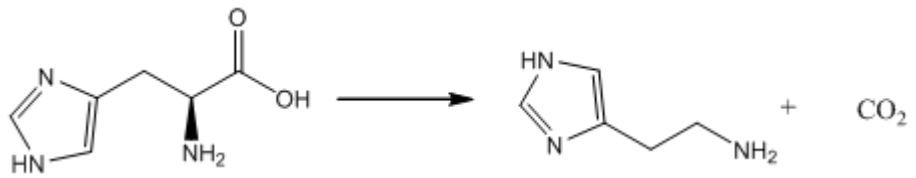

Scheme 4.8: L-Histidine decarboxylation.

To study the effect of the length of the chelating ligand, alkyldiamines of different length such as *en*, *pn* and *bn* (Scheme 4.9) have been used.

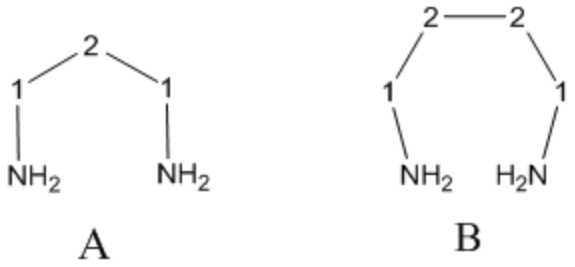

Scheme 4.9: *pn* and *bn* atoms numbering.

Table 4.11 shows the change of chemical shift of Au(III)-*pn* and *bn* complexes (Scheme 4.10) upon reaction with L-histidine. Comparable change of L-histidine chemical shift were observed upon reaction with both Au(III)-*pn* and Au(III)-*bn* complexes.

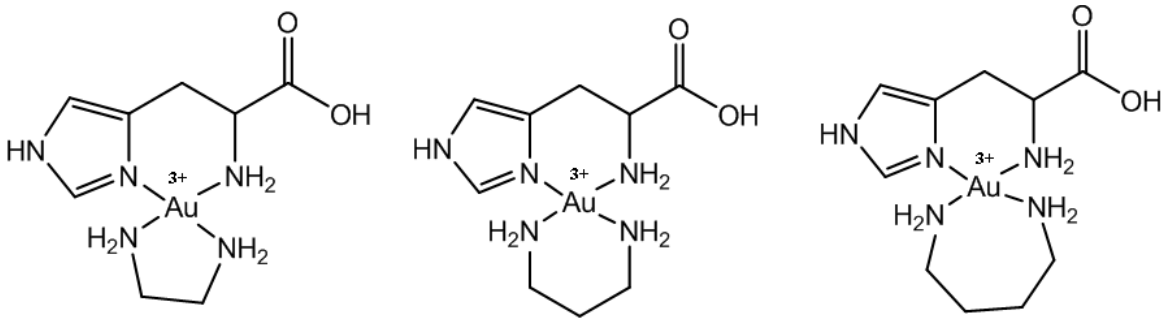

Scheme 4.10: $[(His)Au(alkyldiamine)]^{3+}$.

Table 4.11: ^{1}H NMR chemical shifts of the complexes and ligands of Au(III)-*pn* and Au(III)-*bn* complexes with L-histidine at pD ≈ 3.0.

	H1[a]-*pn*	**H2[a]-*pn***	**H6[c]**	**H5**	**H2**	**H3**	**HO-His**
Pn	3.106	2.051					
$[Au(pn)Cl_2]^+$	2.912	2.098					
His / $[(His)Au(pn)]^{3+}$	3.281	3.249	8.688/ 8.722	7.420/ 7.323	4.190/ 4.495	3.387/ 3.914	8.116
	H1[b]-*bn*	**H2[b]-*bn***					
bn	3.044	1.754					
$[Au(bn)Cl_2]^+$	3.097	1.854					
His / $[(His)Au(bn)]^{3+}$	3.303	3.270	8.695/ 8.727	7.431/ 7.332	4.247/ 4.497	3.418/ 3.974	8.226

a. *pn* atoms numbering refers to scheme 4.9A.

b. *bn* atoms numbering refers to scheme 4.9B.

c. His. atoms numbering refers to scheme 4.2.

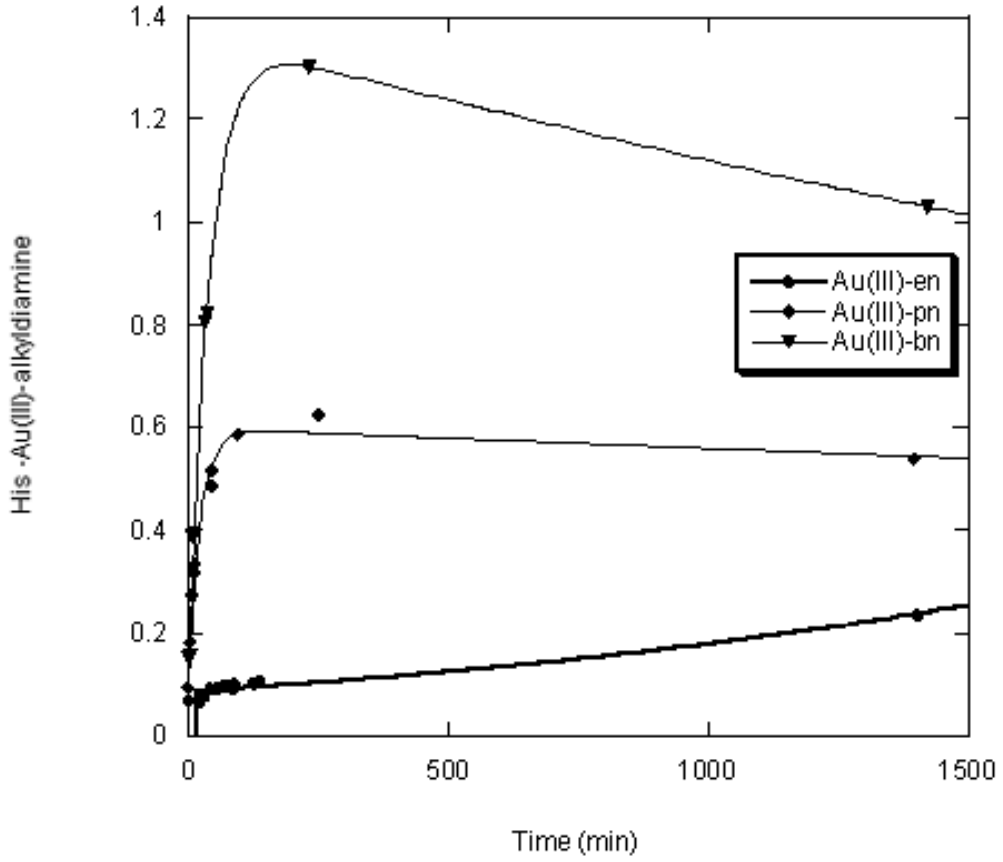

Figure 4.6: Intensity (a.u.) of L-histidine-H5 ^{1}H NMR signal in $[(His)Au(alkyldiamine)]^{3+}$ vs. time for L-histidine reaction with $[Au(\textit{en})Cl_2]^{+}$, $[Au(\textit{pn})Cl_2]^{+}$ and $[Au(\textit{bn})Cl_2]^{+}$ at 25 ^{o}C and pD ≈ 3.0.

Time dependant spectra of binding of Au(III)-*en*, Au(III)-*pn* and Au(III)-*bn* with L-histidine were studied. Monitoring of reacted L-histidine-H5, figure 4.6 shows faster reaction for larger metallacycle ring size. No significant electronic difference is expected for *en*, *pn* and *bn* ligands, but ligands can be arranged according to ligand chain length as *bn* > *pn* > *en*, so faster reaction were with longer chain ligands. This conclusion is supported by Combariza *et al* [82]. They reported that in solution, when chelating ring size increase from five to seven a substantial increase of stability in gas phase is observed. However in solution a poorer metal-ligand overlap takes place as ligand size increases.

Gold(III) complexes with several imidazole derivatives were prepared and found to have a square planar structure [83]. Reaction of [Au(*en*)Cl_2]Cl with imidazole was carried out at three different pD's, 1.5, 5.0 and 6.5. ^{1}H NMR chemical shifts are shown in table 4.8. No reaction was observed at pD 1.5, the reactivity increases at pD 5.0, while even faster reaction was observed at pD 6.5. at pD = 6.5 > imidazole pK_a (6.00), so the pyrrole nitrogen is more deprotonated, so mere electron density is available for donation so it binds stronger (Scheme 4.11).

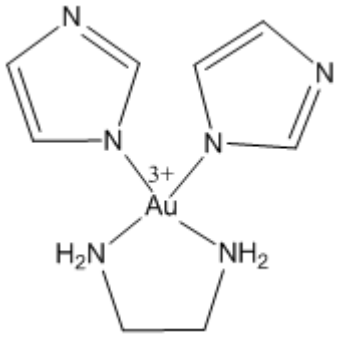

Scheme 4.11: $[(Imi)_2Au(en)]^{3+}$.

Time dependent UV-Vis absorption intensity (at 305 nm) of $[Au(en)Cl_2]^+$ complex reaction with L-histidine at pH = 2.9 was measured (Figure 4.7). L-Histidine showed a slope of 1.11 at constant Au(III)-complex concentration (Table 4.12) while Au(III)-complex showed a slope of 1.14 at constant L-histidine concentration (Table 4.13).

Data are shown in tables 4.12 and 4.13 along with calculated k′ at pH = 2.9 and both components show first order rate equation. Hence the rate expression for the reaction is

$$\textbf{Rate}=k[\text{Au-complex}]\,[\text{His}][H^+]^x$$

At constant pH, the rate equation becomes

$$\textbf{Rate}=k'[\text{Au-complex}]\,[\text{His}]$$

Where $\mathbf{k' = k\,[H^+]^x}$

Similar systems were not found in literature in which rate constant was measured, however, k_{obs} was reported to be 110 $M^{-1}.s^{-1}$ for $HAuCl_4$ reaction with histidine by Soni *et al* [84] that is three times faster than $[Au(en)Cl_2]^+$ reaction with histidine. The difference in k_{obs} could be a result of trans effect caused by *en* ligand, but the difference in trans directing of *en* and chloride is not crucial [85], however, the reason could be the availability of more exchangeable chloride ligands in $HAuCl_4$ than in $[Au(en)Cl_2]^+$ complex where one side is blocked by *en* ligand.

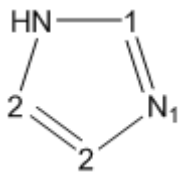

Scheme 4.12: Imidazole atoms numbering

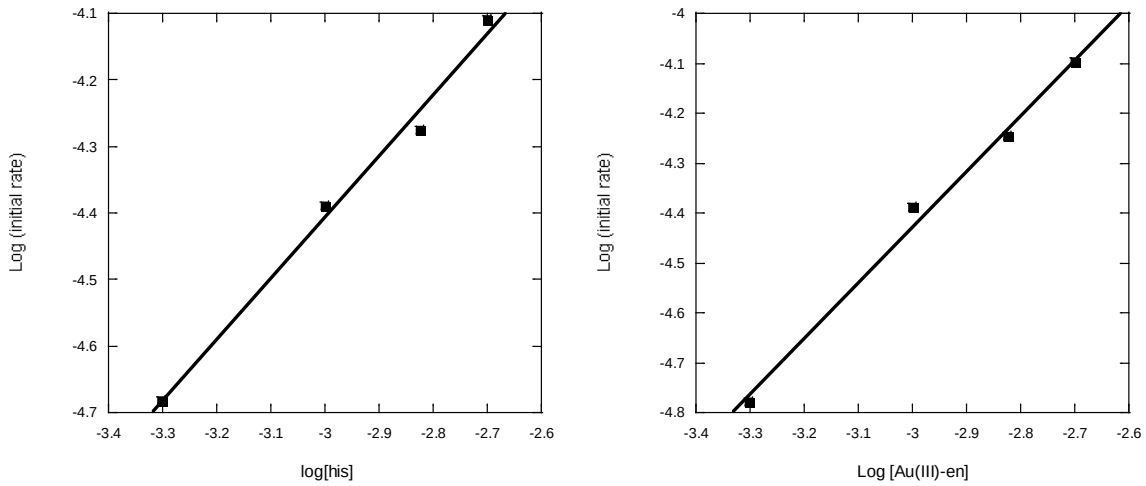

(A) (B)

Figure 4.7: (A) log (initial rate) vs. log [His] in solution ranging from 0.5 to 2.0 mM at constant $[Au(en)Cl_2]^+$ concentration (1.0 mM). (B) log (initial rate) vs. log ($[Au(en)Cl_2]^+$) ranging from 0.5 to 2.0 mM in solution at constant L-histidine concentration (0.5 mM). All solutions were prepared using 0.01M phosphate buffer at pH = 2.9.

Table 4.12: kinetic data for the absorption change of $[Au(en)Cl_2]^+$ complex at different L-histidine concentrations and constant $[Au(en)Cl_2]^+$ concentration of 1.0 mM at 25 ^oC and pH = 2.9.

[His] mM	Initial rate (v)	log [His]	log (v)	k'(L•mol^{-1}•s^{-1})
0.50	2.08 x 10^{-5}	-3.30	-4.68	41.6
1.00	4.09 x 10^{-5}	-3.00	-4.39	40.9
1.50	5.30 x 10^{-5}	-2.82	-4.28	35.3
2.00	7.78 x 10^{-5}	-2.70	-4.11	38.9

Table 4.13: kinetic data for the UV absorption change of $[Au(en)Cl_2]^+$ complex at different $[Au(en)Cl_2]^+$ concentrations and constant L-histidine concentration of 1.0 mM at 25 ^oC and pH = 2.9.

$[Au(en)Cl_2]^+$ (mM)	Initial rate (v)	log ($[Au(en)Cl_2]^+$)	log (v)	k'(L•mol^{-1}•s^{-1})
0.50	1.67 x 10^{-5}	-3.30	-4.78	33.3
1.00	4.09 x 10^{-5}	-3.00	-4.39	40.9
1.50	5.67 x 10^{-5}	-2.82	-4.25	37.8
2.00	8.00 x 10^{-5}	-2.70	-4.10	40.0

4.3. [Au(*en*)Cl_2]Cl interaction with L-methionine and DL-Seleno-methionone.

4.3.1 [Au(*en*)Cl_2]Cl interaction with L-methionine (Met).

Met is an essential α-aminoacid classified as nonpolar, and together with L-cysteine, constitute the two sulfur-containing proteinogenic amino acids [86]. It is also one of the most important bio-ligands that affect the efficacy of antitumor complexes [57]. Interaction of Met with *cis*-platin (*cis*-[$(NH_3)_2PtCl_2$]) was studied by El-Khateeb *et al* [26]. They reported that Met binds to *cis*-platin first by hydrolysis, then the chloride ligand is exchanged by H_2O, which is later exchanged by Met-S ligation, then it rearranges to N, S chelate complex. Thioethers, as in thiols, are oxidized into sulphoxide forms by gold complexes. This was found to be the source of their toxicity [57].

We are here reporting the interaction of Met with Au(III) with one side blocked by the chelating *en* ligand.

Table 4.14 shows ^{1}H NMR chemical shifts data for Met reaction with [Au(*en*)Cl_2]$^+$ and $HAuCl_4$. Significant de-shielding was observed of Met protons upon reaction, H4 and H5 resonances show the largest down-field change in chemical shift indicating bonding through sulfur. After 18 hours, ~ 86 % of *en* ligand has dissociated from [Au(*en*)Cl_2]$^+$.

Table 4.14: ^{1}H NMR chemical shifts for Met interaction with $[Au(en)Cl_2]^+$ in D_2O at 25 ^{o}C, pD = 3.8.

	en	**H5**	**H4**	**H3**	**H2**
Met		1.987	2.486	1.960	3.724
Met + $[Au(en)Cl_2]^+$	3.115	2.375	2.706, 2.602	2.196	3.829
Met + $HAuCl_4$	-	2.552	2.225	2.932, 2.875	4.080

Table 4.15: ^{13}C NMR chemical shifts of Met reaction with $[Au(en)Cl_2]^+$ in D_2O at 25 ^{o}C, pD = 3.8.

	en	**C1**	**C2**	**C3**	**C4**	**C5**
Met	-	174.97	54.64	30.44	29.62	14.73
$[(Met)Au(en)]^{3+}$	51.65	173.69	53.65	32.52	49.95	24.40

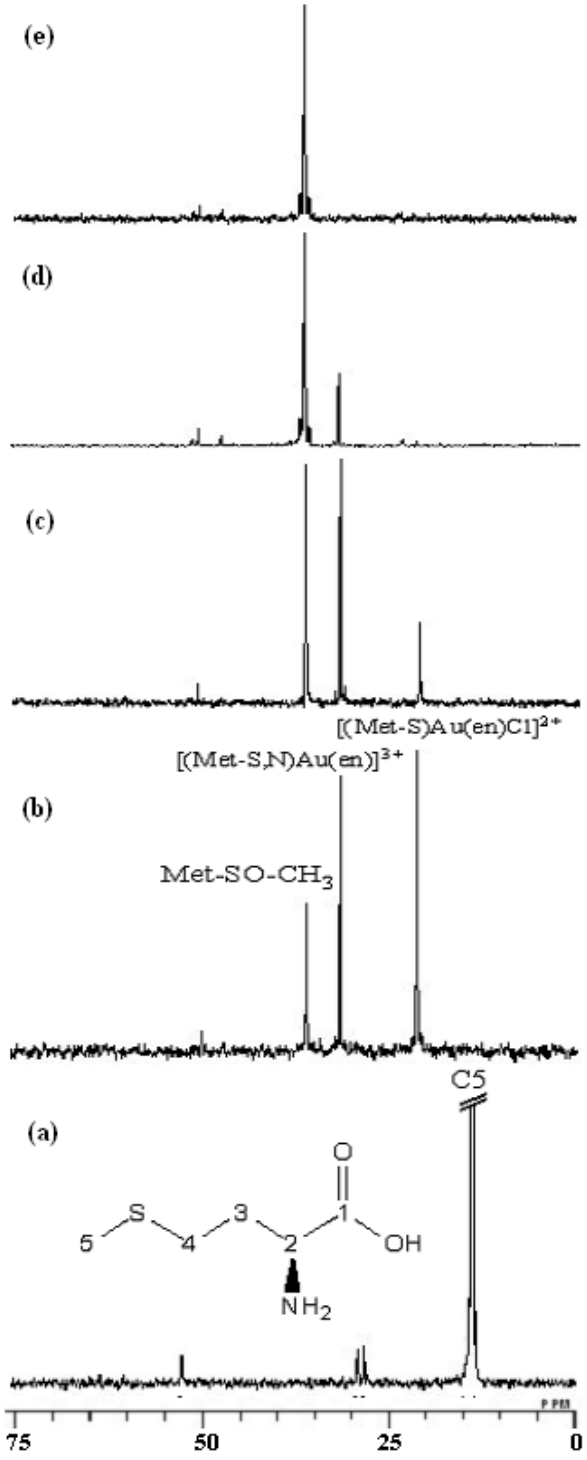

Figure 4.8: ^{13}C NMR spectra of (a) free Met-$^{13}C5$ while spectra (b) to (e) are for Met-$^{13}C5$ after reaction with $[Au(en)Cl_2]^+$, (b) after 17 min, (c) after 34 min, (d) after 44 min, and (e) after 7 hours, in D_2O at 25 ^oC, pD = 3.8.

Figure 4.8 shows ^{13}C NMR spectra for Met-$^{13}C5$ reaction with $[Au(en)Cl_2]^+$, signal at 14 ppm, which is due to $^{13}C5$ disappeared and three signals appeared in the spectrum, 17 min after mixing (Figure 4.8b), corresponding to three different forms of Met in solution. The signals at 23, 33 and 37 ppm are assigned to Au(III)-Met, $[(Met\text{-}S,N)Au(en)]Cl_3$ and Met-SO-CH_3, respectively.

Several experiments were carried out by reacting Met with H_2O_2 and $HAuCl_4$. These experiments are intended to confirm our assignments.

The signal at 23 ppm corresponding to $[(Met\text{-}S)Au(en)]^{3+}$, was decreasing until it completely disappeared after 1 hour. The signal at 33 ppm also decreased and the signal at 37 ppm became dominant after 7 hours. This indicates a complete oxidation of Met to Met-SO-CH_3 along with Au(III) reduction into Au(I). The chemical shift assignments are shown in Table 4.15.

Table 4.15 shows the release *en* ligand from $[Au(en)Cl_2]^+$ complex after reaction. An experiment, where Met ^{13}C-labeled at C5 is oxidized by H_2O_2, was carried out. It resulted in the disappearance of the signal at 15 ppm and the appearance of two signals corresponding to C5 that represents oxidation products of Met.

^{13}C NMR Met-$^{13}C5$ oxidation by H_2O_2, signal at 37 ppm was formed after reaction that correspond to Met-SO-CH_3, while signal at 23 and 33 ppm were not found indication that these signals correspond to Met-gold complexes.

Figure 4.9 shows ^1H NMR spectra for Met reaction with $HAuCl_4$, the reaction was carried out at pD = 3.8 that higher pH will cause the hydrolysis of $[Au(en)Cl_2]Cl$ complex [5]. Down field shift of H5, H3 and H2 is observed after coordination ion to gold. The multiplet signal corresponds to C3 as shown for Se-Met reaction with $NaAuCl_4$ by Isab [87]. Polymeric $[Au(Met)]_n$ complex precipitated out of solution after few days.

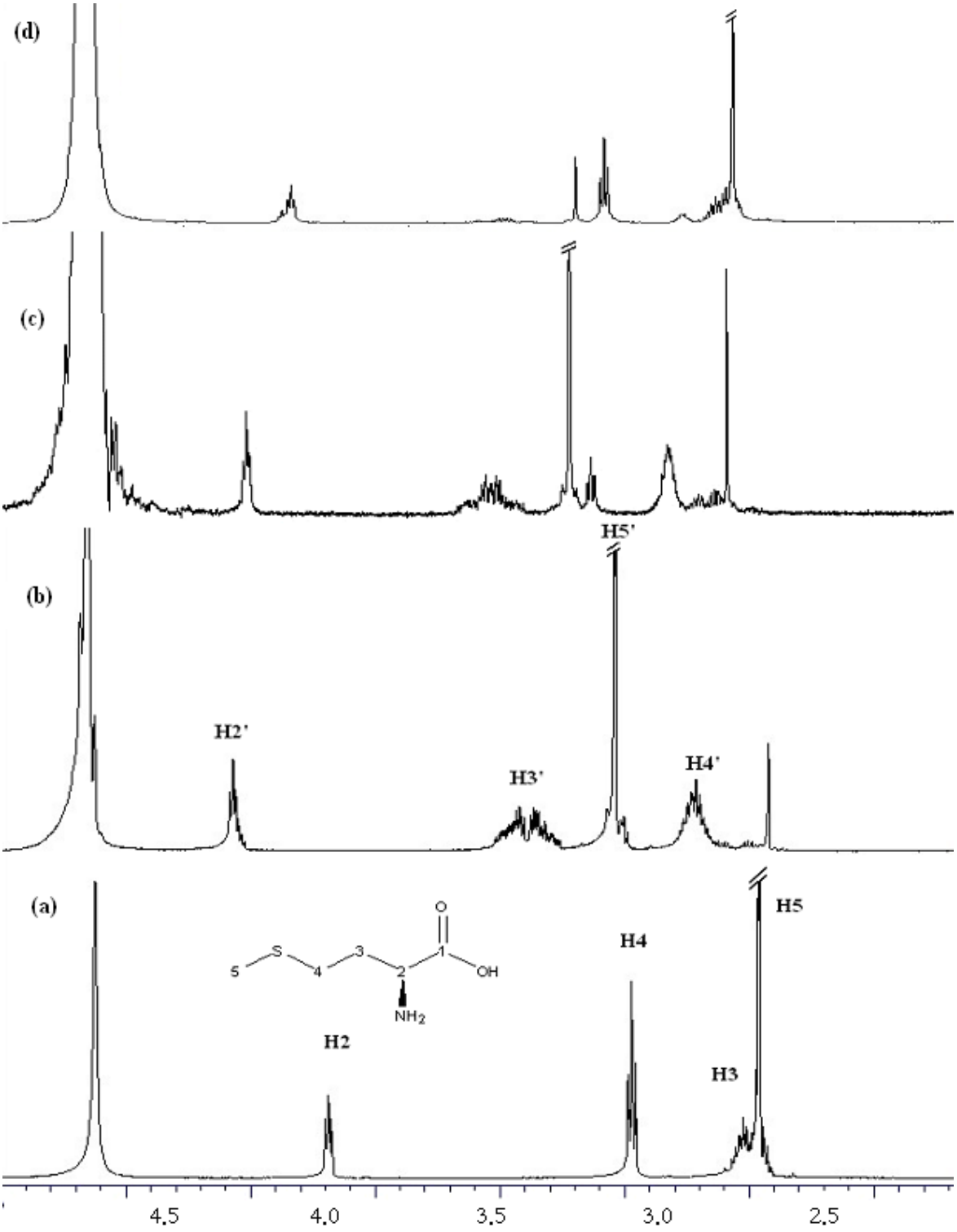

Figure 4.9: ^{1}H NMR spectra of (a) Met, spectra (b) after mixing with $HAuCl_4$ (white ppt formed in solution), (c) after $Na_2S_2O_3$ added to solution (d) after 10 days in D_2O at 25 ^{o}C, pD = 3.8.

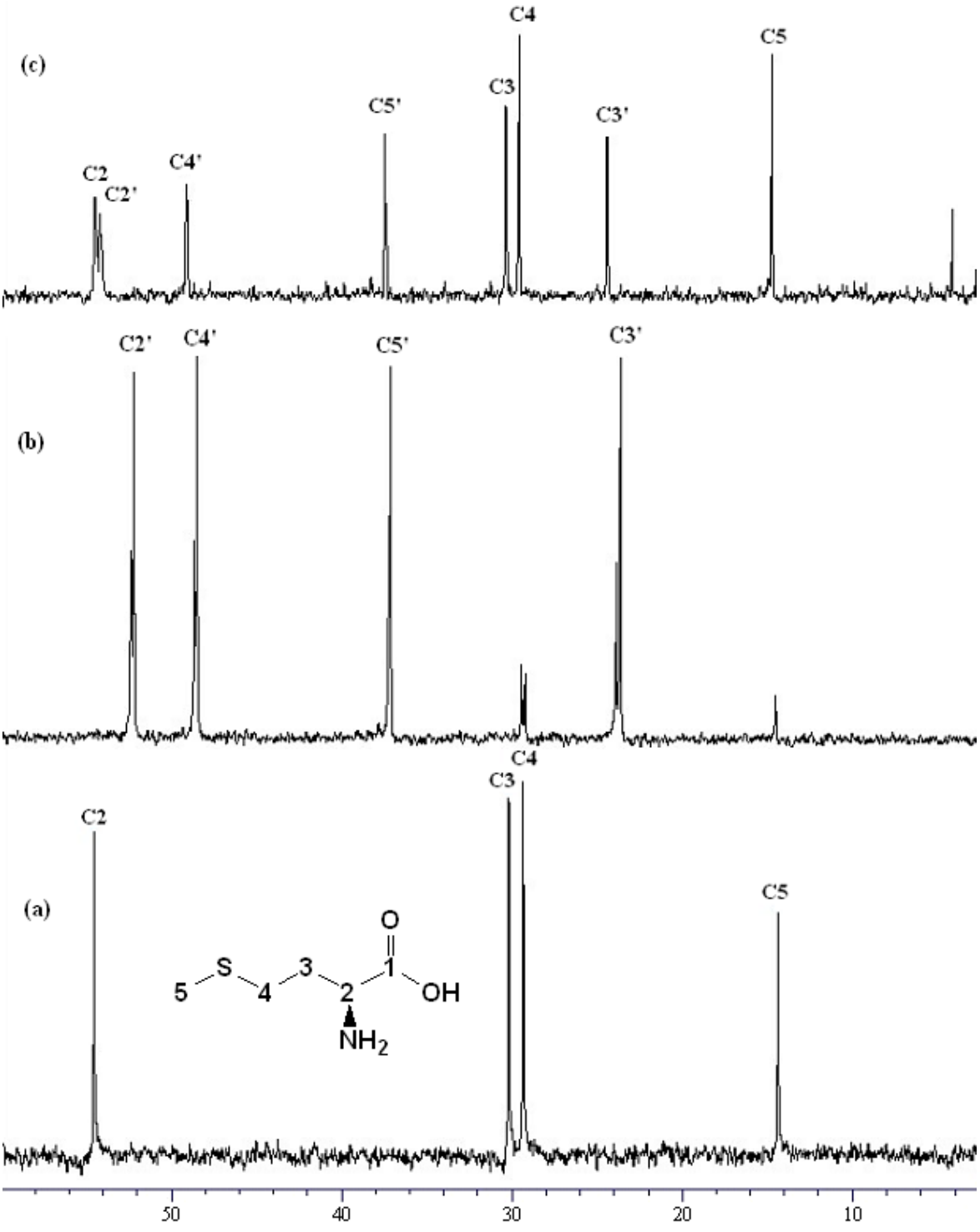

Figure 4.10: ^{13}C NMR spectra of (a) Met, spectra (b) after mixing with $HAuCl_4$ (white ppt formed in solution and clear solution decanted) (c) after $Na_2S_2O_3$ added to solution, in D_2O at 25 ^oC, pD = 3.8.

Figure 4.10 shows ^{13}C NMR spectra for Met that are recorded before and long period of time after reaction with $HAuCl_4$ (2 day). Figure 4.10b shows a signal at 37 ppm attributed to Met-SO-CH_3 indication of Met oxidation by gold(III) that is reduced to gold(I). Polymeric $[Au(Met)Cl]_n$ was precipitated out of solution, and when $Na_2S_2O_3$ was added to the solution, reduction of Met-SO-CH_3 took place. The reactions could be described by equations (1) and (2).

$$HAuCl_{4(aq)} + 2Met_{(aq)} \longrightarrow Met\text{-}SO\text{-}CH_{3(aq)} + [Au(Met)Cl]_{n(ppt)} \quad (1)$$

$$Met\text{-}SO\text{-}CH_3 \xrightarrow{Na_2S_2O_3} Met \quad (2)$$

Vujačić *et al* [88] have studied Met reaction with $HAuCl_4$ that shows that Met binding on Au(III) metal center takes place via exchange of one chloride ligand and then rearrangment into chelating Met-S,N binding. These results are consistent with our finding i.e. the formation of three species of Met that convert finally into Met-SO-CH_3. We propose that $[Au(en)Cl_2]^+$ reacts with Met according to equation (3).

$$[Au(en)Cl_2]^+_{(aq)} + 2Met_{(aq)} \longrightarrow Met\text{-}SO\text{-}CH_{3(aq)} + [Au(Met)Cl]_{n(ppt)} + en \quad (3)$$

From the preceeding discussion we may suggest that the reaction proceeds through the following reaction mechanism (Equations 4 to 7).

$$[Au(en)Cl_2]^+ + Met \longrightarrow [(Met\text{-}S)Au(en)Cl]^{2+} + Cl^- \quad (4)$$

$$[(Met\text{-}S)Au(en)Cl]^{2+} \longrightarrow [(Met\text{-}S,N)Au(en)]^{3+} + Cl^- \quad (5)$$

$$[(Met\text{-}S,N)Au(en)]^{3+} \longrightarrow Met\text{-}SO\text{-}CH_3 + Au^{1+} + en \quad (6)$$

$$Au^+ + Met + Cl^- \longrightarrow [Au(Met)Cl]_n \quad (7)$$

The reaction starts with $[Au(en)Cl_2]^+$ hydrolysis, as expected by comparison with reaction with *cis*-platin complex, as shown by El-Khateeb *et al* [26]. One Cl^- ligand

is exchanged by Met-S ligand that rearranges into chelating mode of Met-S,N (Equation 5). The reduction of Met takes place in the next stage concurrent with *en* ligand dissociation and gold(I) formed in solution (Equation 6). The reaction stops finally by the precipitation of Au(I) with non-oxidized Met as polymeric $[Au(Met)Cl]_n$.

4.3.2 [Au(*en*)Cl_2]Cl interaction with DL-Seleno-methionine (Se-Met).

Selenium compounds have received more attention in the recent decades and found to be an essential element in mammals [89]. It is known that seleno-ligands binds more strongly to gold complexes than thio-ligands [51,90]. DL-Seleno-methionine (Se-Met) interaction with $[Au(en)Cl_2]^+$ was studied in this work and ^{13}C NMR was recorded for the reaction. Reaction of $[Au(en)Cl_2]^+$ with Se-Met was carried out using Se-Met labeled $^{13}C5$. The ^{13}C NMR spectrum was recorded for the resulting solution (Figure 4.11). Fast and complete shift of signal at δ = 4 ppm, corresponding to C5, to 32 and 34 ppm, that are attributed to $[(Se\text{-}Met)Au(en)]^{3+}$ (C5´ signal) and Met-SeO-CH_3 (C5˝ signal), respectively. These signals were assigned by comparison with spectrum resulting from Se-Met-$^{13}C5$ oxidation experiment by H_2O_2. The mechanism suggested for Met is also applicable for Se-Met. Hence the reaction mechanism could be described as chloride ligand exchange by Se-Met followed by Se-Met oxidation while gold(III) is reduced into gold(I) along with *en* ligand dissociation from the reduced gold(III) metal center and the precipitation of white polymeric $[Au(Se\text{-}Met)Cl]_n$.

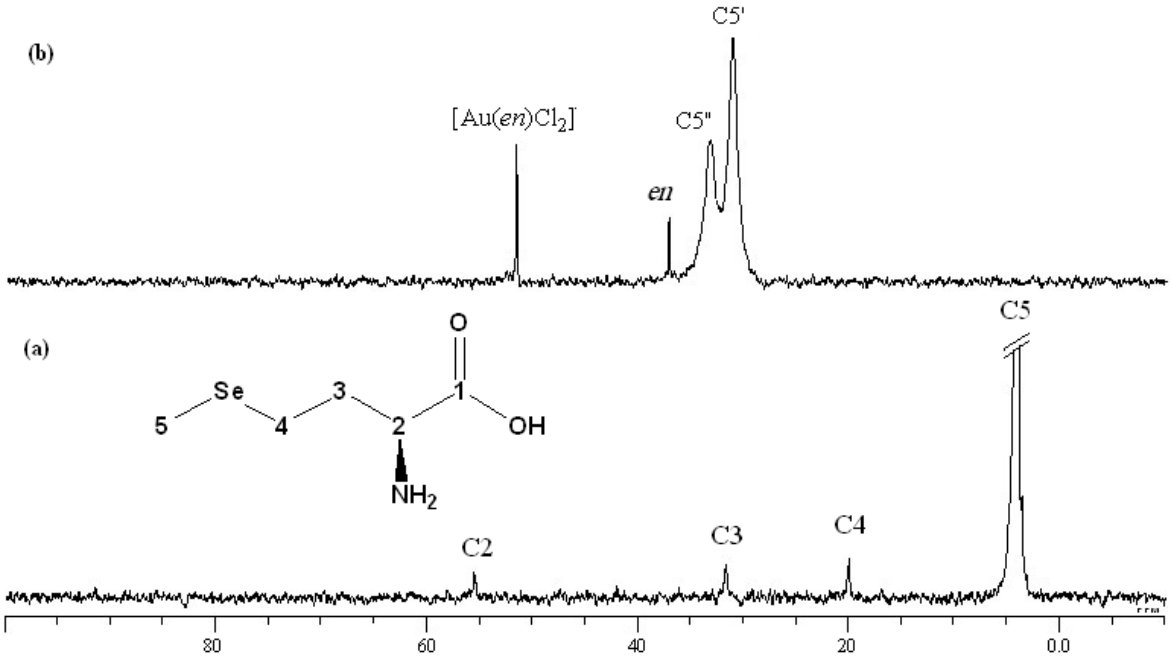

Figure 4.11: ^{13}C NMR spectra for Se-Met-$^{13}C5$ before reaction (a) and after reaction with $[Au(en)Cl_2]^+$ at 1:1 ratio (b), in D_2O at 25 ^oC and pD = 3.7.

4.4 [Au(*en*)Cl_2]Cl interaction with thiols

4.4.1 [Au(*en*)Cl_2]$^+$ interaction with L-cysteine

L-Cysteine is an α-amino acid with the chemical formula $HO_2CCH(NH_2)CH_2SH$, it is classified as a non essential hydrophilic amino acid. Because of the high reactivity of this thiol, L-cysteine is an important structural and functional component of many proteins and enzymes. Cystine is its oxidized dimer (Scheme 4.13) [91].

L-Cysteine has pK_a values 1.92 for -COOH, 10.46 for $–NH_3^+$ and 8.35 for –SH side chain [77] and considered as S- and N- donor nucleophile [92]. Cysteine and penicillamine (Scheme 4.15) generally, form similar complexes with transition metal ions with subtle difference in some redox reactions [93]. Most thiols such as L-cysteine and thiomalic acid reduce gold(III) to gold(I) and form stable complex [93]. Penicillamine was reported to form a stable complex with gold(III) ion if present in excess but will reduce it to gold(I) if present in 1:1 ratio [93].

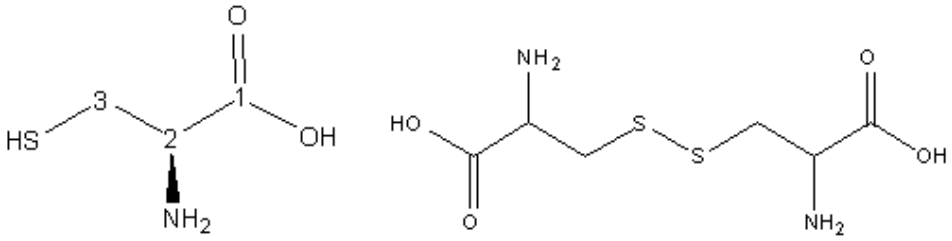

(a) **(b)**

Scheme 4.13: (a) L-Cysteine and (b) L-Cystine.

In the present work, interaction of L-cysteine and penicillamine ligands with $[Au(en)Cl_2]^+$ complex in aqueous solution were studied by ^1H and ^{13}C NMR spectroscopy.

L-Cysteine reaction with $[Au(en)Cl_2]^+$ at 1:1 ratio was carried out and ^1H NMR chemical shifts were recorded and presented in table 4.16. The reaction pD was adjusted to 3.7 before mixing. At acidic pD only the carboxylate group will be ionized, nevertheless ^1H NMR chemicals shifts of L-cysteine show down-field change in chemical shifts of H2 and H3 signals as shown by table 4.16. Reaction monitoring by ^1H NMR shows *en* ligand dissociation from complex, and after 14 hours a complete release of *en* ligand (signal at 3.222 ppm) is observed. However, ^1H NMR is not much informative according to complex oxidation state. When the pD of the reaction mixture was adjusted to 7, immediate dissociation of *en* ligand from the complex was observed by ^1H NMR. This could be a result of hydrolysis of the complex as shown by Zhu *et al* [5].

Table 4.16: ^{1}H NMR chemical shifts of [Au(*en*)Cl_2]$^{+}$ complex with L-cysteine in D_2O at 25 ^{o}C, pD = 3.7.

	Free *en* / *en* in complex	H2	H3
[Au(*en*)Cl_2]$^{+}$	- / 3.093	-	-
CySH	-	4.176	2.966, 2.945
[Au(*en*)Cl_2]$^{+}$ + CySH	3.222 / 3.087	4.252	3.277, 3.134

* Atoms numbering refer to Scheme 4.13(a)

Table 4.17: ^{1}H NMR chemical shifts of [Au(*en*)Cl_2]$^{+}$ complex with D-penicillamine, pD = 3.7 in D_2O at 25 ^{o}C.

	free en / Au(III)-*en*	H2	H4
PaSH		3.610	1.414, 1.334
[Au(*en*)Cl_2]$^{+}$ + PaSH	3.192 / 3.089	3.821	1.712, 1.620

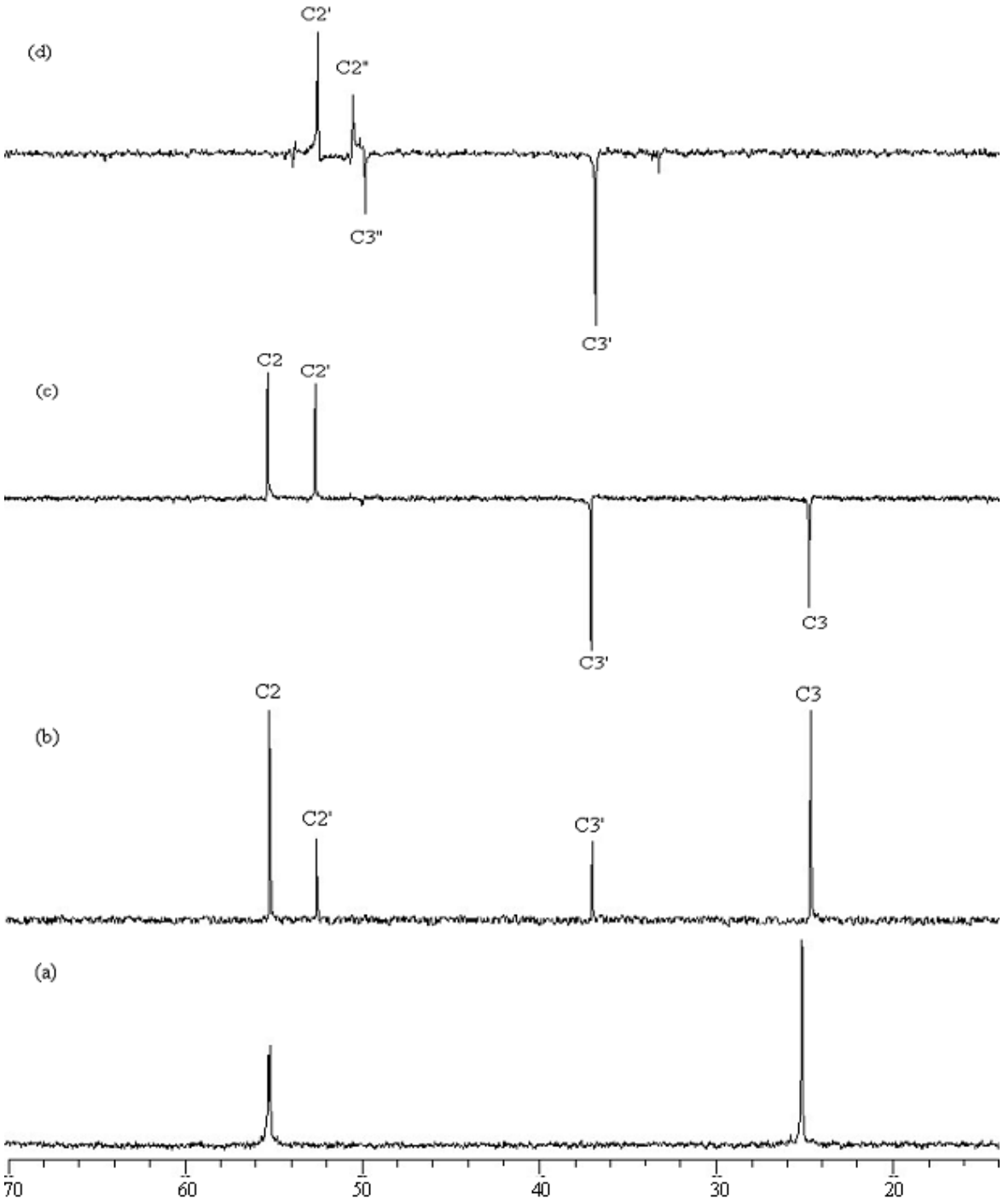

Figure 4.12: (a) ^{13}C NMR spectra for L-cysteine before and (b) after reaction with H_2O_2, while (c) and (d) are ^{13}C-DEPT NMR spectra after reaction with H_2O_2 at 1:1 ratio and when excess H_2O_2 reacted, respectively, in D_2O at 25 ^{o}C.

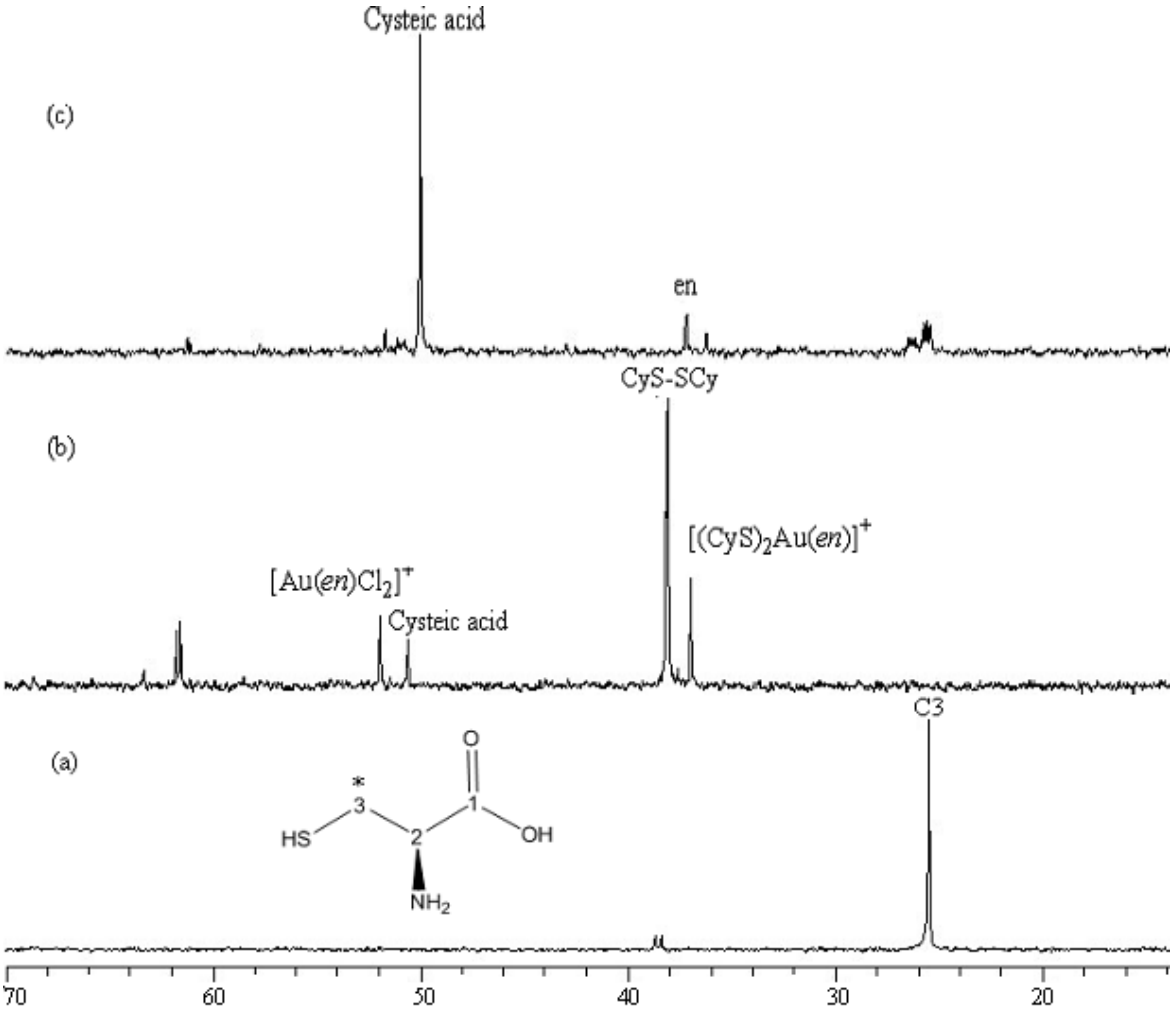

Figure 4.13: ^{13}C NMR for (a) L-$^{13}C3$-cysteine (b) 13 min after reaction with $[Au(en)Cl_2]^+$ and (c) 24 hours after mixing, at 1:1 ratio in D_2O at 25 ^oC, pD = 3.7.

^{13}C NMR spectra for L-cysteine before and after oxidation by H_2O_2 are shown in Figure 4.12, chemical shift assignments were made by ^{13}C-DEPT NMR experiment (Figure 4.12c). Figure 4.12d shows that when excess H_2O_2 is used, it reacted to form cystine, which was further oxidized into cystic acid as shown by Shaw *et al* [57].

Figure 4.13 shows ^{13}C NMR spectra of labeled L-$^{13}C3$-cysteine before and after reaction with $[Au(en)Cl_2]^+$ at 1:1 ratio in D_2O at 3.7. We observe the formation of a signal at 36 ppm corresponding to $[(CyS)Au(en)]^{2+}$, this signal decays very fast and is converted to the signal at 38 ppm that correspond to cystine (Figure 4.13 (b)). The signal at 51.0 ppm also gradually increased. This was assigned to cysteic acid. Ethylenediamine ligand dissociation from the complex is observed, which is a good indication of Au(III) reduction.

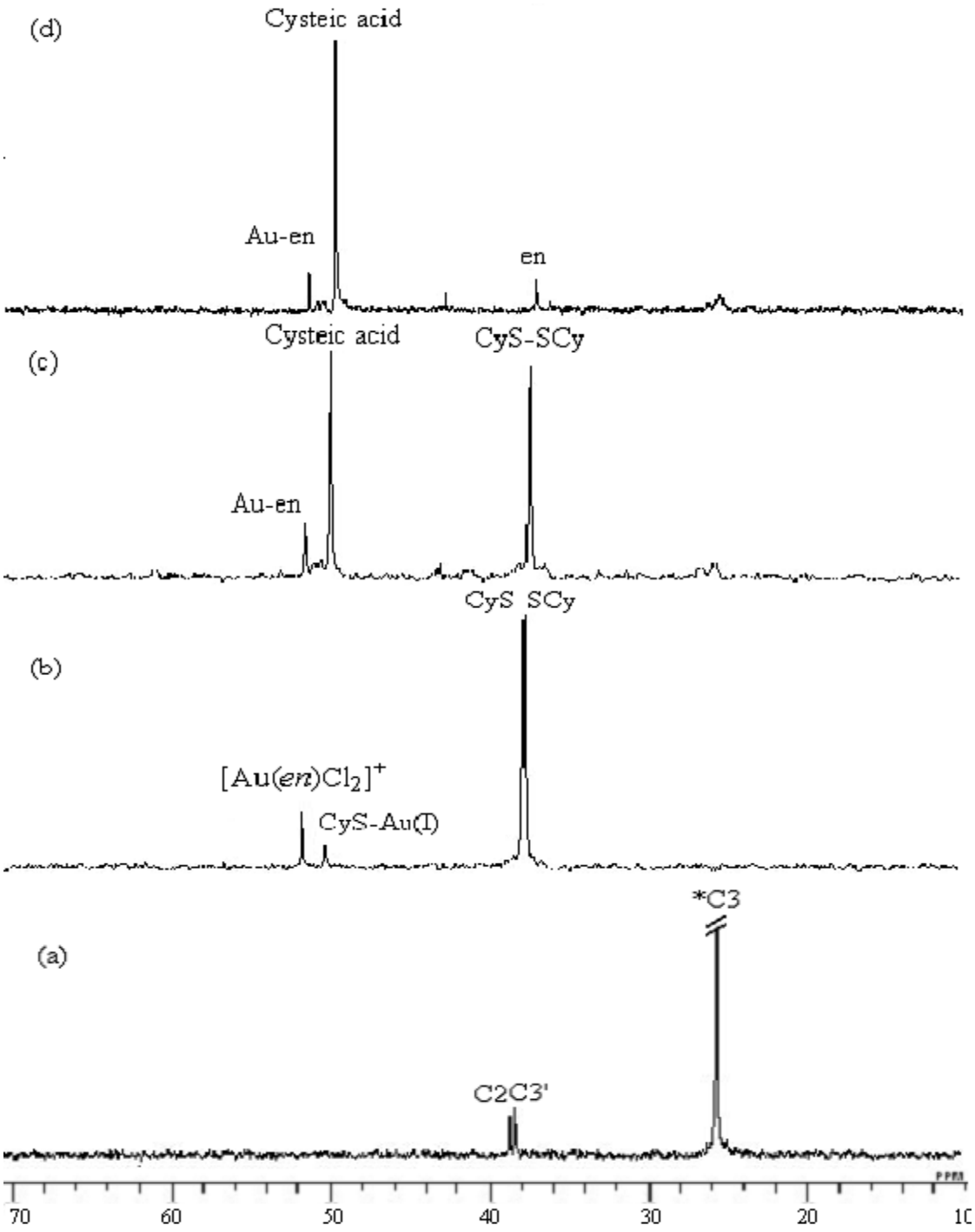

Figure 4.14 ^{13}C NMR spectra of ^{13}C3 labeled L-cysteine reaction with $[Au(en)Cl_2]^+$ (a) L-cysteine, (b) 30 min, (c) ~11 hours and (d) ~ 24 hours, at 2:1 ratio in D_2O at 25 ^{o}C, pD = 3.7. (atom numbering refers to scheme 4.13a)

A reaction was also carried out at 2:1 ratio of L-cysteine : Au(III) (Figure 4.14). We observe in these spectra that L-cystine is formed faster, i.e. complete conversion after 30 min, (Figure 4.14b). The signal corresponding to $[(CyS)Au(en)]^{2+}$ was not found in this spectrum. This could be a result of a fast reaction, in which two Cl^- ligands are exchanged fast by L-cysteine followed by reductive elimination of L-cystine along with Au(III) reduction into Au(I) and *en* ligand dissociation. After standing 24 hours (Figure 4.14 d), L-cystine was completely oxidized into cystic acid (δ = 51.0 ppm) as shown earlier for cystine oxidation by Shaw *et al* [57].

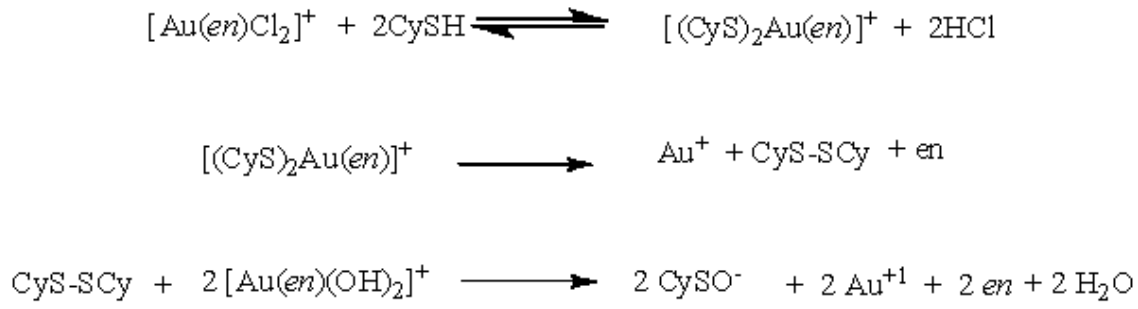

Scheme 4.14: L-Cysteine reaction mechanism with $[Au(en)Cl_2]^+$.

We propate that the reaction of L-cysteine with $[Au(en)Cl_2]^+$ complex goes into three main steps as shown by scheme 4.14. First the exchange reaction of chloride ligand by L-cysteine takes place so C3 signal shifted down-field to 36 ppm. Then L-cysteine oxidation and Au(III) reduction into Au(I) occur so intensity of C3 signal at 36 ppm decreases gradually and L-cystine signal appear at 38 ppm. The later is oxidized to cystic acid (signal at 51 ppm). The signal corresponding to $[Au(en)Cl_2]^+$ did not vanish completely, indicating the catalytic behavior of this complex.

4.4.2 $[Au(en)Cl_2]^+$ interaction with D-penicillamine

D-Penicillamine is a pharmaceutical of the chelator class. It is a metabolite of penicillin, although it has no antibiotic properties [95], D-penicillamine interaction with gold is a very important interaction in rheumatoid disease treatment as shown by Pritchard *et al* [96].

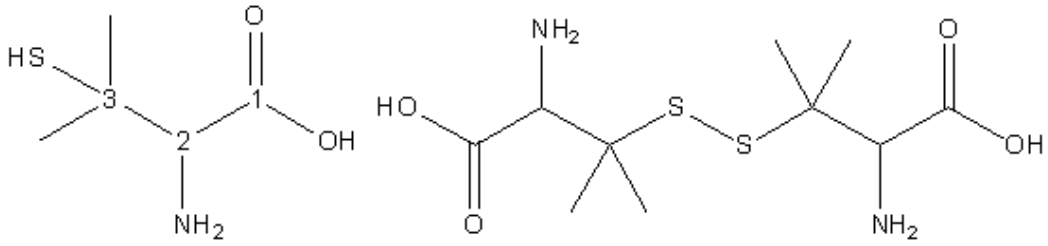

(a) (b)

Scheme 4.15: (a) D-Penicillamine and (b) D-Penicillamine dimer.

Figure 4.15 shows ^1H NMR spectra for D-penicillamine before and after reaction with $[Au(en)Cl_2]^+$, correspond to free *en* ligand, at 3.19 ppm, and in $[Au(en)Cl_2]^+$ complex, at 3.08 ppm, are shown in spectra (b) and (c). Free *en* signal was found to increase at the same rate as decreasing $[Au(en)Cl_2]^+$ signal. Chemical shifts for this reaction are given in table 4.17 .

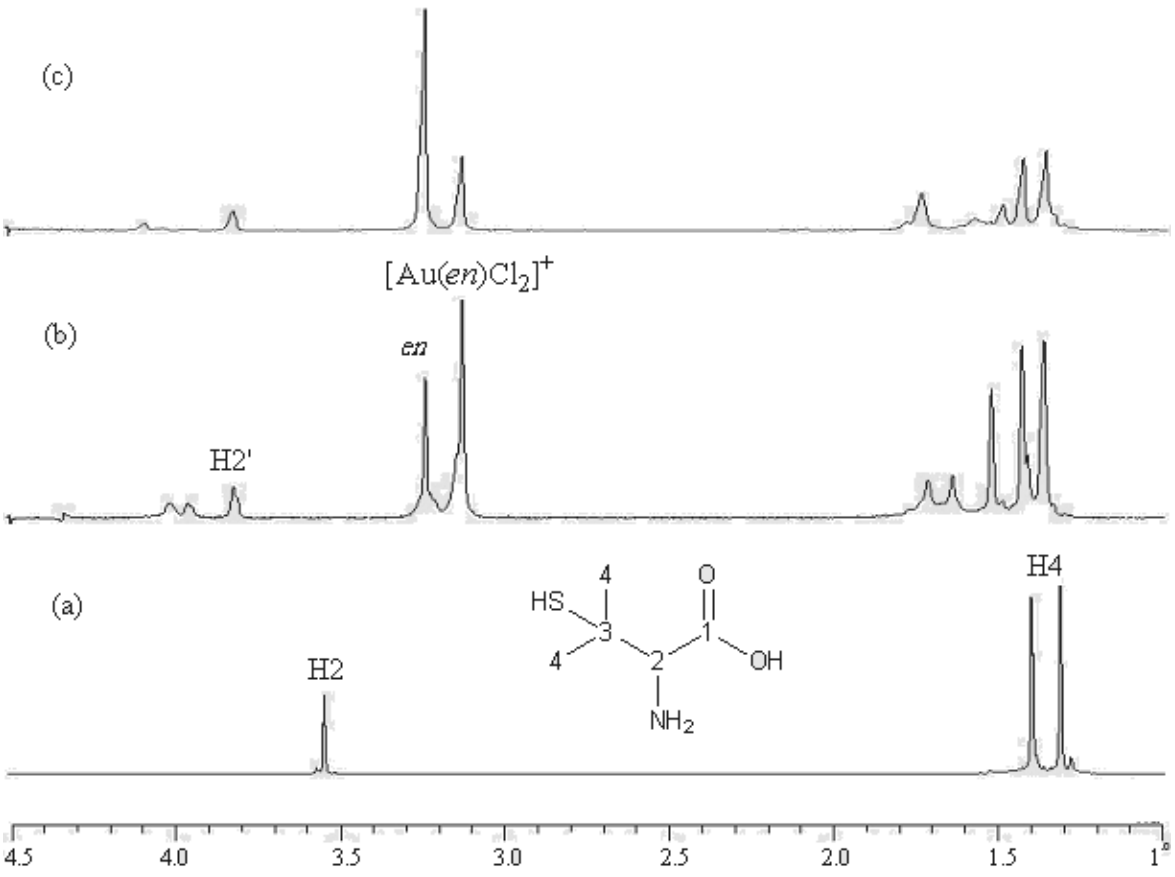

Figure 4.15: ^{1}H NMR spectra for D-penicillamine, (a) before mixing (b) 10 min after reaction and (c) 2 hours after reaction with $[Au(en)Cl_2]^+$, in D_2O at 25 ^{o}C.

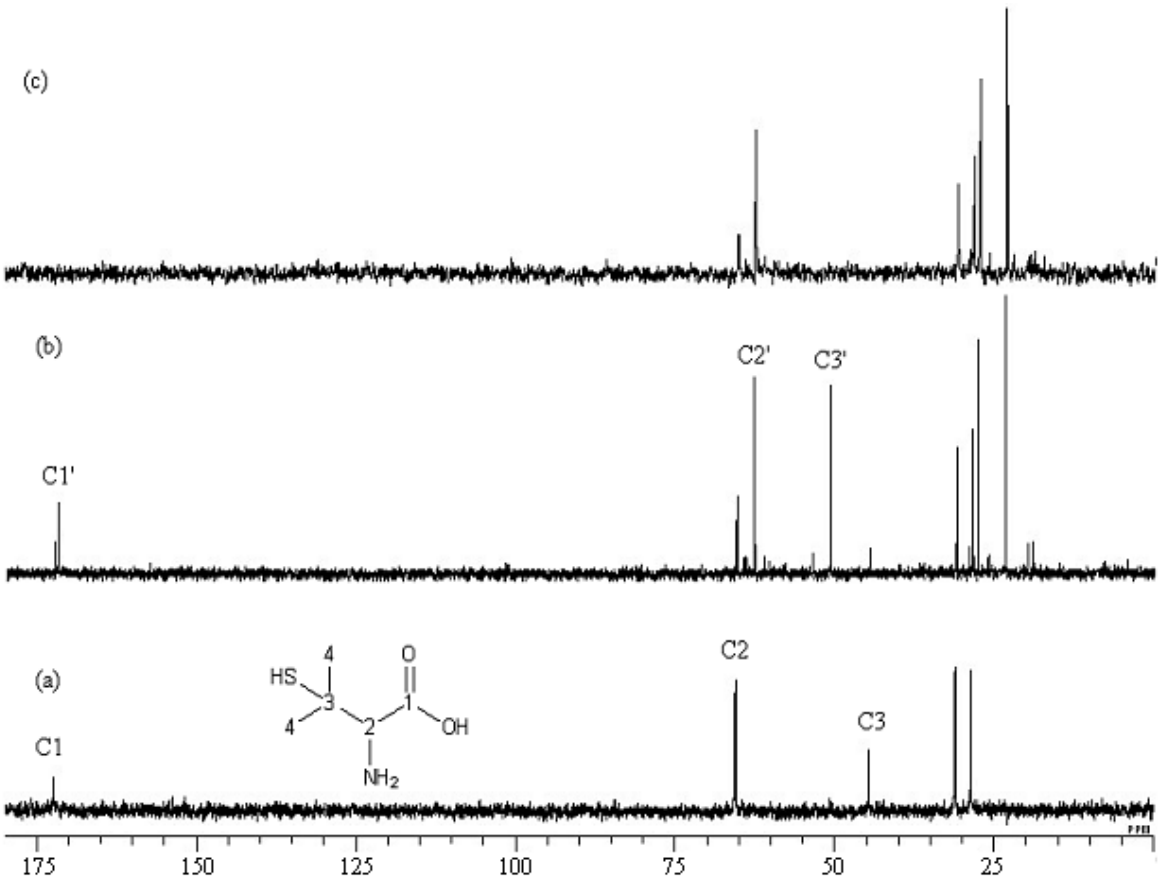

Figure 4.16: ^{13}C NMR spectra for D-penicillamine (a) before reaction, (b) after reaction with H_2O_2 (c)^{13}C-DEPT spectrum after reaction with H_2O_2, in D_2O at 25 ^{o}C.

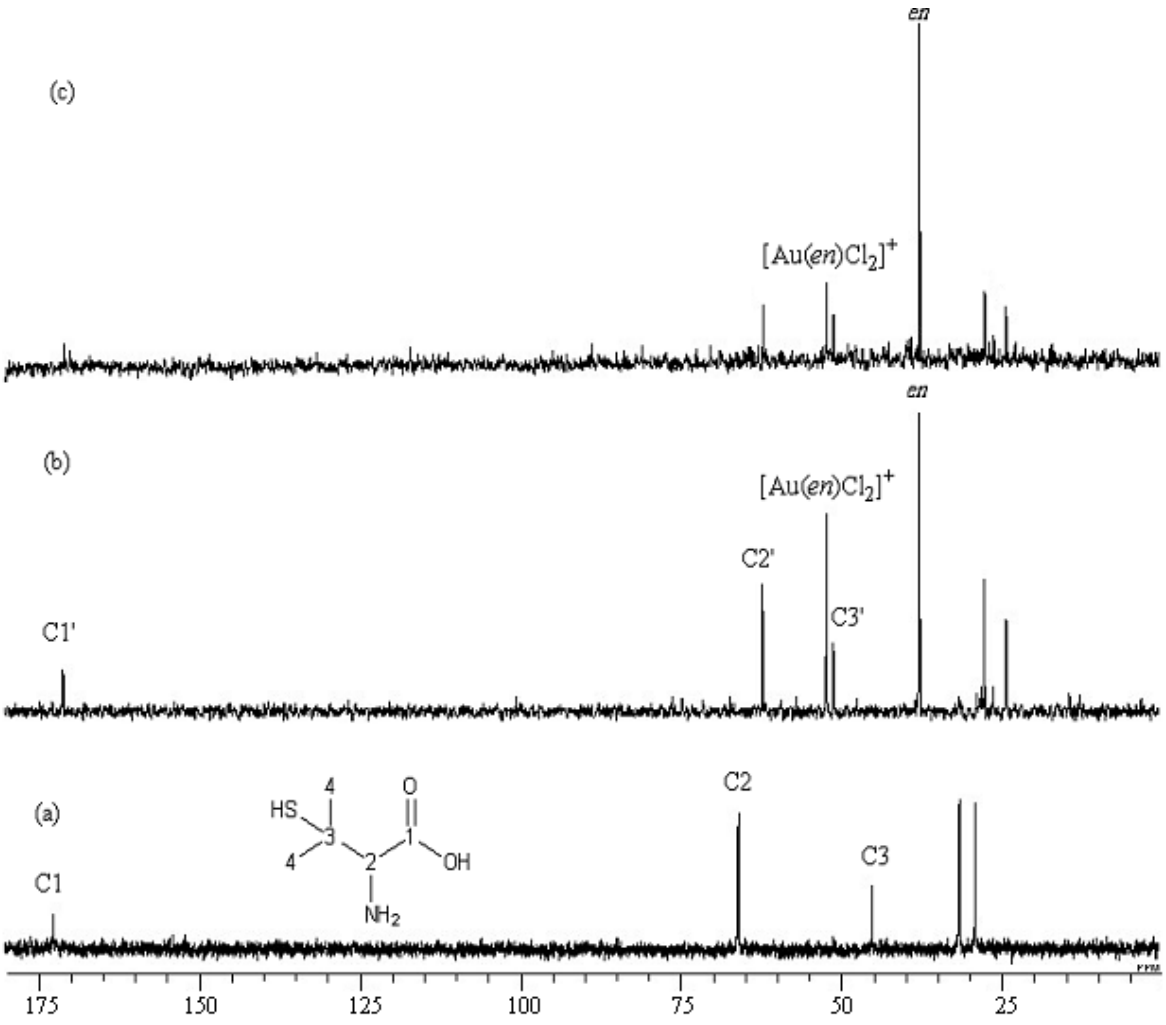

Figure 4.17: ^{13}C NMR spectra for (50 mM) D-penicillamine (a) before reaction, (b) 3 hours after reaction and (c) 6 hours after reaction with $[Au(en)Cl_2]^+$, reactant mixed at 1:1 ratio in D_2O at 25 ^oC, pD = 3.7.

^{13}C NMR chemical shifts assignment for D-penicillamine after oxidation were done by oxidizing D-penicillamine using H_2O_2 solution. The disappearance of the signal at ~50 ppm in ^{13}C DEPT NMR spectrum (Figure 4.16(c)) indicates that it corresponds to D-penicillamine-C3.

Signals corresponding to D-penicillamine C1, C2 and C4 were found to be shifted up-field upon reaction, while C3 was found to shift down field due to electron donation through sulfur.

Figure 4.17 shows ^{13}C NMR spectra for D-penicillamine reaction with $[Au(en)Cl_2]^+$, the signal corresponding to $[Au(en)Cl_2]^+$ complex decreased gradually, while *en* ligand dissociation takes place, (signal at ~37 ppm). After 6 hours ~ 80 % of $[Au(en)Cl_2]$ complex released its *en* ligand, as measured by ^1H NMR spectroscopy.

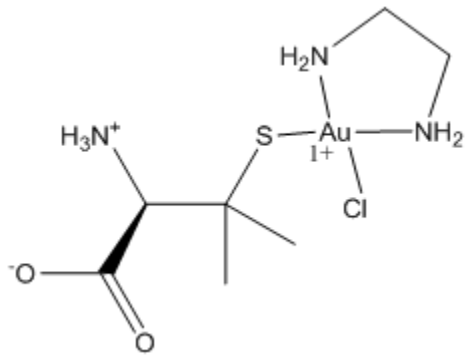

Scheme 4.16: $[(Pa\text{-}S,N)Au(en)]^{3+}$ structure

This reaction could be summarized as follows: D-penicillamine exchanges a chloride ligand from $[Au(en)Cl_2]^+$ complex, (Scheme 4.16). This is followed by D-penicillamine oxidation into the di-sulfide, while Au(III) reduced into Au(I), along

with *en* ligand release from the complex. No signals were observed that correspond to penicillamine dimer as found for cysteine, which could be hindered by steric factor of the bulky penicillamine ligand.

4.4.3 [Au(*en*)Cl_2]Cl interaction with Captopril

Captopril is an angiotensin-converting enzyme inhibitor used for the treatment of hypertension and some types of congestive heart failure [97]. It is present in two conformers *cis* and trans (Scheme 4.17) both forms are present in solution with dominancy according to solution pH [98,99]. Rabenstein *et al* [100] reported that *trans* conformer is dominant at low pH, while both conforms will be present as pH raised.

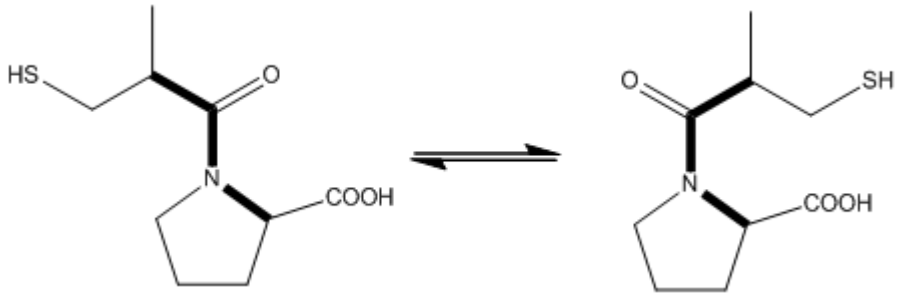

(A) **(B)**

Scheme 4.17: (A) trans- and (B) *cis*- captopril.

Captopril consists of 3-mercapto-2-methyl propanal and the proline moieties which behave differently in solution and have distinct signals in NMR. Captopril was reported to have pK_a for carboxylate 3.7 and 9.8 for the thiol group [101].

In this work we studied captopril interaction with $[Au(en)Cl_2]^+$ at ~ pD = 3.6 and monitored by NMR techniques.

Interaction studies of $[Au(en)Cl_2]^+$ complex with captopril were performed by mixing D_2O solutions of 140 mM at 1:1 ratio at pH 3.5. Immediate change of color to yellow and then to milky was observed right after mixing, indicating a fast reaction.

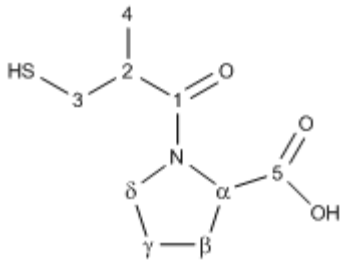

Scheme 4.18: Captopril atoms numbering.

^{1}H NMR spectra showed up-field shift to captopril-Hα (at 4.3 ppm), while H3 signal (at 2.8 ppm) was shifted but could not be distinguished after reaction, indication of immediate reaction through sulfur.

^{13}C DEPT NMR spectra were recorded for captopril reaction with H_2O_2, which were used for signals assignment. Figure 4.18(b) shows ^{13}C DEPT NMR spectrum before oxidation and (c) shows spectrum after oxidation by H_2O_2. C2 was found to be shifted up-field while C3 and Cα show down-field shift after oxidation by H_2O_2.

Figure 4.19 show ^{13}C NMR spectra for captopril before and after reaction with $[Au(en)Cl_2]^+$, *en* ligand signal showed complete dissociation from metal center, while we can observe very high down-field shift of signal corresponding to C3. This could be a result of captopril being bound to gold(III), as assigned using ^{13}C DEPT NMR. Chemical shifts were assigned as shown in table 4.18.

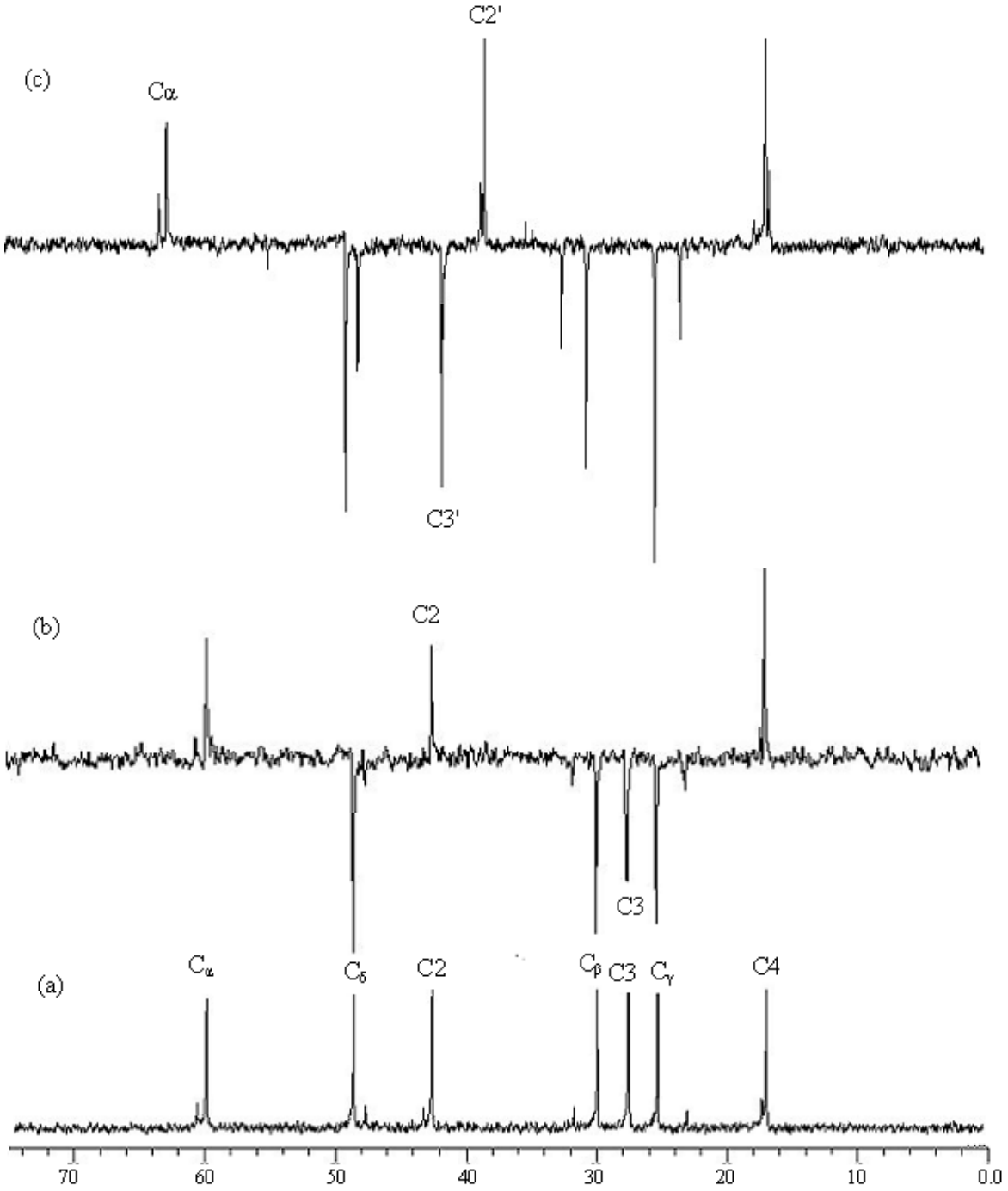

Figure 4.18: ^{13}C NMR spectra for captopril (a) before, (b) ^{13}C DEPT NMR before reaction with H_2O_2 and (c) ^{13}C DEPT NMR spectrum after reaction with H_2O_2, in D_2O at 25 ^{o}C and pD was 3.0.

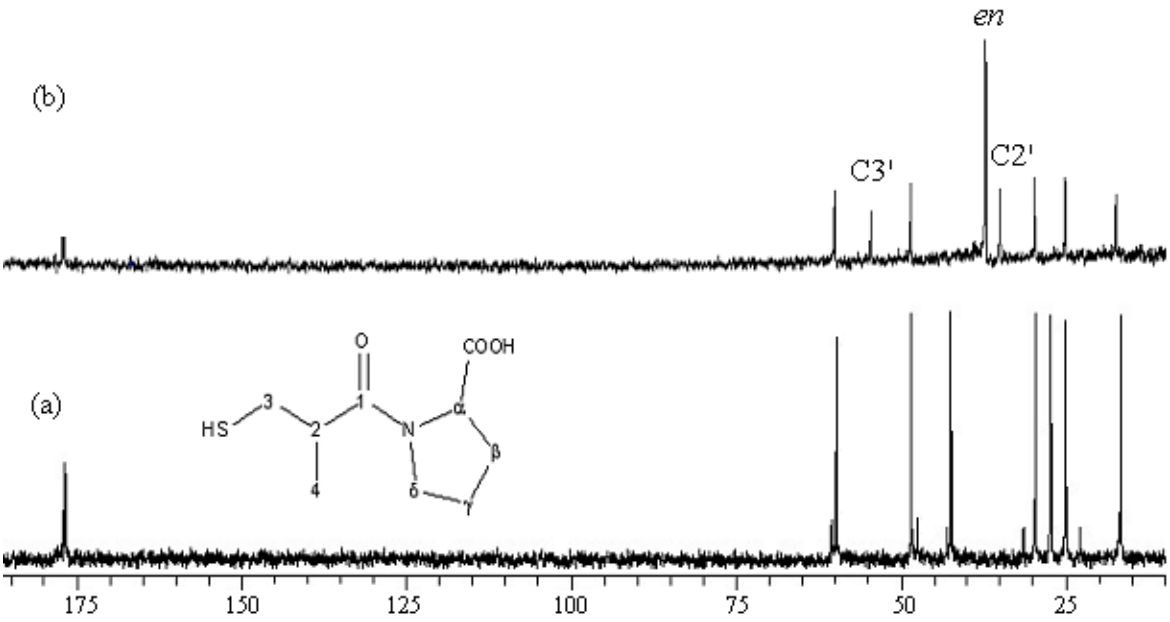

Figure 4.19: (a) ^{13}C NMR spectra for captopril before reaction and (b) after reaction with $[Au(en)Cl_2]^+$, in D_2O at 25 ^oC and pD = 3.5.

Table 4.18: ^{13}C NMR chemical shifts of $[Au(en)Cl_2]^+$ complex reaction with captopril in D_2O at and 25 ^oC, pD = 3.5.

	en	CO_2	Cα	Cβ	Cγ	Cδ	CON	C3	C2	C1
cis-Captopril		-	60.61	31.66	22.97	47.76	177.87	-	43.27	17.23
trans-Captopril		177.14	60.06	29.85	25.25	48.71	177.56	27.50	42.60	16.85
Captopril + $[Au(en)Cl_2]^+$	37.33	176.91	60.14	29.85	25.23	48.62	178.36	54.68	34.59	17.52

Table 4.19: ^1H NMR chemical shifts of $[Au(en)Cl_2]^+$ reaction with thiomalic acid in D_2O at 25 ^oC, pD = 3.7.

	en	**H3**	**H2**
TmSH	-	3.634	2.808, 2.768
$[(TmS)_2Au(en)]^{3+}$	3.106	3.800	2.926, 2.820

Table 4.20: ^{13}C NMR chemical shifts of $[Au(en)Cl_2]^+$ complex reaction with thiomalic acid in D_2O at and 25 ^oC, pD = 3.7.

	en	C=O	C4	C3	C2
TmSH		177.55	175.62	40.17	36.72
TmSH + $[Au(en)Cl_2]^+$	37.31	174.96	175.19	36.41	48.46,48.14

Table 4.18 shows ^{13}C NMR chemical shifts for *cis* and *trans* conformers at pH 3.5 before and after reaction with $[Au(en)Cl_2]^+$. Immediate dissociation of *en* ligand from metal center takes place. This is an indication of Au(III) reduction into Au(I), which accompanies generally captopril oxidation into the di-sulfide form. However the later was not detected after completion of the reaction. C3 signal shows change in chemical shift to 54.68 ppm that is assigned to $[(Cap\text{-}S)_2Au]^+$. This down-field shift of C3 is concurrent with the up-field shift of C2 signal by 8 ppm. That could be an indication of binding through oxygen at C1 and Sulfur. Corresponding spectra are shown in Figure 4.19. Similar mechanism for captopril could be suggested for other thiols.

4.4.4 $[Au(en)Cl_2]^+$ interaction with Thiomalic acid

Gold thiomalic acid complexes are used mainly for their anti-inflammatory action in the treatment of rheumatoid arthritis [57]. Interaction of thiomalic acid with $[Au(en)Cl_2]^+$ is presented.

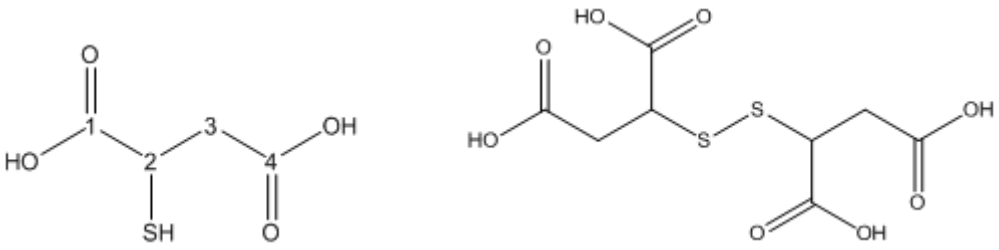

(a) (b)

Scheme 4.19: (a) Thiomalic-acid and (b) Thiomalic-acid dimer.

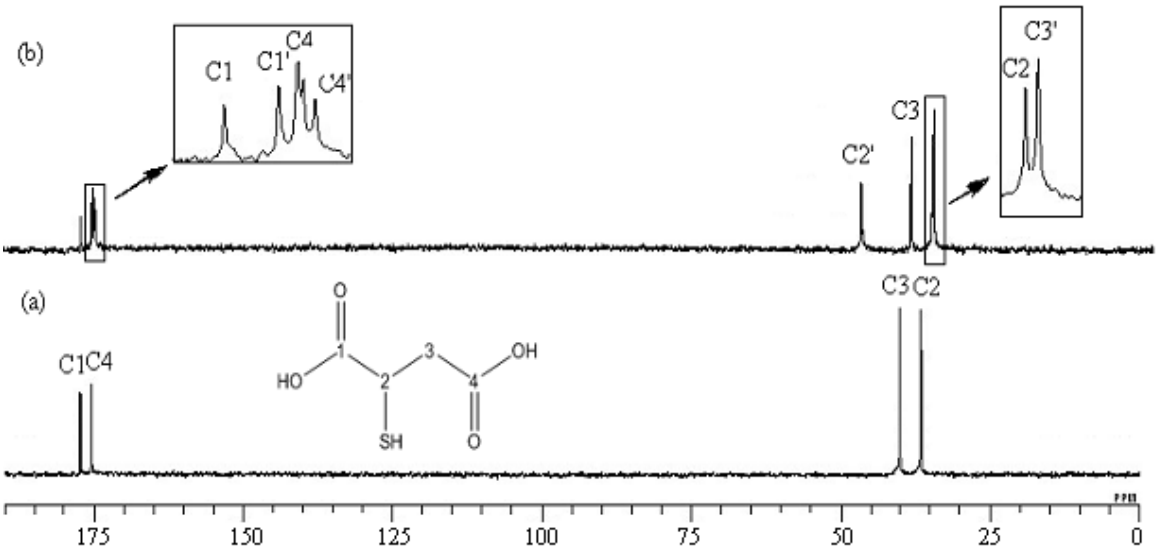

Figure 4.20 : ^{13}C NMR of thiomalic acid (a) before and (b) after reaction with H_2O_2 in D_2O at 25 ^oC.

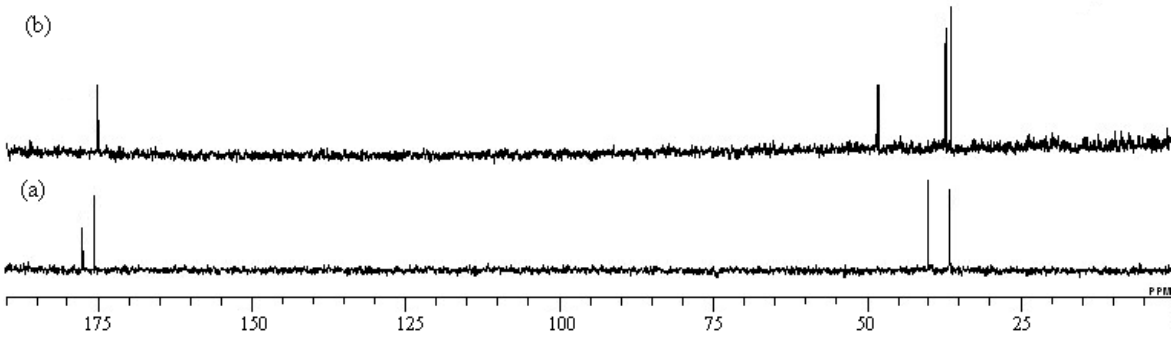

Figure 4.21: ^{13}C NMR of thiomalic acid (a) before and (b) after reaction with $[Au(en)Cl_2]^+$ at 1:1 ratio, in D_2O at 25 ^oC, pD = 3.7.

^{1}H NMR chemical shifts for thiomalic acid before and after interaction with $[Au(en)Cl_2]^+$ are given in table 4.19. As expected, a downfield change in chemical shifts for both H2 and H3 signals is obserevd, with larger down-field shift for H3. This is an indication of a reaction through sulfur.

Thiomalic acid (TmSH) was oxidized by H_2O_2. ^{13}C NMR spectra are shown in figure 4.20, C2' signal shifted down-field to 48 ppm, while C3' shows up-field shift after dimerization to 36 ppm. C1 and C4 also shows up-field shift after dimerization. C2' was the most affected by this reaction.

^{13}C NMR spectrum of the species resulting from the reaction of thiomalic acid and $[Au(en)Cl_2]^+$ is shown in figure 4.21. This shows similar changes of chemical shifts as shown in the H_2O_2 experiment (Figure 4.20). The main reaction occur after mixing the components at 1:1 ratio is the thiomalic acid oxidation that produces the disulfide dimer, while Au(III) is reduced into Au(I) that causes the release of *en* ligand. Chemical shift assignments are given in table 4.20. C2 signal shows ~14 ppm downfield shift, while C3 signal shifted up-field by ~ 4 ppm after reaction. The signal corresponding to free *en* ligand in solution appears at 37 ppm right after mixing.

4.4.5 [Au(*en*)Cl_2]Cl interaction with L-glutathione

Glutathione (GSH) is a tripeptide that contains an unusual peptide linkage between the amine group of L-cysteine and the carboxyl group of the glutamate side chain. Glutathione along with glutathione reductase enzyme work as an antioxidant in living cells [102]. Glutathione reduces any disulfide bond formed within cytoplasmic proteins to cysteine by donating electrons while being converted to glutathione disulfide (GSSG). Glutathione reductase then transforms GSSG back to GSH [102]. The ratio of reduced glutathione to oxidized glutathione within the cells is used as a measure of cellular toxicity [102].

Lewis *et al* [55] discussed the reaction of gold(I) with glutathione and reported bonding GS-Au interaction to be through sulfur. Gold(III) reduction by glutathione was reported as pH dependent [103].

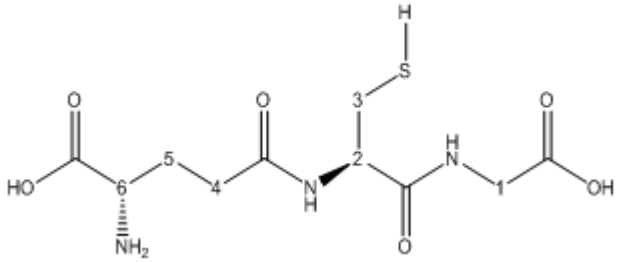

Scheme 4.20: L-Glutathione atoms numbering.

In this work we studied [Au(*en*)Cl_2]$^+$ interaction with glutathione by means of ^{1}H and ^{13}C NMR spectroscopy. A comparison of this reaction with oxidation by H_2O_2 (Figure 4.22) was performed.

^{1}H NMR chemical shifts show minor changes upon reaction so they were not much informative in this reaction, except that *en* ligand can easily be monitored. It was found to dissociate from Au(III) complex over 13 hour.

Figure 4.22 shows ^{13}C NMR spectra of L-glutathione oxidation by H_2O_2 solution. The signal at 27 ppm corresponding to C3 was found to decrease while C3' signal assigned for GSSG was found to increase (at 39 ppm). C2 signal also shifted up-field upon L-glutathione dimerization. Figure 4.22 (b) shows signal after oxidation of L-glutathione, So C3 and C2 signals shifted to C3' and C2', respectively. Figure 4.22 (c) shows the resulting spectrum after L-glutathione reaction with $[Au(en)Cl_2]^+$. In this spectrum we observed the dissociation of *en* ligand and the GSSG formation, after 10 hours of reaction. A brown precipitate also formed in solution after gold(III) reduction into metallic gold.

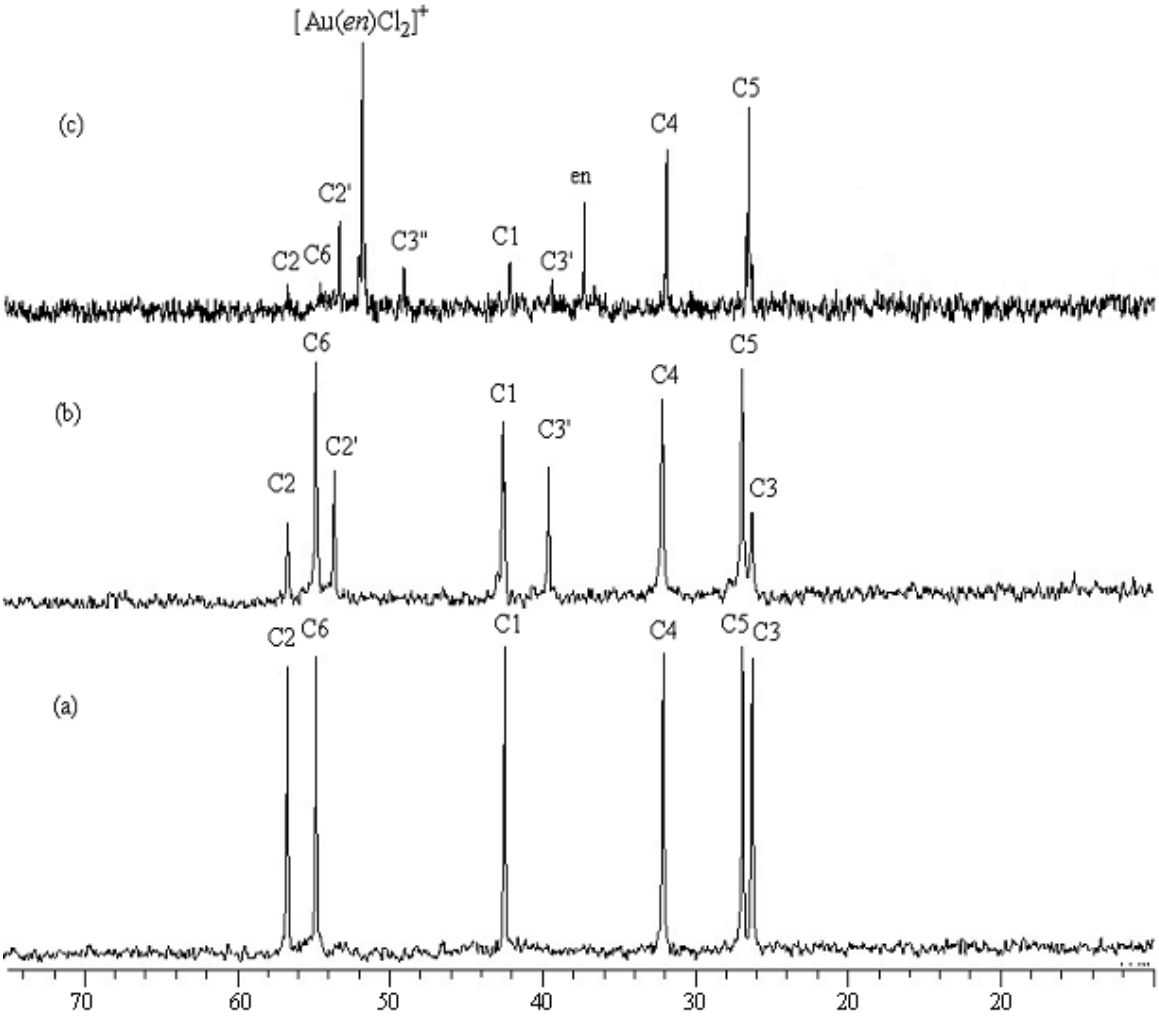

Figure 4.22: ^{13}C NMR of glutathione, (a) before, (b) after oxidation by H_2O_2 and (c) after 6 hours of L-glutathione reaction with $[Au(en)Cl_2]^+$ at 1 to1 ratio, in D_2O solution at 25 ^oC and pD = 3.7.

Table 4.21: ^{13}C NMR chemical shifts of $[Au(en)Cl_2]^+$ complex reaction with glutathione in D_2O at 25 ^oC, pD = 3.7.

	en	***C=O***	***C2***	***C6***	***C1***	***C4***	***C5***	***C3***
GSH		178.05, 175.60, 174.09, 173.33	56.49, 56.34	54.32	42.10	31.87	26.67	26.14
GSH + $[Au(en)Cl_2]^+$	51.78	176.13, 174.97, 173.89, 173.77, 172.41	53.01	54.12	42.08	31.77	26.17	39.48
GSH + $[Au(en)Cl_2]^+$ 13 hour	51.72, 37.64	175.06, 173.61, 172.22, 172.04, 170.94	53.01	53.33	41.97	31.72, 32.18	26.28, 26.06	39.38, 49.82

Atoms numbering refers to scheme 4.20.

^{13}C NMR chemical shifts are given in table 4.21, down-field change of C3 chemical shift was observed to 39 ppm. This is indication of bonding through sulfur. After 13 hours we observe a small up-field change in chemical shift of C6 indication of bonding through -NH_2. Carbonyl signal shows general up-field shift after reaction with $[Au(en)Cl_2]^+$ after 13 hours indication of reaction progress. Four C=O signals appear in spectra which shows up-field change in chemical shift after mixing, up-field shift increases after 13 hours and a signal appears at 39 ppm corresponding to GSSG compound which is expected to form in solution.

Therefor we suggest the reaction mechanism to take place first by chloride exchange reaction by L-glutathione at gold(III) metal ion through sulfur, followed by di-sulfide reductive elimination. Au(III) is then reduced into Au(I). Excess glutathione will cause Au(I) reduction into metallic gold but the reaction at 1:1 ratio causes L-glutathione binding to Au(I) and precipitation of $[(GS)_2Au]^+$. After standing, chelating likely occurs through amine group, so C6 signal is shifted up-field. Ethylenediamine ligand found to be continuously dissociate from the $[Au(en)Cl_2]^+$ complex along with gold(III) reduction into gold(I).

4.5 [Au(alkyldiamine)Cl_2]Cl with ergothionene and thiones

4.5.1[Au(*en*)Cl_2]$^+$ with ergothionene (ErS)

L-Ergothionene (ErS) is a unique, naturally occurring antioxidant that is abundant in most plants and animals [104]. High concentration of ergothioneine is found in the red blood cells [104] and tissues including liver, kidney, the eye, seminal fluid, and erythrocytes [104]. ErS exists in a thiol (ErSH), thione (ErS) equilibrium, as

given in scheme 4.21. Thione is found to be dominant in the solid state and at pH = 7 [104-106].

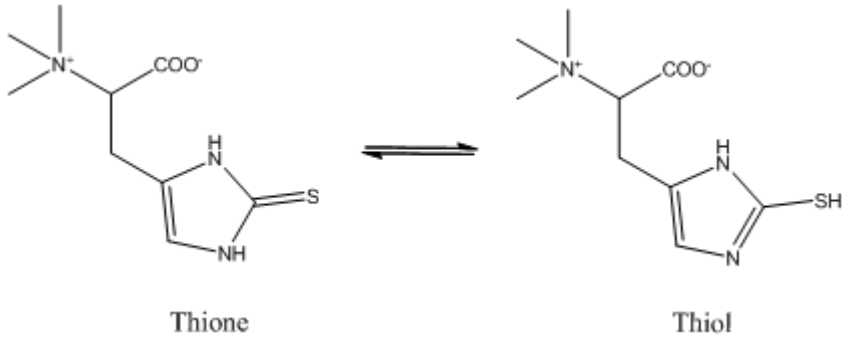

Thione Thiol

A **B**

Scheme 4.21: Ergothionene thione - thiol isomerization

Reaction of ergothionene with $[Au(en)Cl_2]^+$ was carried out and monitored by ^1H and ^{13}C NMR spectroscopy.

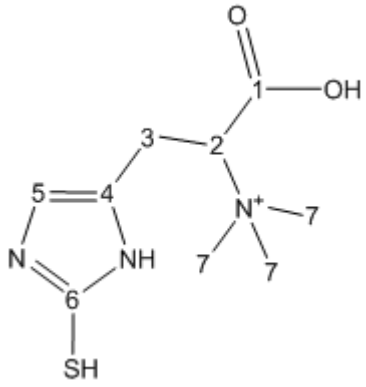

Scheme 4.22: Ergothionene (ErS) atoms numbering.

^1H NMR chemical shift for ErSH before and after reaction with $[Au(en)Cl_2]^+$ are given in Table 4.22. The down-field shift of H5 signal soon after reaction is an indication of high reactivity and conversion of ergothioneine into its thiol form. The de-shielding of protons takes place because of the ring aromaticity in the thiol form.

Table 4.22: ^{1}H NMR chemical shifts of ergothioneine upon reaction with $[Au(en)Cl_2]^+$ at 2:1 ratio in D_2O at 25 ^{o}C and pD = 3.7.

	$[Au(en)Cl_2]^+$/ free-*en*	**H5**	**H2**	**H7**	**H3**
ErSH	-	6.672	4.031	3.141	3.186
ErSH + $[Au(en)Cl_2]^+$	3.141/ 3.214	7.212	3.915	3.166	3.374

Atoms numbering according to scheme 4.22.

Table 4.23: ^{13}C NMR chemical shifts of ergothioneine upon reaction with $[Au(en)Cl_2]^+$ at 2:1 ratio in D_2O and 25 ^{o}C, pD = 3.7.

	en	**C1**	**C2**	**C3**	**C6**	**C5**	**C4**	**C7**
ErSH	-	169.64	75.75	23.39	157.01	116.58	123.82	53.20
ErSH + $[Au(en)Cl_2]^+$ 7 hours	37.30	170.06	76.50	23.58	150.87	117.56, 118.55	125.7	53.14
ErSH + $[Au(en)Cl_2]^+$ 3 days	37.29	170.28	76.78	23.59	148.35	117.87, 118.62	127.17	53.19

Atoms numbering according to scheme 4.22.

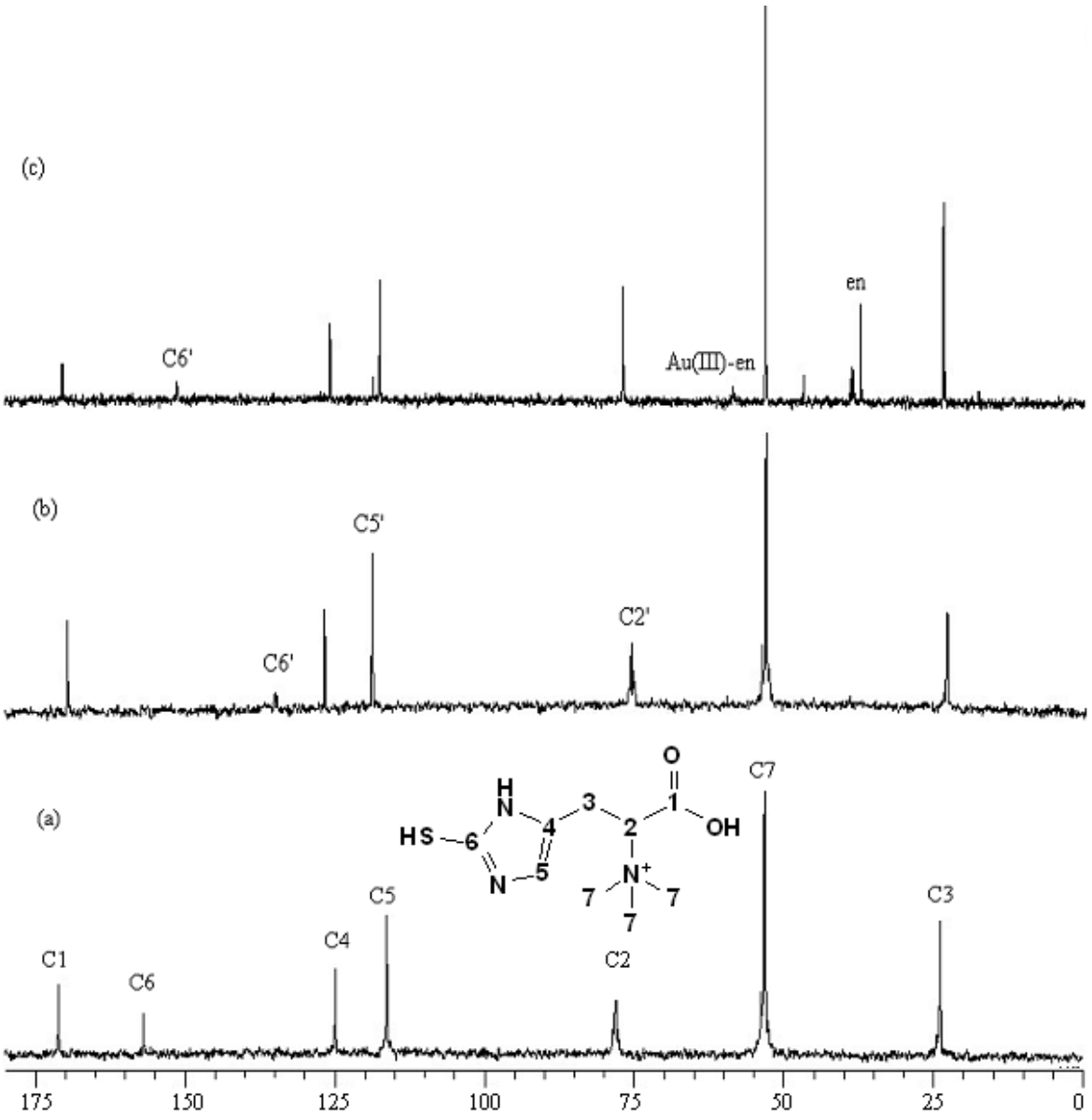

Figure 4.23: ^{13}C NMR spectra for ergothioneine (a) before reaction, (b) after reaction with H_2O_2 and (c) 7 hours after reaction with $[Au(en)Cl_2]^+$ in D_2O at 2:1 ratio at 25 ^oC, pD = 3.7.

As shown by Figure 4.23(a) ergothionene at pD = 3.7 is present as thiol. Figure 4.23(b) stands for ergothioneine after oxidation by H_2O_2. By comparison with Figure 4.23 (a) we can observe up-field shift of C6 and C2 signals while C5 shifted down-field. C6´ shifted to 134 ppm after dimerization. ^{13}C NMR spectrum of ergothioneine after reaction with $[Au(en)Cl_2]^+$ at 2:1 ratio is shown in Figure 4.23(c). In this figure we can observe an up-field shift of C6 by 6 ppm (δ = 151 ppm) indicating legation through thiol group. No signs were found for ergothioneine dimerization by comparison with H_2O_2 reaction discussed earlier. However after three days, the ^{13}C NMR spectrum C6 is shifted to 148 ppm, indicating the Au(III) reduction into Au(I) as shown by Ahmad *et al* [104]. Ethylenediamine ligand was found to dissociate from the complex after 7 hours (Figure 4.23(c)) and this supports the hypothesis of Au(III) reduction to Au(I), as discussed previously. ^{13}C NMR chemical shifts for reactants before and after reaction are given in table 4.23.

The up-field shift of C6 after legation through sulfur to the metal center can be rationalized as due to the electron deficiency produced that promotes electron compensation from the surrounding nitrogens.

4.5.2 [Au(alkyldiamine)Cl_2]Cl with thiones.

Gold-thiones have found great interest in recent research due to potent gold sulfur interaction which found several medicinal applications [1,59]. Thione heterocyclic rings with various metal ions, have received much interest [48,107,108]. Myocrisin and solganol used for the treatment of rheumatoid arthritis are gold-sulfur compounds [60,61]. Considerable work has been carried out on thione complexes with gold(I) [63], very little is known about Au(III) complexes with thiones.

Imidazolidine-2-thione and its derivative ligands were reacted with gold(III)-alkyldiamine complexes in 2:1 mole ratio. This resulted in formation of several complexes that were characterized by melting point and elemental analysis, while structural analysis were done by IR spectroscopy and ^{13}C and ^{15}N solid-state NMR.

This work reports the synthesis of gold(III)-alkyldiamine reaction with imidazolidine-2-thione and its derivatives such as Imt, Diaz and Diap.

Table 4.24: IR frequencies, $\nu(cm^{-1})$ of [Au(*en*)Cl_2]Cl complex with Imt, Diaz and Diap.

Complex	**$\upsilon_{(N-H)}$, cm^{-1}**	**$\upsilon_{(C=S)}$, cm^{-1}**	-N-C=S Asym str
Imt	3200	506	-
$[(Imt)_2Au(en)]Cl_3$	3426 w	495	2052
$[(Imt)_2Au(pn)]Cl_3$	3426 s	497	2017
$[(Imt)_2Au(bn)]Cl_3$	3400 w	496	2026
[(Imt)Au(N,N'-Me-en)]Cl	3462, 3141	495	-
[(Imt)Au(N,N'-*i*Pr_2-en)]Cl	3431, 3184	493	2039
Diaz	3166	516	-
$[[(Diaz)_2Au(en)]Cl_3$	3423 w	518	2044 w
$[(Diaz)_2Au(pn)]Cl_3$	3444 m	517	2015
$[(Diaz)_2Au(bn)]Cl_3$	3413 sh	499	2010
$[(Diaz)_2Au(N,N'-iPr_2-en)]Cl_3$	3447	489	-
$[(Diaz)_2$ Au(N,N'-Me-en)]Cl_3	3445	517	2043
$[(NN'$-di-Et-Diaz$)_2Au(en)]Cl_3$	3428 m	-	-
Diap	3224	527a	-
$[(Diap)_2Au(en)_2]Cl$	3418 m	505	2019
$[(Diap)_2Au(pn)_2]Cl$	3428 m	519	2020
[(Diap)Au(bn)]Cl	3403 sh	495	2013
$[(Diap)_2$ Au(N,N'-Me-en)]Cl_3	-	489	-
$[(Diap)_2Au(N,N-iPr_2-en)]Cl_3$	-	491	-

IR frequencies for the prepared complexes were recorded in the range 4000-400 cm^{-1} using KBr pellet, selected IR frequencies are given in Table 4.24, vibrational frequency for thione ligands $\upsilon_{(C=S)}$ shows red shift upon complexation as a result of electron donation from sulfur to the metal center that promote π-back donation to thione π* orbital, this causes weakening of the C-S bond. N-H vibrational frequency $\upsilon_{(N-H)}$ were found to shift to higher wavenumber (blue shift) indication of N-H bond strengthening in complex compared to the free ligand as a result of electron donation form sulfur [109]. Stretching frequencies in the range 2010-2052 cm^{-1} were also recorded for the prepared complexes corresponding to $\upsilon_{(-N-C=S)}$ band as reported by Ray *et al* [110].

Solution NMR data were not found to be descriptive for complexes, because of lack of stability of complexes in solution. So NMR measurements in the solid state were preformed. The chemical shifts found are given in table 4.25.

Table 4.25: Solid-state ^{13}C Isotropic Chemical Shifts (δ_{iso}) and Principle Shielding Tensors (σ_{xx}) of [Au(alkyldiamine)Cl_2]Cl complexes with Imt, Diaz, and Diap ligands.

Complex	Nnd ucleus	δ_{iso}	σ_{11}	σ_{22}	σ_{33}	Span	Skew	Other
$[(Imt)_2Au(en)]Cl_3$	^{13}C	155.41						46.78
	^{15}N	-260.14, -335.83						
$[(Imt)_2Au(pn)]Cl_3$	^{13}C	177.03	257	183	90	167	0.116	46.58
	^{13}C	154.90	221	163	81	139	0.175	
	^{15}N	-258.2						
$[(Imt)_2Au(bn)]Cl_3$	^{13}C	176.93	252	193	86	167	0.289	46.29
	^{15}N	-259.6						
$[(Diaz)_2Au(en)]Cl_3$	^{13}C	166.74	241	186	73	168	0.351	42.70, 19.41
	^{13}C	149.37	223	143	82	141	-0.127	
	^{15}N	-357.60						
$[(Diaz)_2Au(pn)_2]Cl_3$	^{13}C	167.31						43.48, 19.50
	^{15}N	-337.47						
$[(Diaz)_2Au(bn)]Cl_3$	^{13}C	171.69	244	189	83	161	0.319	44.74, 27.46
	^{15}N	-205.2						
$[(Diap)_2Au(en)_2]Cl$	^{13}C	172.46	273	201	44	229	0.366	45.22, 27.66
	^{15}N	-258.2, -333.5						
$[(Diap)_2Au(pn)_2]Cl$	^{13}C	172.08	227	211	78	148	0.792	45.90, 27.75
	^{15}N	-257.0, -263.9						
[(Diap)Au(bn)]Cl	^{13}C							44.84, 26.78
$[(Diaz)_2Au(N,N'\text{-Me-en})]Cl_3$	^{13}C	154.32	226	153	84	142	-0.035	51.62, 41.15,
$[(Diaz)_2Au(N,N'\text{-}i\text{Pr}_2\text{-en})]Cl_3$	^{13}C	146.16	194	141	10	90	-0.170	71.82, 61.34,
$[(Diap)_2 Au(N,N'\text{-Me-en})]Cl_3$	^{13}C	159.17	216	154	10	108	-0.153	46.58, 28.53

Isotropic shielding, $\sigma i = (\sigma_{11} + \sigma_{22} + \sigma_{33})/3$; $\Delta\sigma = \sigma_{33} - 0.5(\sigma_{11} + \sigma_{22})$; $\eta = 3(\sigma_{22} - \sigma_{11}) / 2\Delta\sigma$; [2,73,74].

4.6 [Au(*alkyldiaimine*)Cl_2]$^+$ interaction with Imt

Interaction of [Au(*en*)Cl_2]$^+$ complex with imidazolidine-2-thione (Imt) has been studied by ^{1}H and ^{13}C NMR spectroscopy. Reactants were mixed at (1:2) and (1:1) ratios in D_2O at 25^{o}C , pD= 3.7. After mixing at 2:1 ratio, very fast reaction was observed and the solution color changed turn from yellow into turbid orange. ^{1}H NMR chemical shifts showed fast dissociation of *en* ligand (signal at ~3.1 ppm decrease) from gold complex due to Imt exchange or due to gold(III) reduction. Imt signal shifted to 3.87 ppm. When the reaction was carried out at 1:1 ratio, *en* ligand signal showed signals for both free *en* at 3.20 ppm and for metal bound ligand, while Imt showed two distinct signals at 3.67 ppm corresponding to Au(III)-Imt and a signal at 3.83 ppm corresponding to Imt-dimer.

The reaction of [Au(*en*)Cl_2]$^+$ with Imt was carried out at 1:1 ratio and monitored with time using the peak at 3.08 ppm, which corresponds to the *en* in [Au(*en*)Cl_2]$^+$, after 10 hours this signal was vanished almost completely, so it required 36 min for 60 % of bond *en* ligand to dissociate, while the rest of the *en* required more than 10 hours to dissociate.

Table 4.26: ^{1}H NMR Chemical shifts for Imt reaction with H_2O_2 and $[Au(en)Cl_2]^+$ complex in D_2O at 25 ^{o}C and pD = 3.7.

	en	**N-H**	**H1**	**Imt-S-S-Imt**
Imt			3.532	
Imt + H_2O_2				3.898
$[Au(en)Cl_2]^+$ + Imt	3.084, 3.195	3.911	3.674	3.836
1eq : 1eq				
$[Au(en)Cl_2]^+$ + Imt	3.191	3.954	3.713	3.865
1eq : 2eq				

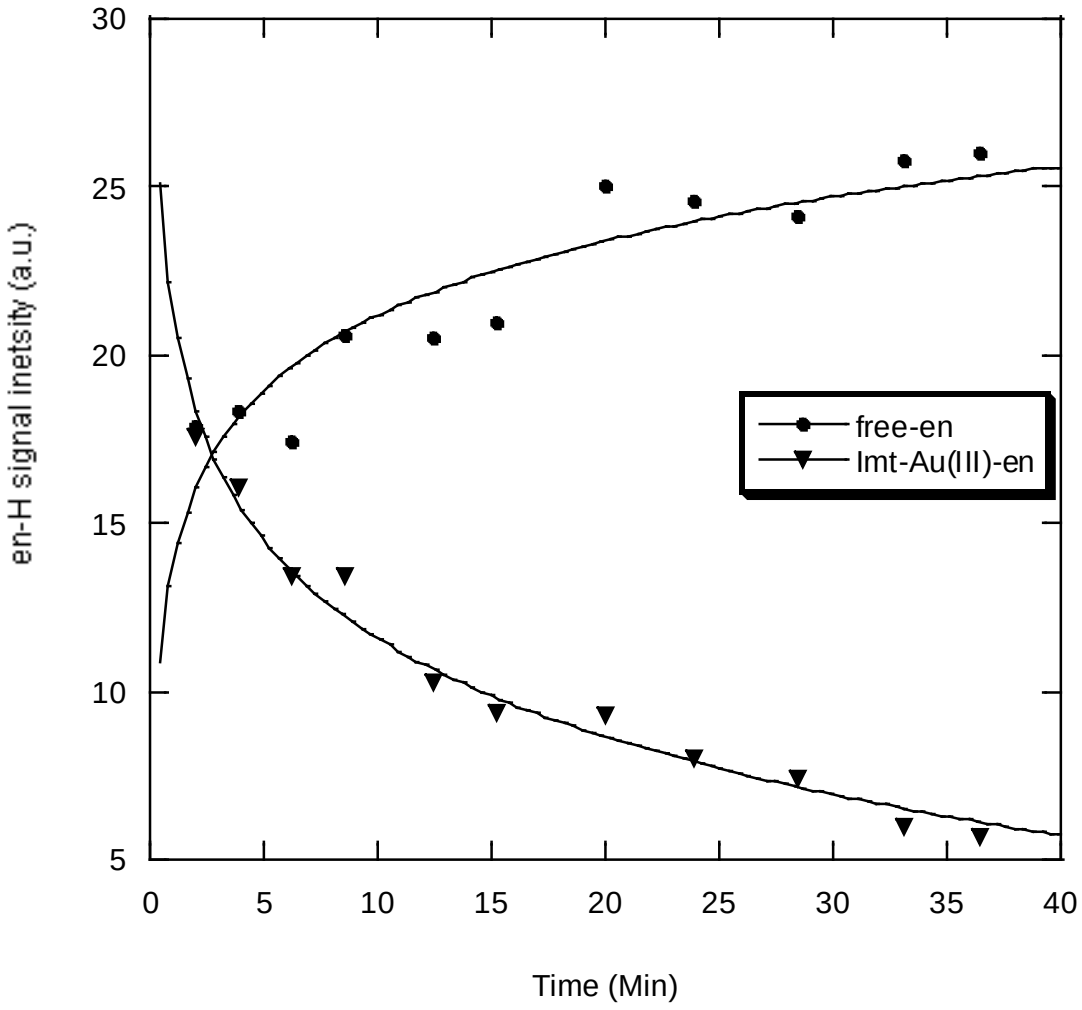

Figure 4.24: ^{1}H NMR monitoring of *en*-H signal intensity (a.u) vs. time. (●) refer s to free en and (▼) refer s to $[(Imt)_2Au(en)]^{3+}$ complex at 25 ^{o}C, pD = 3.7.

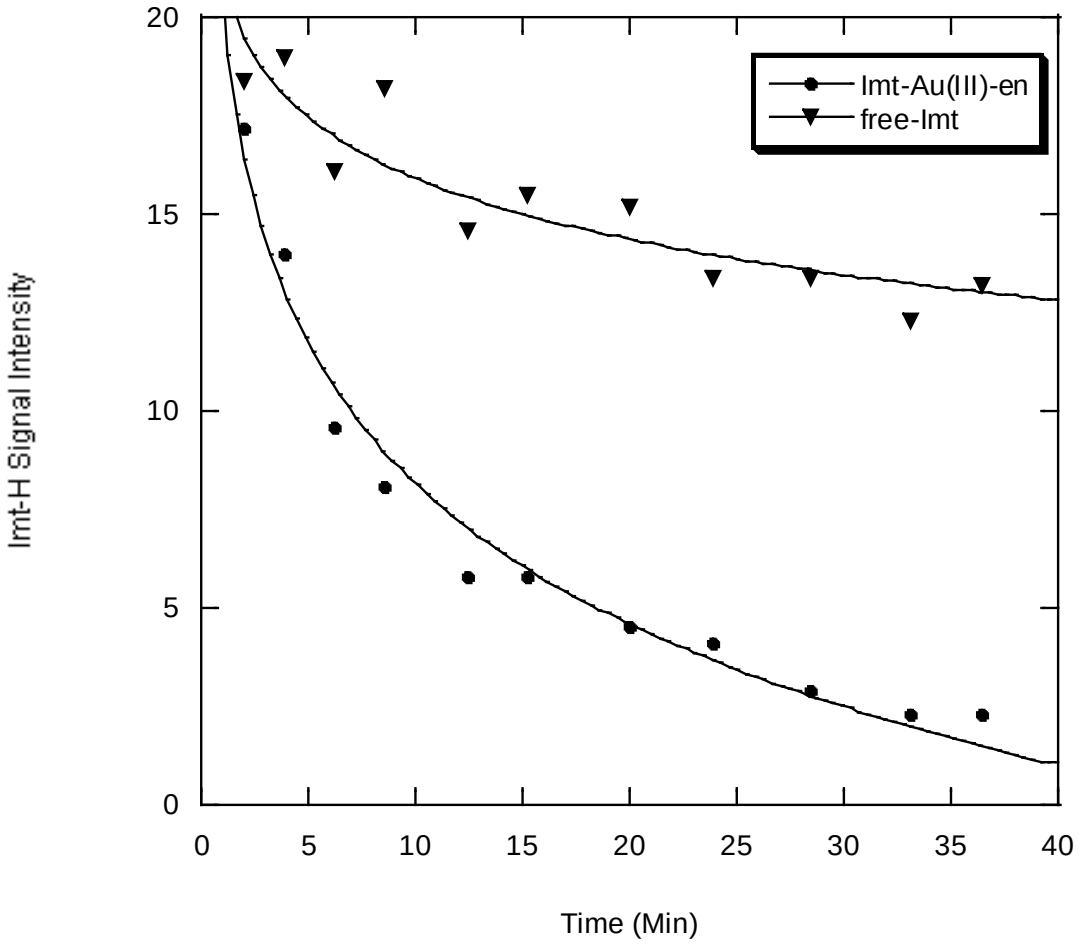

Figure 4.25: ^{1}H NMR monitoring of Imt-H signal intensity (a.u) vs. time. (▼) refers to free Imt and (●) refers to $[(Imt)_2Au(\textit{en})]^{3+}$ complex at 25 ^{o}C, pD = 3.7.

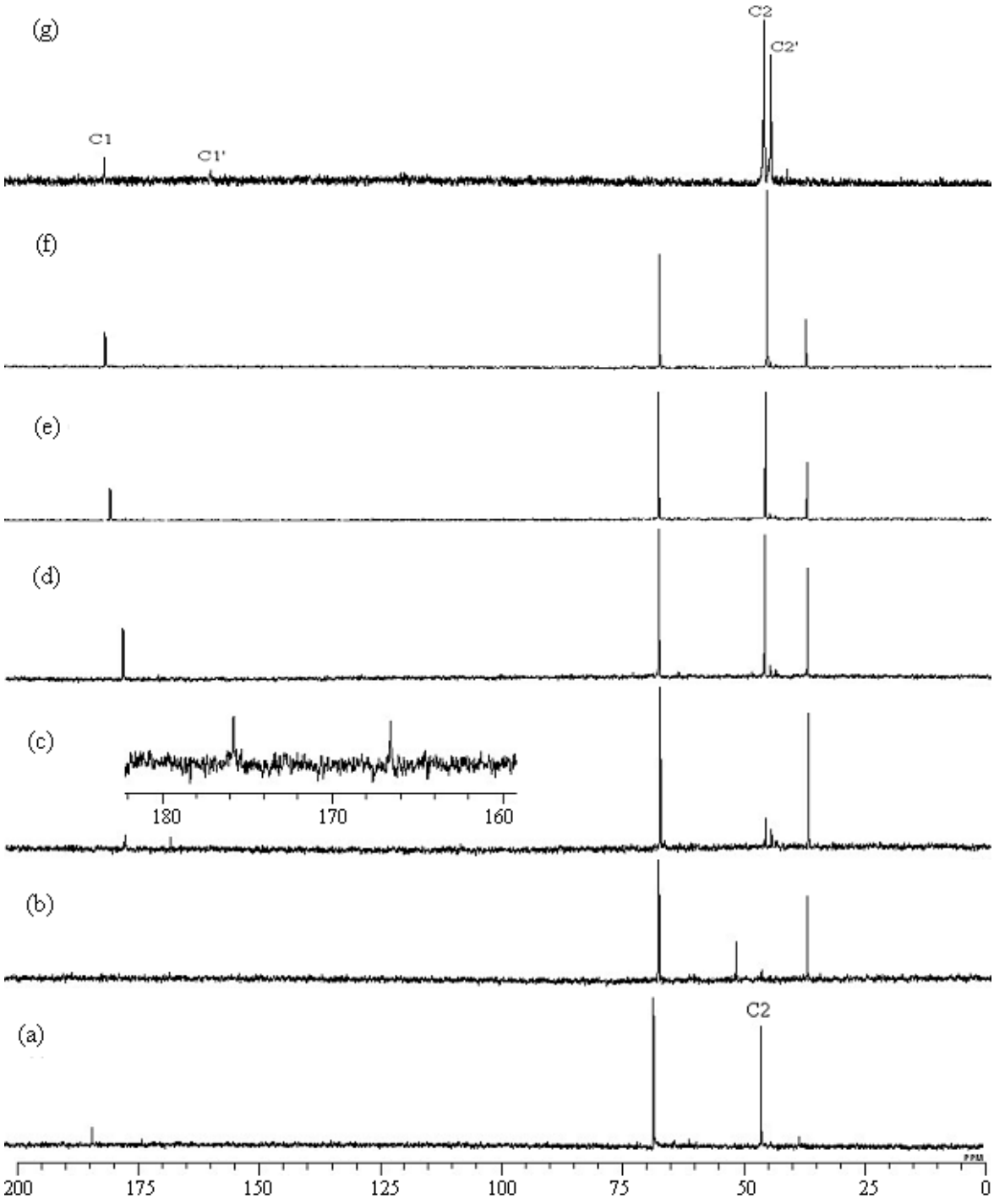

Figure 4.26: ^{13}C NMR spectra of (a) Imt before reaction, (b to f) Imt after reaction with $[Au(en)Cl_2]^+$ and (g) after reaction with H_2O_2, at 25 ^oC.

Figure 4.26 (a) shows ^{13}C spectrum of Imt. The reaction with $[Au(en)Cl_2]^+$ was monitored and spectra (b-f) were obtained. Imt ligand C2 shifted up-field indicating binding to Au(III) but after standing di-sulfide starts to form and Au(III) is reduced into Au(I). The signals were assigned by comparison with Imt oxidation experiment by H_2O_2 as shown by figure 4.26 g. C2 corresponding to Imt-di-sulfide (Imt-S-S-Imt) was found in solution (δ = 166 ppm). Ethylenediamine ligand was found to be released from $[Au(en)Cl_2]^+$ complex after reaction indicating Au(III) reduction. We can therefore suggest that the reaction starts with Imt ligand binding to gold(III) which is reduced very fast into gold(I). This leads to *en* ligand dissociation from $[Au(en)Cl_2]^+$ complex, Imt is oxidized into Imt-S-S-Imt and the corresponding chemical shift appeared at 166 ppm. The signal corresponding to Imt-Au(I) was found at 179 ppm.

4.7 **Gold(III)-tetracyanide interactions with L-cysteine, glutathione, captopril, L-methionine and DL-Se-methionine.**

$[Au(CN)_4]^-$ interaction with different thiols and thioethers were carried out by mixing reactants at different ratios, and reactions were monitored by NMR and UV-visible absorption techniques. Selected data that show reaction progress are presented here. Signals assignments were carried out based on literature [16,103].

4.7.1 L-Cysteine interaction with $[Au(CN)_4]^-$

The reaction was carried out for CySH with $[Au(CN)_4]^-$ at 1:1 ratio and monitored by ^1H NMR. ^1H NMR chemical shifts for CySH reaction with $[Au(CN)_4]^-$ are given in table 4.27. Downfield shift of signals corresponding to H2 and H3 were observed

after reaction. H3 signal showed more downfield shift indicating binding through sulfur atom, but ^{1}H NMR is not much informative about gold ion oxidation state and cyanide ligand binding mode. CySH reaction with $[Au(CN)_4]^-$ was montored by ^{13}C NMR (Figure 4.27c), CySH-^{13}C3 signal shifted downfield (from δ = 25 ppm to δ = 38 ppm) indication of oxidation into L-cystine, while Au(III) were reduced to Au(I) i.e. $[Au(CN)_2]^-$ (δ = 156 ppm) [41,103]. Triplet signal at 112 ppm was assigned to cyanogen that may be reductively eliminated from auricyanide as was suggested by Ettorre *et al* [42] for the reductive elimination of Br_2 from $[Au(CN)_2Br_2]^-$. It is observed here that the signal corresponding to cyanogen (δ = 112 ppm) appears as a deceptive triplet due to fully labeled cyanogen which has a spin system of AA'XX'. The large one bond ^{13}C-^{13}C coupling in the spin system provides a deceptive triplet [112-114].

No intermediates were detected from reaction, so it is not possible to shed light on the reaction mechanism. So further experiments where CySH-^{13}C3 were reacted with $[Au(CN)_4]^-$ at 0.5:1 equivalents, 1:1 equivalents; and at 2:1 equivalents, respectively, CySH-^{13}C3 were used for better monitoring of reaction in the NMR time scale, UV spectrophotometry was also employed for reaction monitoring in this work.

Table 4.27: ^{1}H NMR chemical shifts of $[Au(CN)_4]^-$ complex with CySH ligands at 1:1 ratio in D_2O at 25 ^{o}C, pD = 7.4.

	H2	**H3**
CySH	3.922	2.980, 2.904
$[Au(CN)_4]^-$ + CySH	4.045	3.295, 3.268

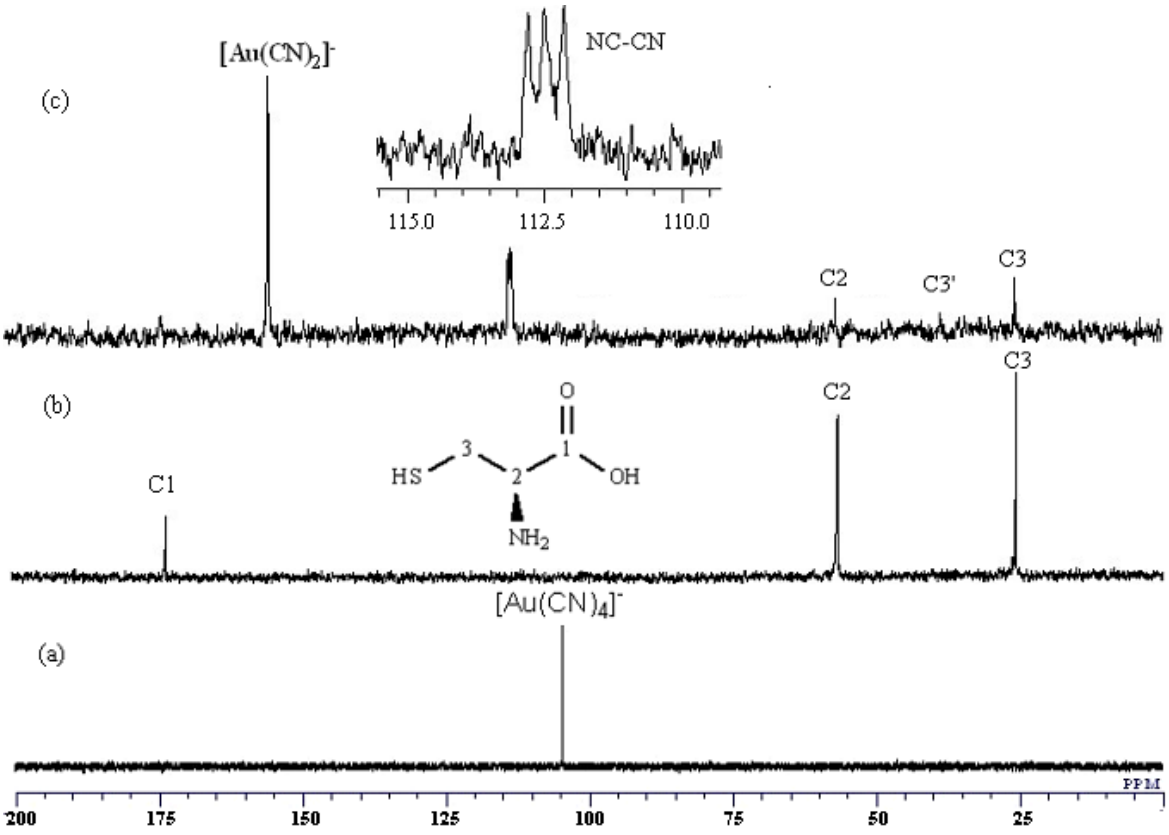

Figure 4.27: ^{13}C NMR of spectra for (a) $[Au(CN)_4]^-$ (b) CySH and (c) 30 hours after reaction with $[Au(CN)_4]^-$ at 2:1 ratio in D_2O at 25 ^oC, pD = 7.4.

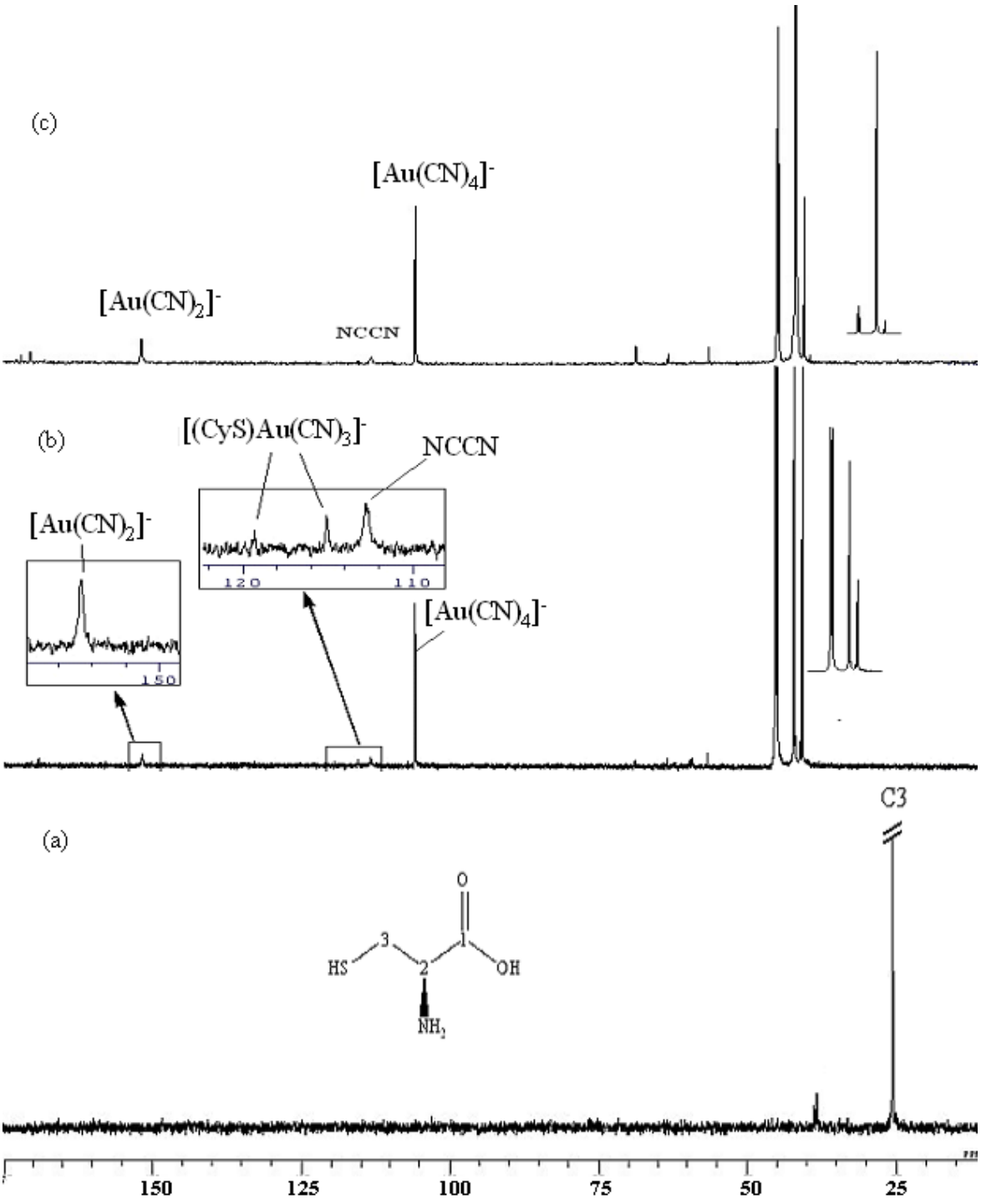

Figure 4.28: ^{13}C NMR spectra for $[Au(CN)_4]^-$ reaction with CySH-$^{13}C3$ at 1:0.5, (a) for CySH-$^{13}C3$ before reaction (b) 16 hours after reaction and (c) 36 hours after reaction, in D_2O and 25 ^oC, pD = 7.4.

Figure 4.28 presents ^{13}C NMR spectra for $[Au(CN)_4]^-$ reaction CySH at 1:0.5 ratio in D_2O at pD 7.4. A complete shift of C3 corresponding signal was observed right after mixing, which splits into four new signals. The signal at 33.0 ppm corresponds to mono-substituted complex $[(CyS)Au(CN)_3]^-$. The signal at 38.5 ppm is attributed to sulfenic acid [115]. These two signals are converted gradually to CyS-SCy (38.2 ppm) and L-cysteic acid ($CySO_3H$) (35 ppm). L-cysteic acid chemical shift was found almost the same as reported by Shaw *et al* after referencing to dioxin [57]. After 4 days all species were converted into L-cysteic acid (35 ppm).

Figure 4.29 shows CySH reaction with $[Au(CN)_4]^-$ at 1:1 ratio. CySH-C3 signal shifted downfield from 25 ppm (Figure 4.29b) to 33 ppm (Figure 4.29c). This is a result of fast cyanide exchange by CySH. Three signals correspond to cyanide were found in the spectrum (Figure 4.29c), i.e. $[Au(CN)_4]^-$ (δ = 104 ppm), $[Au(CN)_2]^-$ (δ = 156 ppm) and $[(CyS)Au(CN)_3]^-$ (δ = 115 ppm). It is observed that initially there is a decay of $[Au(CN)_4]^-$ in solution and then an increase (Figure 4.29c).

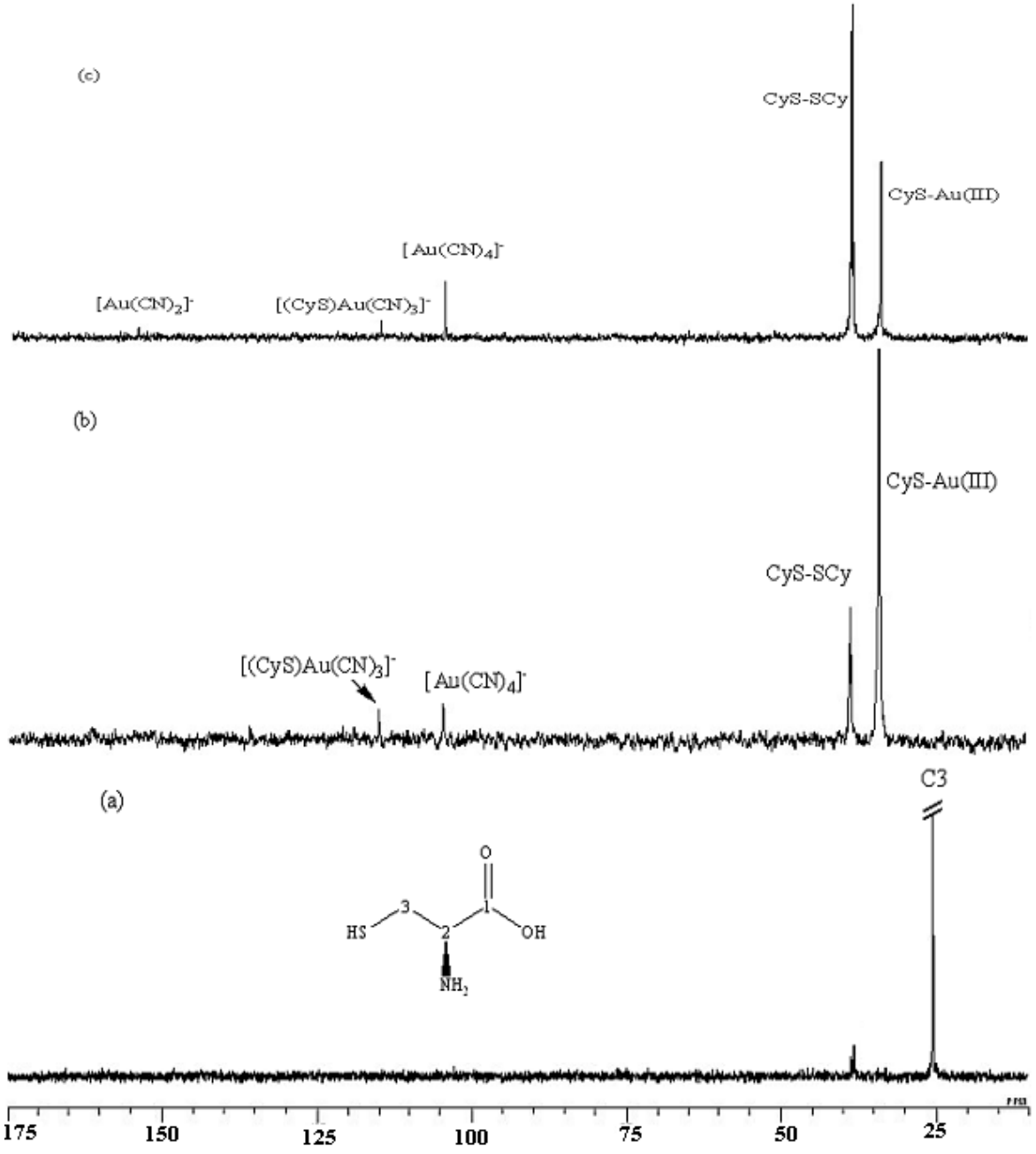

Figure 4.29: ^{13}C NMR spectra for $[Au(CN)_4]^-$ reaction with CySH-$^{13}C3$ at 1:1, (a) for CySH-$^{13}C3$ before reaction (b) 2 hours after reaction and (c) 24 hour after reaction, in D_2O and 25 ^oC, pD = 7.4.

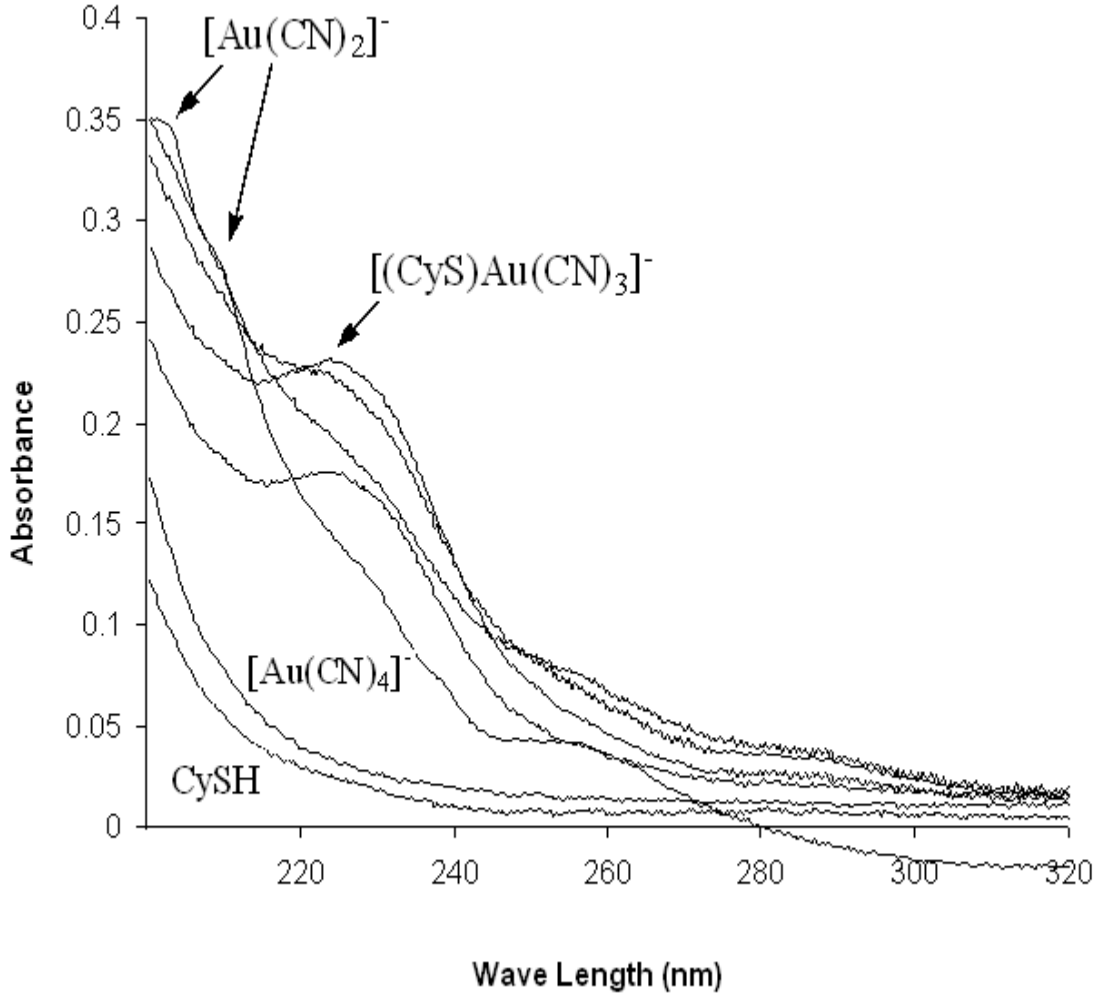

Figure 4.30: UV absorbance for $[Au(CN)_4]^-$ (0.1 mM) and CySH (0.2 mM) before and after reaction at 1:0.5 mole ratio, in the range 200-310 nm at 25 ^oC and pH = 7.4 (0.1M phosphate buffer).

Figure 4.30 shows the UV absorption spectra for $[Au(CN)_4]^-$ reaction with CySH at 1:0.5 mole ratio (pH = 7.4). Absorption band at 228 nm (band I) corresponding to $[(CyS)Au(CN)_3]^-$ increased to its maxima in 3 minutes and then started converting gradually into set III bands after 8 days, indicating that the reaction is mainly progressing through one cyanide ligand exchange that is followed by $[Au(CN)_2]^-$ formation with very low formation of the second cyanide exchange procedure, as shown by the very small intensity signal at ~ 289 nm in figure 4.30 .

Based on earlier discussion, the following mechanism (Scheme 4.23) can be suggested.

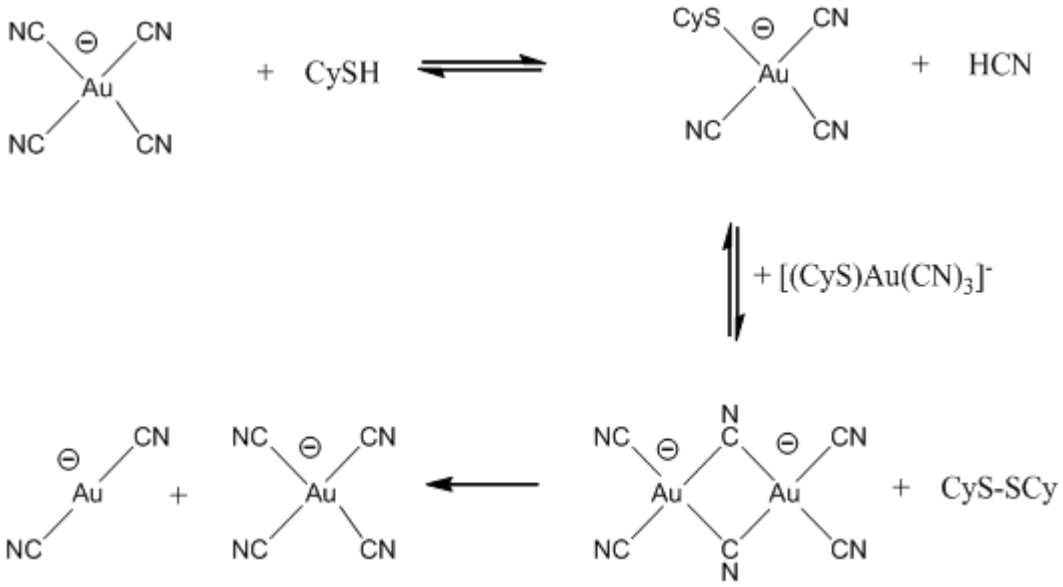

Scheme 4.23: Suggested mechanism for $[Au(CN)_4]^-$ reaction with CySH at 1:0.5 and 1:1 mole ratio.

The reaction starts with cyanide exchange by CySH (Scheme 4.23), the corresponding signal is shown as CyS-Au(III) UV absorption at 228 nm. Bands at

250 and 289 nm, corresponding to the disubtitute product, were not intense this indicate that CyS-SCy produced by reductive elimination from two adjacent $[(CyS)Au(CN)_3]^-$ species resulted in the formation of CyS-SCy and hexacyano-diaurate (Scheme 4.23), which undergoes disproportionation reaction into $[Au(CN)_4]^-$ and $[Au(CN)_2]^-$ in solution. The corresponding ^{13}C NMR signals appear at 104.6 and 156 ppm respectively. The increase of cyanide signal intensity at 104.6 ppm (corresponding to $[Au(CN)_4]^-$) is an indication of the disproportionation mechanism occurrence, that could regenerate the $[Au(CN)_4]^-$ in solution after its consumption during the initial step.

Figure 4.31 shows UV absorption spectra for $[Au(CN)_4]^-$ reaction with CySH at 1:1 ratio pH = 7.4. A faster reaction occurs compared at 1:0.5 ratio (Figure 4.30). Bands from 204 to 240 nm were distinct after 4 hours, while mono- and di-substitution corresponding bands are concurrently present in solution. So it can be concluded that the reaction proceeds through two subsequent cyanide exchange steps by CySH followed by reductive elimination when relatively higher CySH ratio is present in solution.

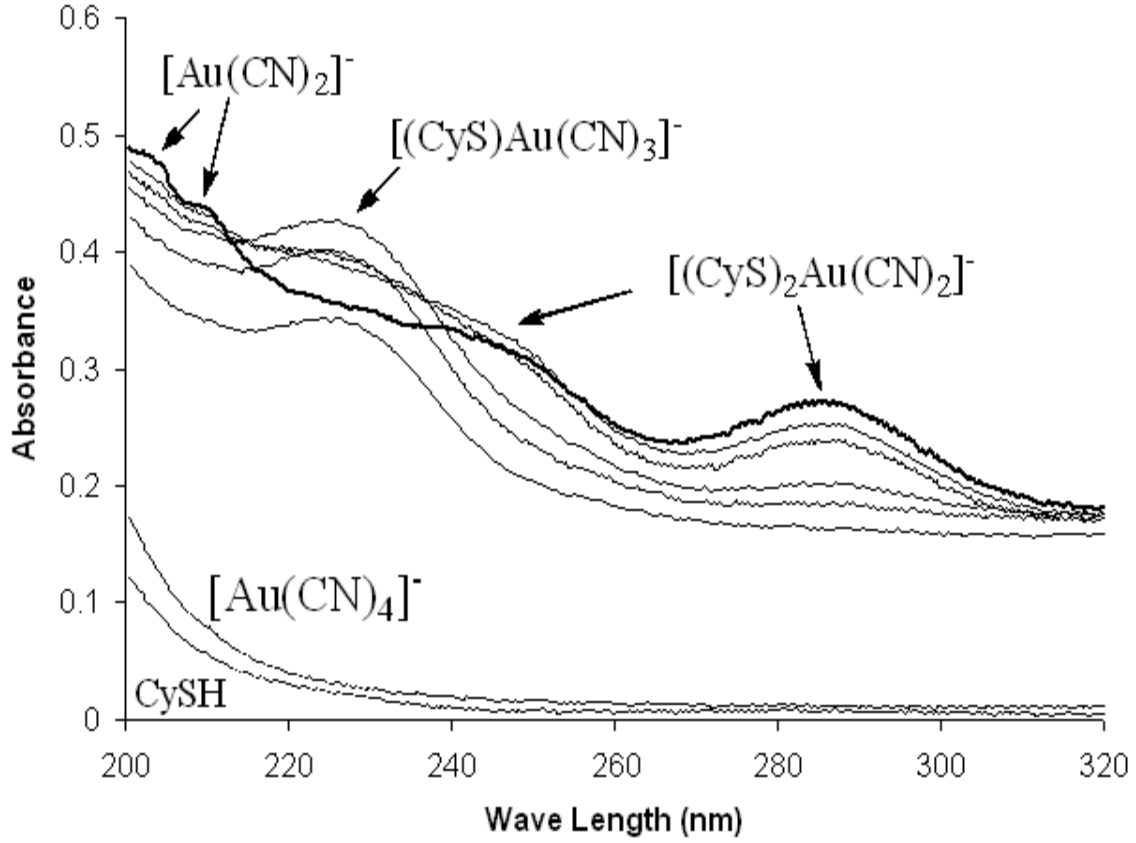

Figure 4.31: UV absorbance for $[Au(CN)_4]^-$ (0.1 mM) and CySH (0.2 mM) before and after reaction at 1:1 mole ratio, at 25 ^oC and pH = 7.4 (0.1 M phosphate buffer).

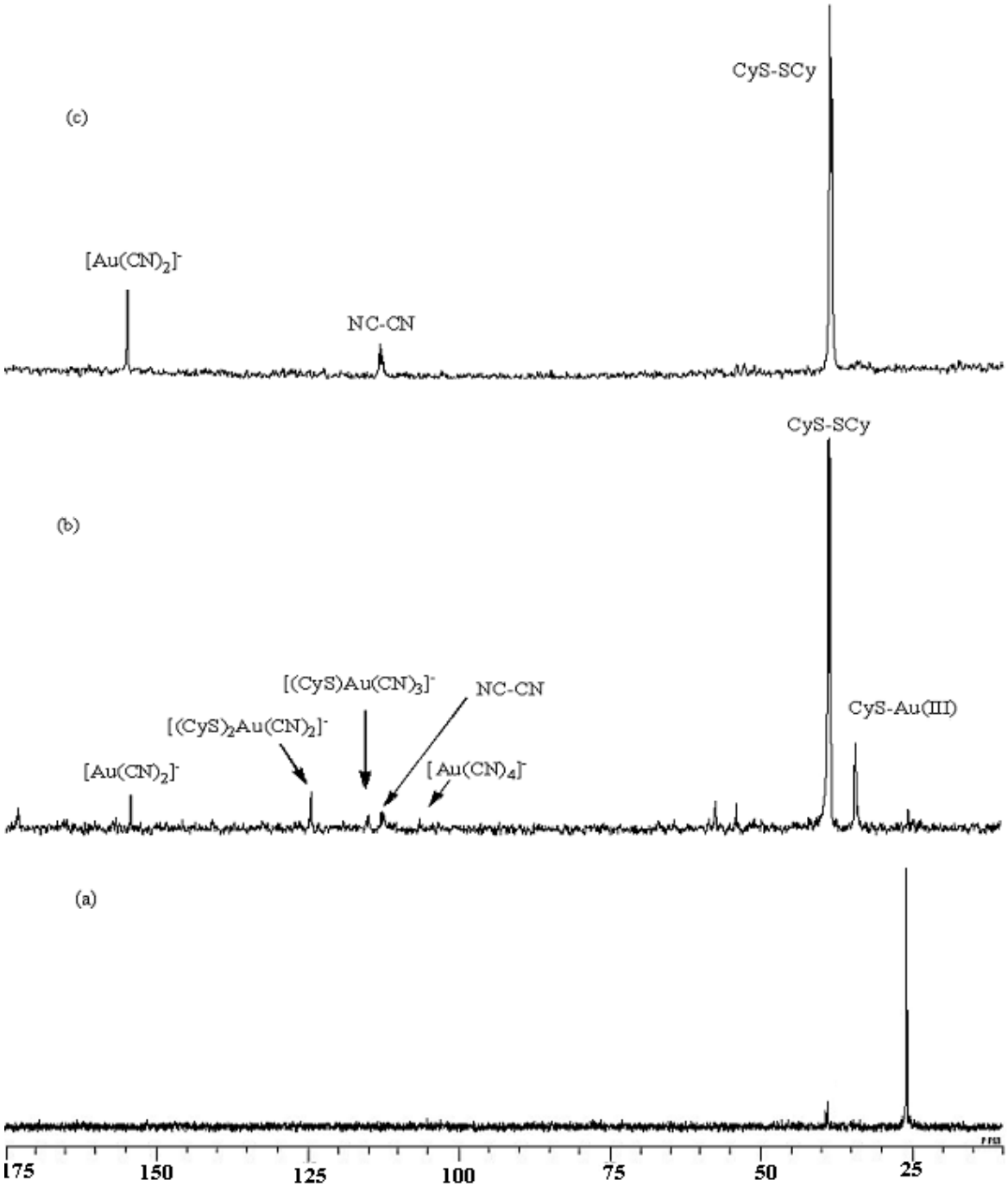

Figure 4.32: ^{13}C NMR spectra (a) for CySH-$^{13}C_3$, (b) after 14 hours of reaction with $[Au(CN)_4]^-$ at 1:2 ratio, in D_2O and 25 ^oC, pD = 7.4 and (c) after 32 hours of reaction.

Figure 4.32 shows representative ^{13}C NMR spectra for $[Au(CN)_4]^-$ reaction with CySH at 1:2 ratio. It is noted that CyS-SCy formation was much faster when CySH mole ratio increased. Five signals in the cyanide region were found in figure 4.32b that represent five different species in solution; $[Au(CN)_4]^-$ (δ = 104 ppm), $[(CyS)Au(CN)_3]^-$ (δ = 115 ppm), $[(CyS)_2Au(CN)_2]^-$ (δ = 124 ppm), NCCN (δ = 112 ppm) and $[Au(CN)_2]^-$ (δ = 156 ppm). The spectra show the formation of cyanogen (δ = 112 ppm), $[Au(CN)_4]^-$ reduction into $[Au(CN)_2]^-$, CySH oxidation into CyS-SCy and formation of $[(CyS)_2Au(CN)_2]^-$ in solution (Figure 4.32c).

$[Au(CN)_4]^-$ reaction with CySH was also carried out at 1:2 ratio and monitored by UV spectrophotometry, as shown in figure 4.33. The first exchange of cyanide take place very fast so the band at 228 nm appears at the first minute of reaction time and then it is converted into bands at 250 and 289 nm in less than 3 minutes, indication of very fast consecutive exchange reaction, that converted later, after 30 min into bands from 204 to 240 nm corresponding to reduced $[Au(CN)_2]^-$ resulting from fast reduction reaction when increased CySH mole ratio found in solution.

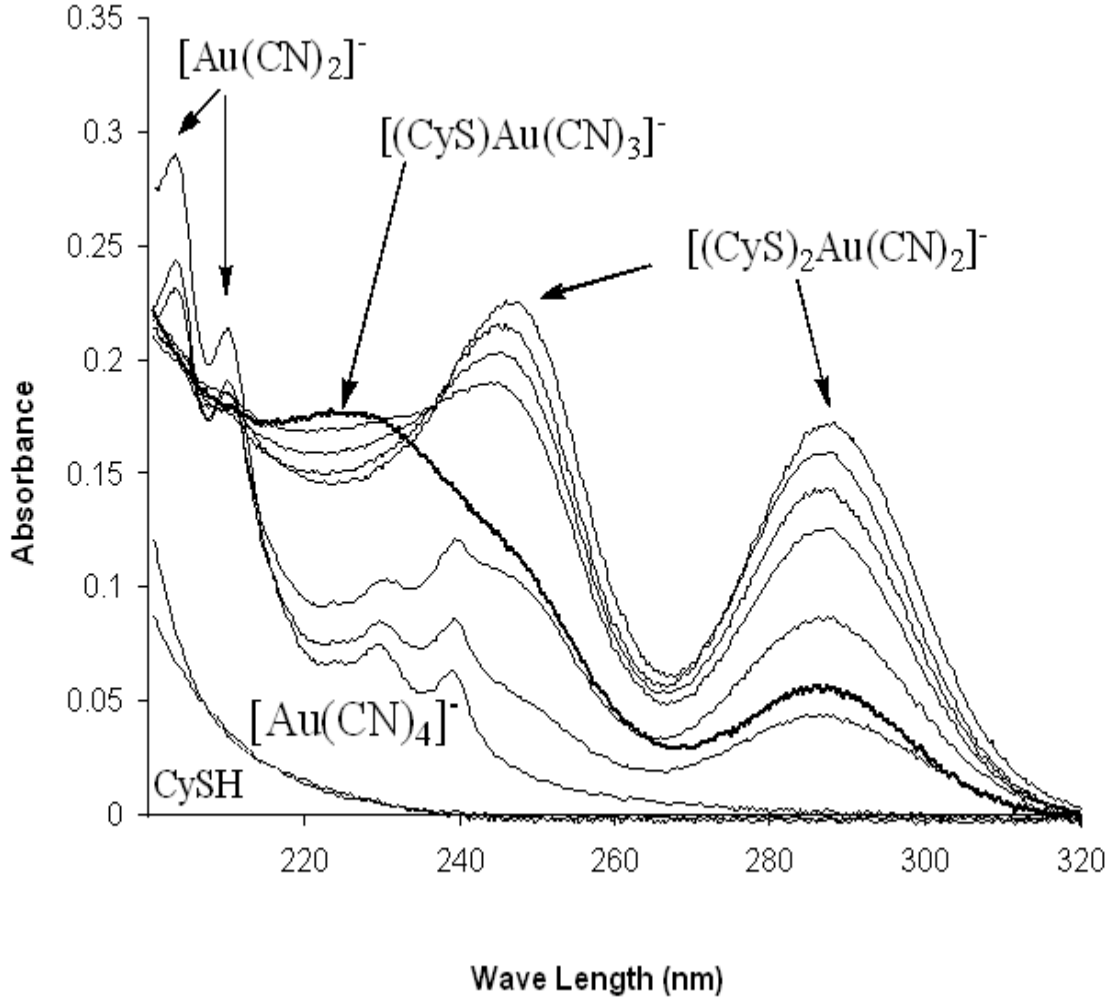

Figure 4.33: UV absorbance for $[Au(CN)_4]^-$ (0.1 mM) and CySH (0.2 mM) before and after reaction at 1:2 mole ratio, at 25 ^oC and pH= 7.4 (0.1 M phosphate buffer).

UV absorption study reveals that the reaction proceeds through two consecutive cyanide ligand exchanges that take place very fast. However, some stability is found for $[(CyS)_2Au(CN)_2]^-$ because of *cis/trans* isomerization. The complex ion in the *cis* form will go very fast into reductive elimination reaction of CyS-SCy, while gold(III) reduced to gold(I) in the form of $[Au(CN)_2]^-$. Suggested mechanism is shown in scheme 4.24.

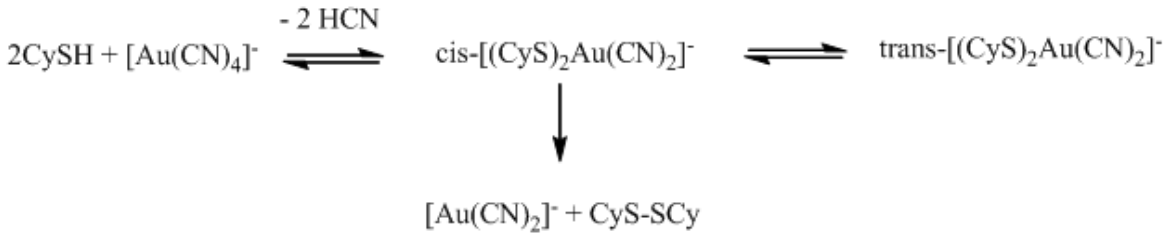

Scheme 4.24: Suggested mechanism for $[Au(CN)_4]^-$ reaction with CySH at 1:2 equivalents.

It can be concluded that higher CySH mole ratio in reaction leads to fast exchange of two cyanide ligands that is followed by reductive elimination of CyS-SCy from *cis*-$[(CyS)_2Au(CN)_2]^-$ and formation of $[Au(CN)_2]^-$.

4.7.2 Glutathione (GSH) interaction with $[Au(CN)_4]^-$

GSH interaction with $[Au(CN)_4]^-$ has been studied in aqueous solution at pH 7.4 by Shaw and co-workers [16]. They reported that the formation of $[(SG)Au(CN)_3]^-$, and $[(SG)_2Au(CN)_2]^-$ species were detected by mass spectrometry. In this work, interaction of GSH with auricyanide was studied using ^1H and ^{13}C NMR to compare the mode of interaction with other thiols.

Figure 4.34 shows ^{13}C NMR spectra of GSH before and after reaction with $[Au(CN)_4]^-$. The C5 signal shifted down-field from 27 to 39 ppm, while C4 signal shifted up-field, indicating the formation of GSSG, the corresponding signals are C4' and C5' respectively [16,41]. Cyanide signals appeared at 156 ppm corresponding to $[Au(CN)_2]^-$ and at 112 ppm and 115 ppm corresponding to NC-CN and $[(GS)Au(CN)_3]^-$, respectively.

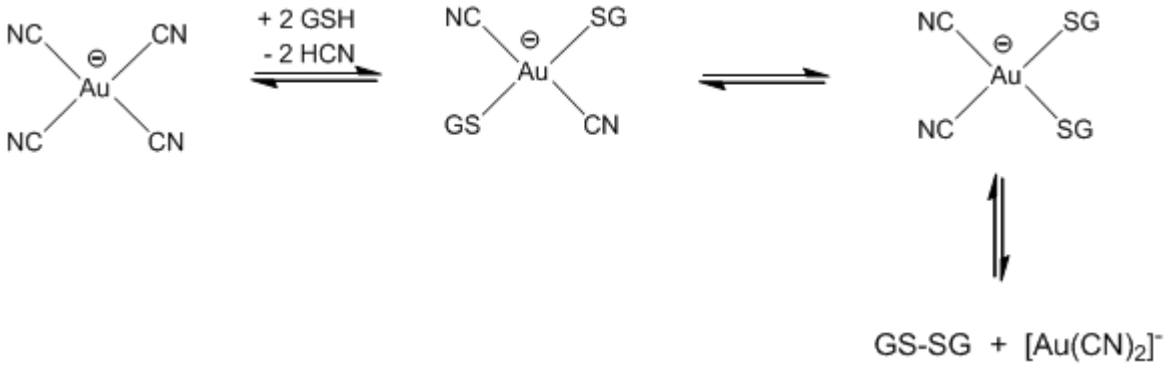

Scheme 4.25: Suggested mechanism for $[Au(CN)_4]^-$ interaction with GSH in D_2O and 25 ^oC.

Scheme 4.25 shows a suggested mechanism that may account for GSH reaction with $[Au(CN)_4]^-$. The reaction starts with two cyanide exchange by GSH, *cis/trans* isomerization takes place next, and the *cis*-isomer will go further into disulfide dimer by reductive elimination.

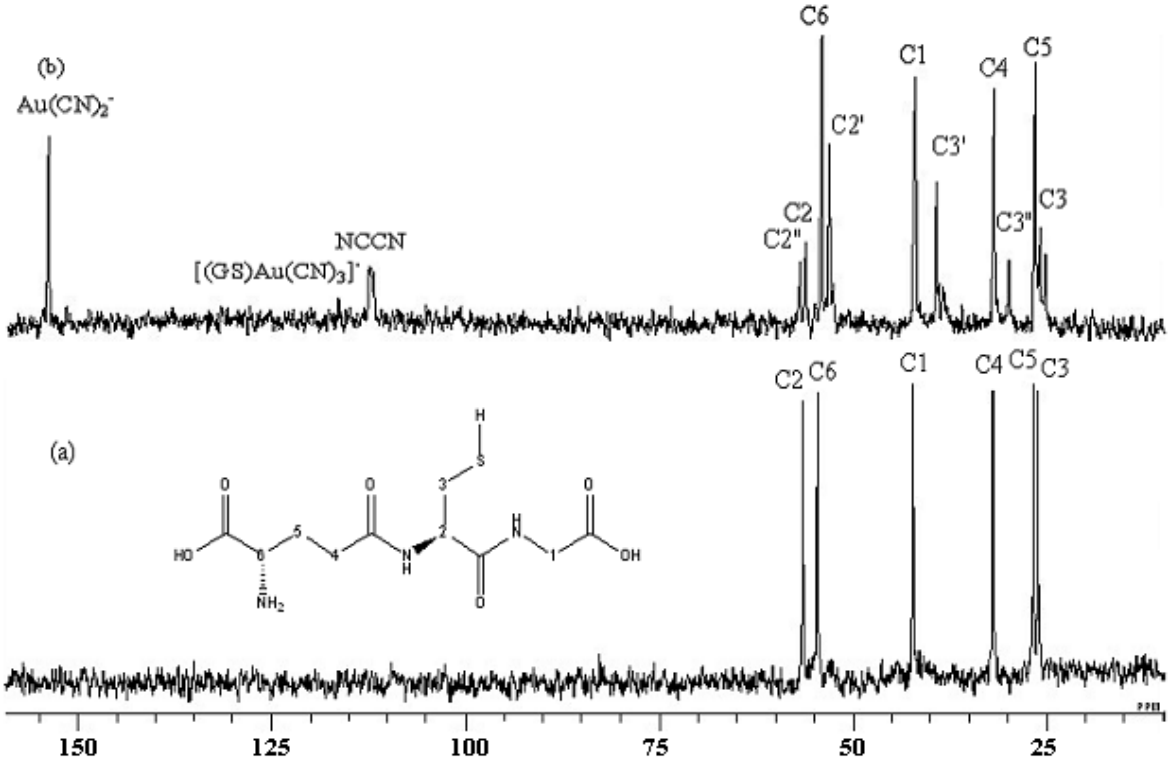

Figure 4.34: ^{13}C NMR of GSH (a) before and (b) after reaction with $[Au(CN)_4]^-$ oxidation at 2:1 ratio in D_2O at 25^oC, pD = 7.4.

4.7.3 Captopril (Cap) interaction with $[Au(CN)_4]^-$

Cap isomerizes in solution into *cis* and *trans* isomers. The ratio of these isomers depends mainly on solution pH [100a-c], however, at pH 7.4 both isomers exist with a higher concentration of *trans* isomer (~ 60 %) as reported by Rabenstein *et al* [100d]. Oxidation of cap by H_2O_2 was carried out, and the products were analyzed using ^{13}C NMR.

Figure 4.35 shows ^{13}C NMR spectra for cap oxidation by H_2O_2. C2 was found to be shifted up-field upon dimerization into di-sulfide while C3 and Cα show down-field shift after oxidation.

^{13}C NMR spectra for cap reaction with $[Au(CN)_4]^-$ in the range (0 to 75 ppm) are given in figure 4.36. The C3 signal was found to shift according to the earlier mentioned mechanism and it was also dependent on the thiol ligand ratio in solution (Figure 4.36b). It was shifted down-field to 41.6 ppm corresponding to Cap-S-S-Cap (Figure 4.36c). Three distinct cap species were found in solution according to spectrum (Figure 4.36c). They correspond to un-reacted cap (referred as C3), cap di-sulfide (referred as C3') and $[(cap)Au(CN)_3]^-$ species (referred as C3''). Other signals corresponding to *cis/trans* cap isomers were also found.

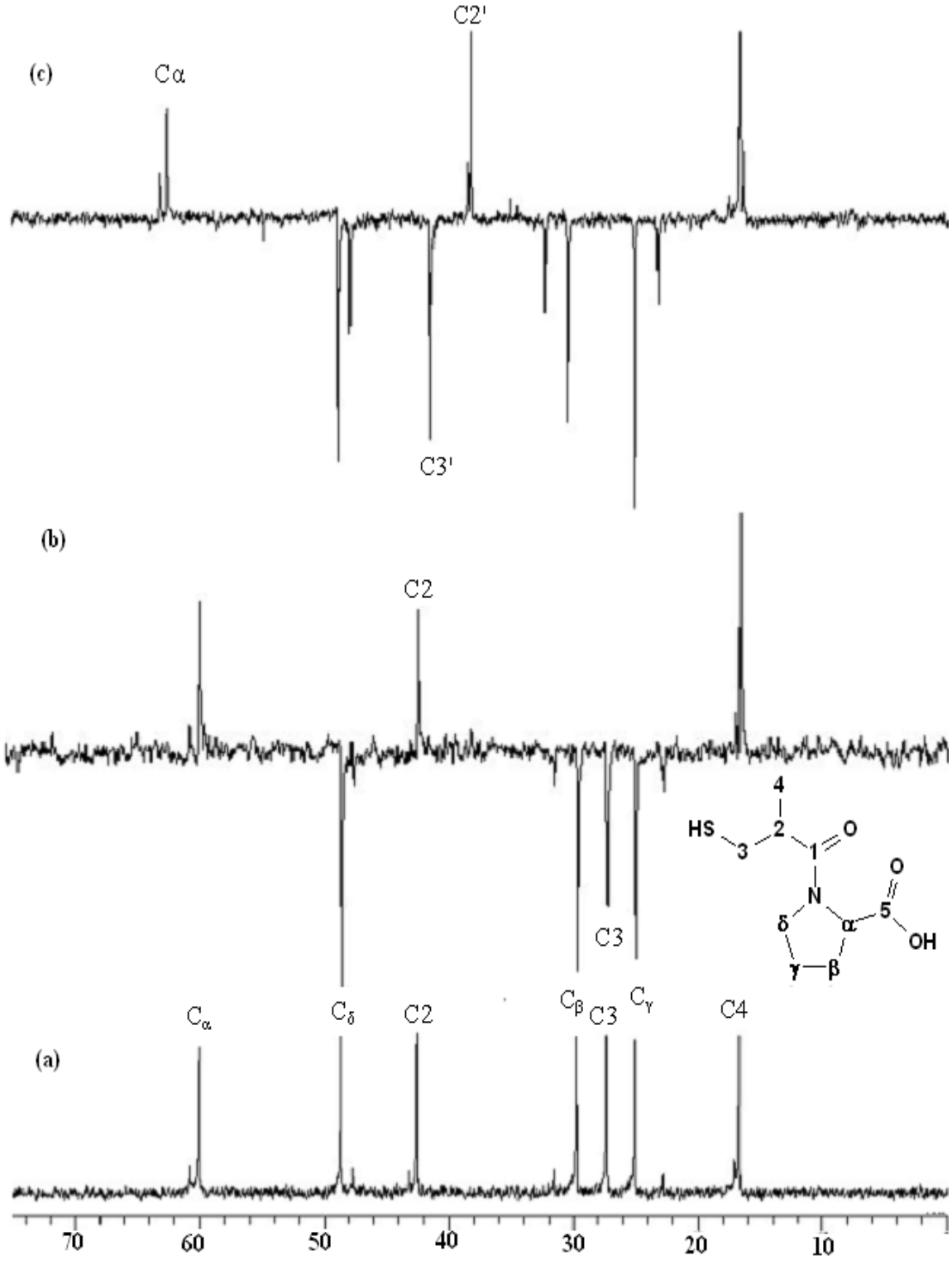

Figure 4.35: ^{13}C NMR spectra for (a) cap (b) cap DEPT spectrum and (c) DEPT spectrum after reaction with H_2O_2 in D_2O at 25 ^oC and pD = 7.4.

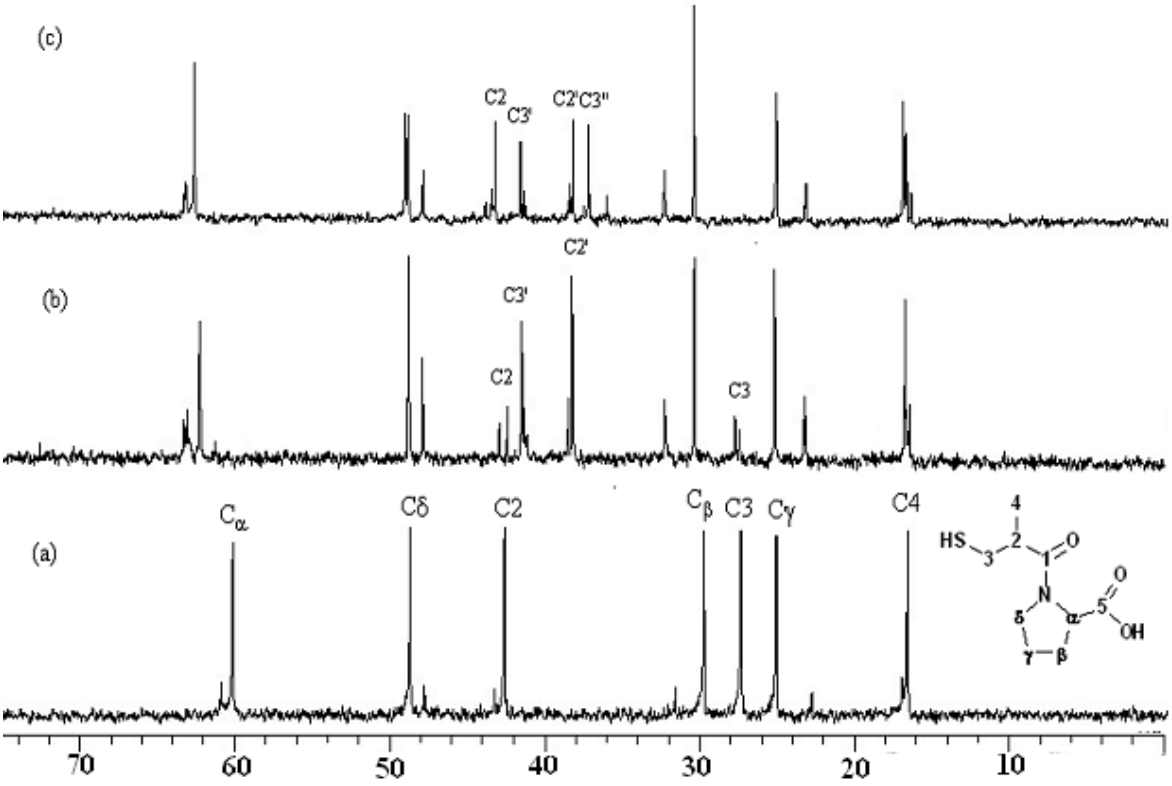

Figure 4.36: ^{13}C NMR (0-75 ppm) spectra (a) for 100 mM cap before reaction, (b) after reaction with $[Au(CN)_4]^-$ at 1:1 ratio and (c) after reaction with $[Au(CN)_4]^-$ at 0.5:1 ratio, in D_2O at 25 ^oC and pD = 7.4.

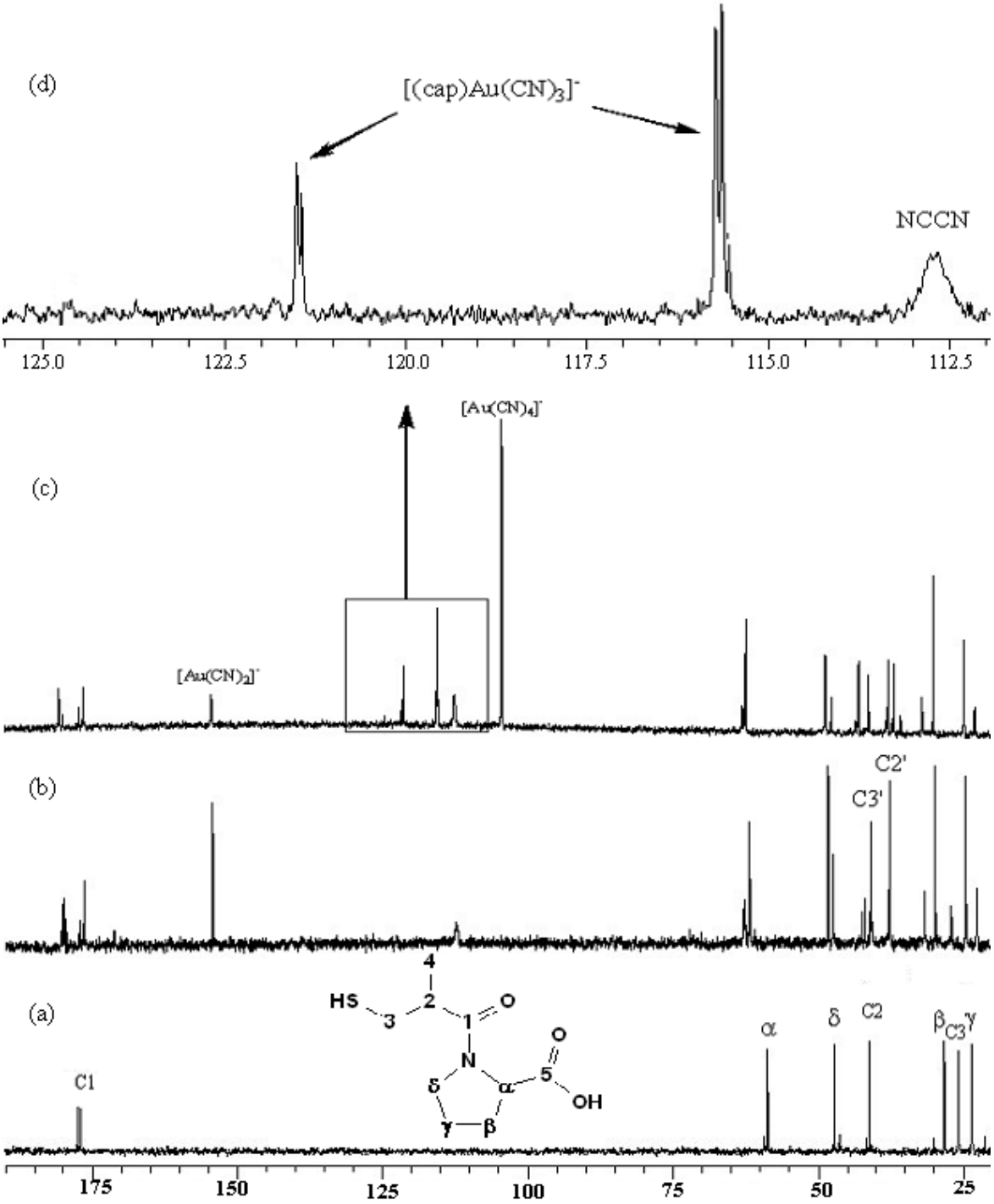

Figure 4.37: ^{13}C NMR (0-190 ppm) spectra (a) for 100 mM cap before reaction, (b) after reaction $[Au(CN)_4]^-$ at 1:1 ratio, (c) and (d) after reaction with $[Au(CN)_4]^-$ at 0.5:1 ratio, in D_2O at 25 ^oC and pD = 7.4.

Figure 4.36 shows ^{13}C NMR for cap reaction with $[Au(CN)_4]^-$ at 1:0.5 mole ratio. Four cyanide signals were found in spectrum corresponding to $[Au(CN)_2]^-$ (δ = 156 ppm), cyanogen (δ = 112 ppm) and (115, 120 ppm respectively) to *cis/trans*-$[(cap)Au(CN)_3]^-$. These results indicate similar reaction intermediates to other thiols described earlier. The reaction proceeds through two cyanide substitution by cap at higher cap/ Au(III) ratio, while mono-substitution reaction takes place followed by disproportionation at lower ratio as shown earlier for CySH reaction with $[Au(CN)_4]^-$. The observation of similar intermediates produced during CySH, cap and GSH reactions with $[Au(CN)_4]^-$ at the similar mole ratio leads to the conclusion that similar reaction mechanisms may be found for all these reactions, with high dependence on species ratio.

4.8 L-Methionine (Met) and DL-Se-Methionine (Se-Met) interactions with $[Au(CN)_4]^-$

Met and Se-Met interactions with auricyanide were studied by mixing the reactants at different ratios. No change was observed at all ratios by both ^1H and ^{13}C NMR at pDs 7 and 12. The monitoring by NMR was continued for more than three days but no reaction was found to take place in solution. However, when Se-Met was mixed with auricyanide at 2:1 ratio and pD adjusted to 12 and stirred for three days, a little $[Au(CN)_4]^-$ was reduced to $[Au(CN)_2]^-$ while Se-Met was oxidized into Met-SeO [116-118]. Signals were assigned by comparison with Se-Met oxidation experiment with hydrogen peroxide [90,119,120]. Se-Met binding to gold metal center is expected to be through selenium or amine group as reported from computational work for methyl-seleno-cysteine by Shoeib *et al* [34].

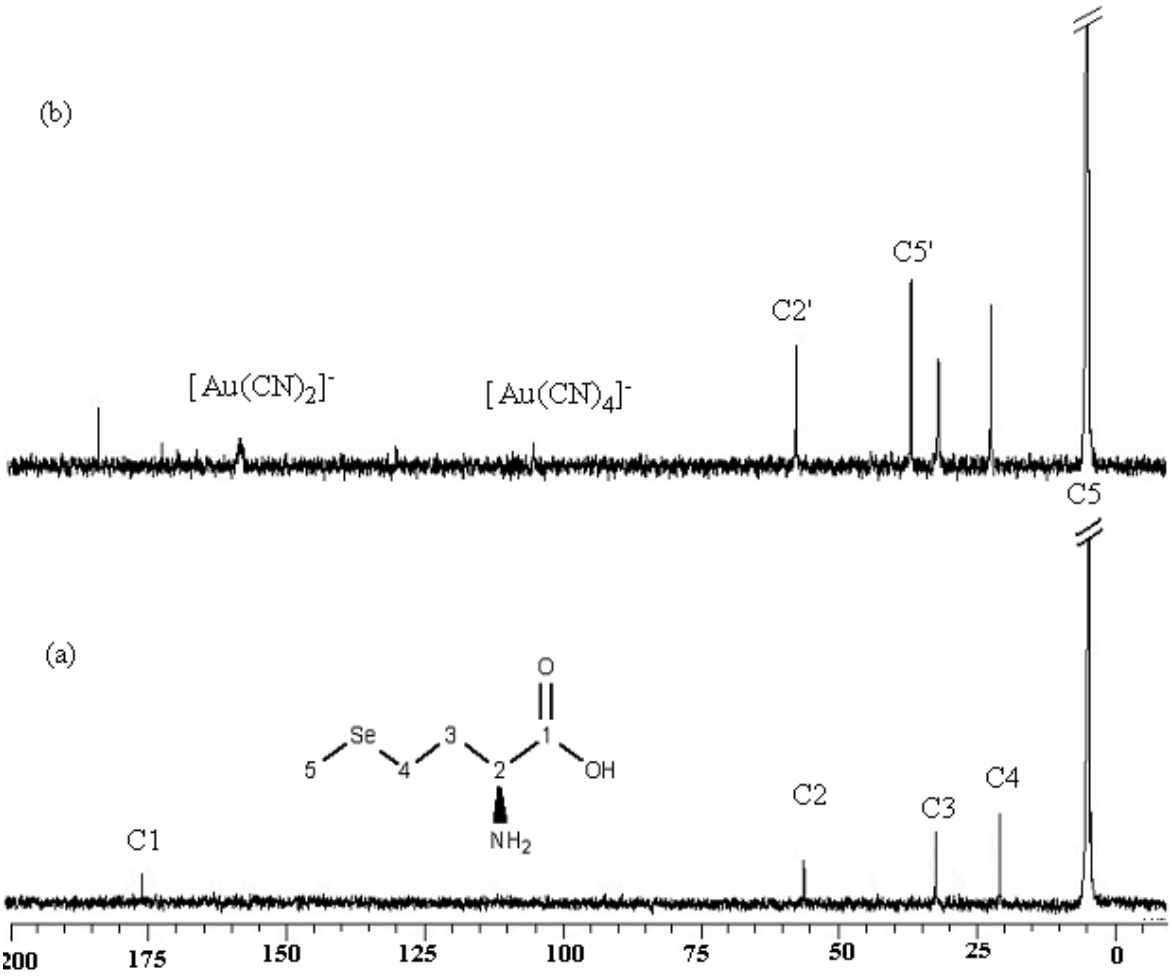

Figure 4.38: ^{13}C NMR for (a) Se-Met-$^{13}C_5$ before and (b) after reaction with $[Au(CN)_4]^-$, in D_2O at 25 ^oC and pD = 12.0.

Met was reported to be highly reactive with Au(III) ion [121], but it showed no reactivity toward auricyanide even after stirring for five days. So it can be concluded that cyanide ligand causes stabilization for Au(III) against reaction with Met and Se-Met [51]. Lack of reactivity of Met and Se-Met with $[Au(CN)_4]^-$ complex could be rationalized in terms of the strong Au(III)-CN bond at pH 7.4. However, at high pH (~12), hydrolysis facilitates the with ligand exchange reaction as shown by El-Khateeb *et al* [26]. They studied the interaction of Met with *cis*-platin (*cis*-$[(NH_3)_2PtCl_2]$) and reported that Met binding to *cis*-platin complexes proceeds first by hydrolysis of the complexes followed by Met-S ligation. The carboxylate and amine groups enhanced the reaction by electrostatic stabilization of the metal ligand complex [122,123].

4.9 Synthesis and characterization of aurocyanide and auricyanide complexes of phosphines, phosphine sulphides and phosphine selenides.

All reactions were done by mixing $KAu(CN)_4$ with L ligands at 1:2 ratios. Product chemical formula, melting point and elemental analysis are given in Table 3.4. IR and UV spectra were measured for all synthesized complexes, the results are as follows. All gold(III) complexes show at least one band corresponding to cyanide in the range 2179-2192 cm^{-1}, this band was missing from all gold(I) complexes.

a. $[((2\text{-}CN\text{-}Et)_3P)_2AuCN]$

IR spectrum shows CN stretching band at 2245 and 2240 cm^{-1} corresponding to the cyanide at $(2\text{-}CN\text{-}Et)_3P$ ligand, and the other band at 2136 cm^{-1} corresponding to CN stretching as reported earlier by Yangyuoru *et al* [16], which is characteristic

of the Au(I)-cyanide. UV spectrum shows absorption bands at 204-240 nm, characteristic for Au(I)-cyanide [16,41].

b. $[(Cy_3P)_2AuCN].KCN$

IR spectrum shows a band at 2140 cm^{-1} that is characteristic for Au(I)-CN moiety in complex [124], and UV absorption spectrum shows absorption bands in the range of 204 to 240 nm corresponding to Au(I)-CN [5].

c. $[(Me_3PS)_2Au(CN)_3]$

IR data show a stretching frequency for the cyanide group at 2186 that is characteristic for Au(III)-CN moiety in complex, and no distinct signals were found in UV.

d. $[(Et_3PS)_3Au(CN)_3]$

IR vibration spectrum shows a band at 2186 cm^{-1} assigned to Au(III)-CN, and no distinct signals were found in UV.

e. **$[(Ph_3PS)_2Au(CN)_3]$**

IR spectrum showed cyanide stretching frequency at 2192 cm^{-1} that is characteristic of Au(III)-CN, and no distinct signals were found in UV.

f. $[(Me_3PSe)_2Au(CN)_3]$

IR data show a CN stretching bands at 2179 cm^{-1}, characteristic of Au(III)-CN, and no distinct signals were found in UV corresponding to Au(I)-CN.

g. **$[(Ph_3PSe)Au(CN)_3].KCN$**

IR data shows CN stretching band at 2189 cm^{-1} characteristic of CN bound to Au(III) as shown by Yangyuoru *et al* [16,41].

Phosphine ligand reaction with $[Au(CN)_4]^-$ results in formation of tri-coordinate complexes. Three coordinate complexes are common in literature for gold phopshine complexes as reported for $[Au(PPh_3)_2Cl]$ complexes by Tiekink *et al* [125]. Several three-coordinate gold(I) phosphine complexes were also reported by Parish [126].

Table 4.30 shows the IR and Far-IR data of the synthesized complexes. $KAu(CN)_4$ complex showed stretching band at 2189 cm^{-1} that correspond to stretching band of Au(III)-CN moiety [16,41], while $KAu(CN)_2$ IR spectrum shows stretching band at 2140 cm^{-1} [124,128,129]. The difference in cyanide IR stretching bands could be a result of more electron density in gold(I) complex that lead to more π–back donation to the cyanide ligand, this increase the occupation in the cyanide anti-bonding (π^*) orbital's, weakening the CN bond. Less number of coordinating ligand in $KAu(CN)_2$ will also increase the electron back donation from metal to ligand, so Au-C get shorter and C≡N get longer these conclusion is consistent with the IR and Far-IR bands for $K[Au(CN)_2]$, the reverse is true for $K[Au(CN)_4]$ complex.

Table 4.28: Solid (KBr-disk) IR and (CsCl-disk) Far-IR data for Au(III) and Au(I)-cyanide complexes with phosphines.

Complex	$\nu_{(C\equiv N)}$, cm^{-1}	$\nu_{(Au-C)}$, cm^{-1}	$\upsilon_{(P-S/P-Se)}$, cm^{-1}	$\upsilon_{(P-S-Au/P-Se-Au)}$, cm^{-1}
$K[Au(CN)_2]$	2140	471*	-	-
$K[Au(CN)_4]$	2189	418	-	-
$[((2\text{-}CN\text{-}Et)_3P)_2AuCN]$	2245, 2240, 2136	437	-	-
$[(Cy_3P)_2AuCN].KCN$	2140	419	-	-
$[(Me_3PS)_2Au(CN)_3]$	2186, 2171, 2148	413	565	557
$[(Et_3PS)_3Au(CN)_3]$	2186, 2144, 2064	419	537	536
$[(Ph_3PS)_2Au(CN)_3]$	2192	410	540	516
$[(Me_3PSe)_2Au(CN)_3]$	2179, 2144, 2066	411	562	516
$[(Ph_3PSe)Au(CN)_3].KCN$	2189, 2143	419	562	561

* As reported by Bowmaker *et al* [127].

Table 4.29: ^{31}P and ^{13}C NMR chemical shifts of synthesized complexes in CD_3OD at 25 ^{o}C.

	L-Au-(CN), ^{13}C $\delta_{(C\equiv N)}$ (ppm)	**L, ^{31}P δ (ppm)**	**L-Au-(CN), ^{31}P δ (ppm)**
KCN	163.60		
$KAu(CN)_2$	152.21		
$KAu(CN)_4$	103.47		
$[((2\text{-}CN\text{-}Et)_3P)_2AuCN]$	120.17, 120.05	-32.21	49.36
$[(Cy_3P)_2AuCN]$	113.04	58.51	61.33, 60.50
$[(Me_3PS)_2Au(CN)_3]$	-	33.68	33.75
$[(Et_3PS)_3Au(CN)_3]$	116.72	56.82	51.41
$[(Ph_3PS)_2Au(CN)_3]$	106.21	43.83	43.85
$[(Me_3PSe)_2Au(CN)_3]$	-	-	48.55
$[(Ph_3PSe)Au(CN)_3].KCN$	117.91	35.89	35.89

Signals correspond to cyanide in IR and UV could be employed for the determination of gold atom oxidation state; cyanide ligand in gold(III) complexes shows at least one stretching band in the range 2192-2186 cm^{-1}, while these band is absent from all gold(I) complexes. The cyanide signal in gold(I) complexes show stretching band at 2142-2136 cm^{-1}, and UV spectroscopy show four absorption bands from 204-240 nm in UV spectrum as was shown by Yangyuoru *et al* [41], this band used as an indication of the gold oxidation state in complex , these bands were absent in UV of gold(III) complexes.

Far infrared of phosphines complexes must be interpreted with caution because of the bending vibrations absorb lower than 550 cm^{-1} of Phenyl-P-Phenyl [130]. Far-IR data shows Au-C bond vibration frequency in $K[Au(CN)_4]$ complex at 418 cm^{-1}, while in $K[Au(CN)_2]$ show vibration frequency at 471cm^{-1} [127]. Difference in stretching bands between the two complexes is due to stronger Au(I)-C bond that cause shift to higher wave number, while the Au(III)-C bond is expected to be longer and a red shift was expected. This interpretation is fully consistent with the experimental results. This property could also be used as criteria to distinguish gold oxidation states in complexes. Table 4.28 shows blue shift of the Au-C stretching band in gold(I) complexes while red shift were observed for gold(III) complexes.

IR stretching band of P-S and P-Se [131] shows decrease in vibration frequency upon complexation. This could be due to electron donation from sulfur and selenium to the metal this enhance π-back donation and lead to more electron density on the π* orbital, that weaken P-S and P-Se bonds after complexation.

^{13}C and ^{31}P NMR chemical shifts are given in Table 4.29. ^{13}C NMR chemical shift of the cyanide ligand in complex was useful in the identification of gold oxidation state in complex. Canumalla *et al* [103] reported that cyanide signal in the complex Au(III)-CN appeared at ~115 for *cis* and 120 for *trans* in D_2O for mono-substituted complex $[LAu(CN)_3]$ while at 125 ppm for the di-substituted complex $[L_2Au(CN)_2]^+$, on the other hand, chemical shift for cyanide ligand attached to gold(I) as $[Au(CN)_2]^-$ was reported to appear at 156 ppm in D_2O [132] and found to be 152 ppm in CD_3OD.

^{31}P NMR shows clear downfield shift for phosphines nuclei in complexes while no change in chemical shift by ^{13}P NMR were found when L is phosphine sulphides or phosphine selenides. This could be due to longer distance between the phosphine and metal, compared to phosphine ligands.

When gold(III) complexes were heated overnight at 60^oC and their ^{13}C NMR recorded, a resonance at 152 ppm appeared indicating reduction from gold(III) to gold(I) complexes.

Table 4.30: Solid-state ^{13}C Isotropic Chemical Shifts (δ_{iso}) and Principle Shielding Tensors (σ_{xx})[a] of cyanide in Gold(III)-tetracyanide complexes with phosphine ligands.

Complex		δ_{iso}[a]	σ_{11}	σ_{22}	σ_{33}	Span (Ω)[b]	Skew
$KAu(CN)_4$		110.0	236	138	-46	282	0.30
$(2\text{-}CN\text{-}Et)_3P$		122.9	231	207	-70	302	0.84
$[((2\text{-}CN\text{-}Et)_3P)_2AuCN]$	(i)	127.1	216	124	41	175	-0.05
	(ii)	123.7	266	193	-88	354	0.59
$[(Me_3PS)_2Au(CN)_2]CN$		105.3	222	123	-29	250	0.22
Ph_3PS		120.4	235	133	-7	243	0.16
$[(Ph_3PS)_2Au(CN)_3]$	(i)	122.9	218	138	13	204	0.22
	(ii)	128.5	220	149	17	203	0.30
Ph_3PSe		122.2	197	128	41	156	0.12
$[Ph_3PSeAu(CN)_3].KCN$	(i)	122.3	216	138	13	203	0.23
	(ii)	125.2	204	142	30	173	0.28

[a] $\delta_{iso} = (\sigma_{11} + \sigma_{22} + \sigma_{33}) / 3$, [b] Span ($\Omega$) = $\sigma_{33} - \sigma_{11}$ and [c] Skew (κ) = $3(\sigma_{22} - \delta_{iso}) / \Omega$, [64,65,133,134]

Solid state ^{13}C NMR data for the synthesized complexes are given table 4.30. Cyanide isotropic signal shows downfield shift in complex by comparison with $KAu(CN)_4$. In aryl- phosphine–gold complexes, cyanide ^{13}C NMR signal are interfering with aromatic ring multiplets, which are more intense, because of the hydrogen attached to carbon. This increase signal intensity in the CPMAS experiment, while cyanide carbon signal was of less intensity and broader. Downfield effect were observed in all complexes when compared to $[Au(CN)_4]^-$ before reaction. The same results found in solution and solid NMR. Another observation is the higher downfield shift found in solid NMR as effect of solvent effect absence, so less shielded nuclei found by solid state NMR as expected.

Solid state ^{31}P NMR isotropic signal and tensors (σ_{xx}) are given Table 4.31, isotropic signal of the complex show clear shift in case phosphine ligands, that in the phosphine complex the phosphorus is directly attached to the Au and as such we expect the largest change [135], while minor change or no change were found for phosphine sulphides and phosphine selenides complexes that are distant from binding site, another explanation for this could be the presence of p_π-d_π bond that will lead to the increase in electron density around phosphorus, thus augmenting its shielding [124].

Table 4.31: Solid-state ^{31}P NMR, isotropic chemical shifts (δ_{iso}) and principle shielding tensors (σ_{xx})[a] for gold(III)-tetracyanide complexes with phosphine ligands.

Compound	δ_{iso}	σ_{11}	σ_{22}	σ_{33}	Span (Ω)[a]	Skew
(2-CN-Et)$_3$P	-32.2	-15	-41	-41	26	-1.00
[((2-CN-Et)$_3$P)$_2$AuCN]	49.5	130	82	-63	193	0.50
[(Cy$_3$P)$_2$AuCN].KCN	50.3	112	98	-59	171	0.83
Et$_3$PS	59.7	109	96	-25	134	0.80
[(Et$_3$PS)$_3$Au(CN)$_3$]	59.8	107	97	-25	131	0.85
Ph$_3$PS	45.3	112	80	-56	167	0.62
[(Ph$_3$PS)$_2$Au(CN)$_3$]	45.4	107	86	-56	163	0.75
Ph$_3$PSe	36.8	111	51	-52	163	0.27
[Ph$_3$PSeAu(CN)$_3$].KCN	36.8	96	60	-46	143	0.50

[a] $\delta_{iso} = (\sigma_{11} + \sigma_{22} + \sigma_{33}) / 3$, [b] Span ($\Omega$) = $\sigma_{33} - \sigma_{11}$ and [c] Skew (κ) = $3(\sigma_{22} - \delta_{iso}) / \Omega$, [64,65,133,134]

4.10 Gold(III)-tetracyanide interaction with imidazolidine-2-thione ligand and its derivatives.

Interactions of gold(III)-tetracyanide with thione ligands were studied by mixing reactants at different ratios.

Imt reaction with H_2O_2 was carried out in D_2O and resulting spectra are presented in Figure 4.38, after oxidation signal at 179.6 ppm appeared in spectrum Figure 4.38b, that correspond to the C1 of the disulphide product, C2 signal split into two non-equivalent carbons after oxidation to the disulphide and two signals appeared at 46.2 and 44.8 ppm.

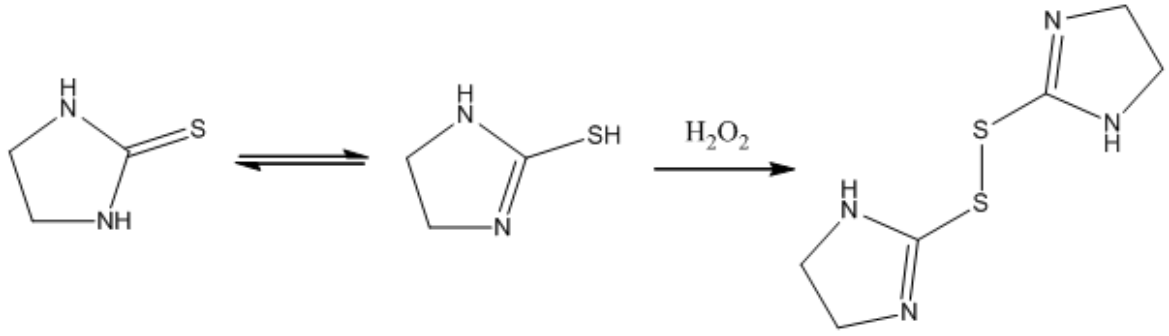

Scheme 4.26: Imt oxidation reaction by H_2O_2.

Figure 4.39 shows ^{13}C NMR spectra for Imt reaction with $[Au(CN)_4]^-$, no reaction was observed after mixing of components in both; D_2O and CD_3OD solutions. However heating of sample overnight at 45 ^oC in methanol-d_4 showed the formation of signal at 152 ppm that correspond to cyanide in $[Au(CN)_2]^-$ complex,(Figure 4.39b).

Table 4.32: ^{13}C NMR chemical shifts for thiones reaction with H_2O_2 and $[Au(CN)_4]^-$ complex at 25 ^oC in D_2O.

Compound	$\delta_{(CN)}$	C1	C2	C3	Ref.
KCN	164.49				[136]
$KAu(CN)_2$	154				[132]
$KAu(CN)_4$	104				[16,103]
Imt	-	182.08	45.37		
Imt + H_2O_2	-	179.63	46.21, 44.81		
$KAu(CN)_4$ + Imt	153.60	181.30	44.56		
Diaz	-	173.29	41.00	19.26	This work
Diaz + H_2O_2	-	171.30, 161.25, 159.70	40.11, 39.92, 37.49	25.73, 21.03, 18.53	
$KAu(CN)_4$ + Diaz	118.78	177.62	41.66	20.53	
Diap	-	183.88	45.84	26.97	This work
Diap + H_2O_2	-	174.50	47.37	27.01	
$KAu(CN)_4$ + Diap	154.86, 134.55, 114.16, 112.96	186.04, 175.03	52-43	28-24	

Table 4.33: ^{13}C NMR chemical shifts for thiones reaction with $[Au(CN)_4]^-$ complex at 25 ^oC in CD_3OD.

Compound	$\delta_{(CN)}$, (ppm)	C1	C2	C3	Ref.
KCN	163.60				This work
$KAu(CN)_2$	153.41				[137]
$KAu(CN)_4$	103.47				This work
Imt	-	186.09	46.01		This work
$KAu(CN)_4$ + Imt	152.53	185.31	46.03		
Diaz	-	205.32	41.65	20.54	This work
$KAu(CN)_4$ + Diaz	134.82, 118.92	162.34,158.89	40.12	21.14, 19.51	
Diap	-	189.43	46.20	27.88	This work
$KAu(CN)_4$ + Diap	162,30, 153.06, 134.28, 114.56	171.32	45.98	30.92,27.42	

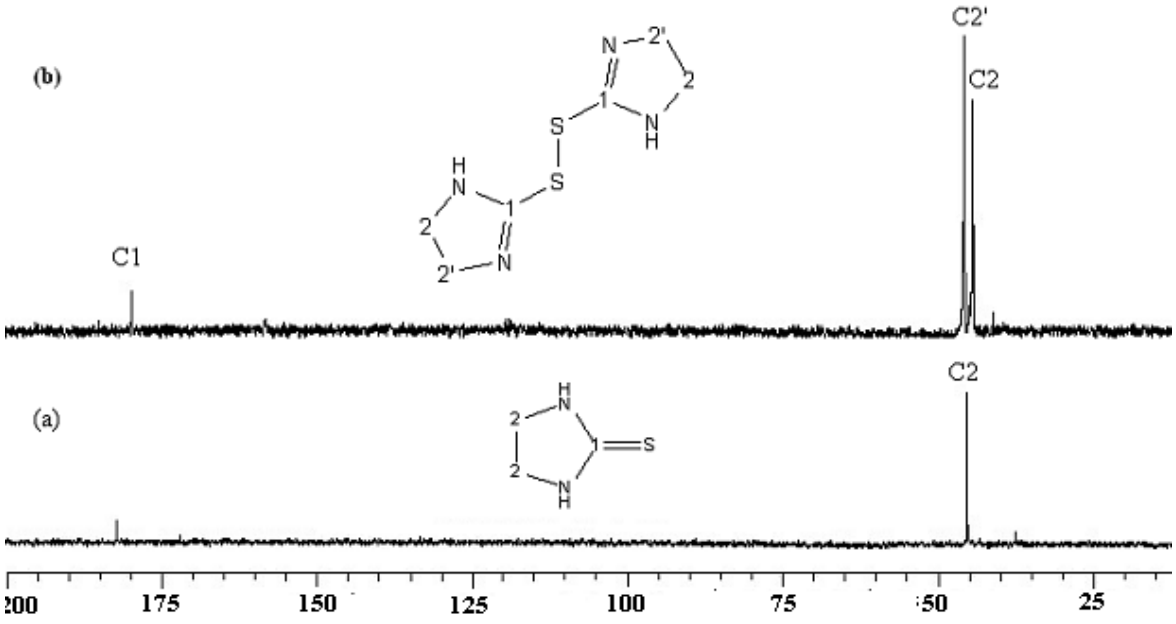

Figure 4.39: ^{13}C NMR spectra of (a) Imt before reaction, (b) after reaction with H_2O_2, at 25 ^{o}C.

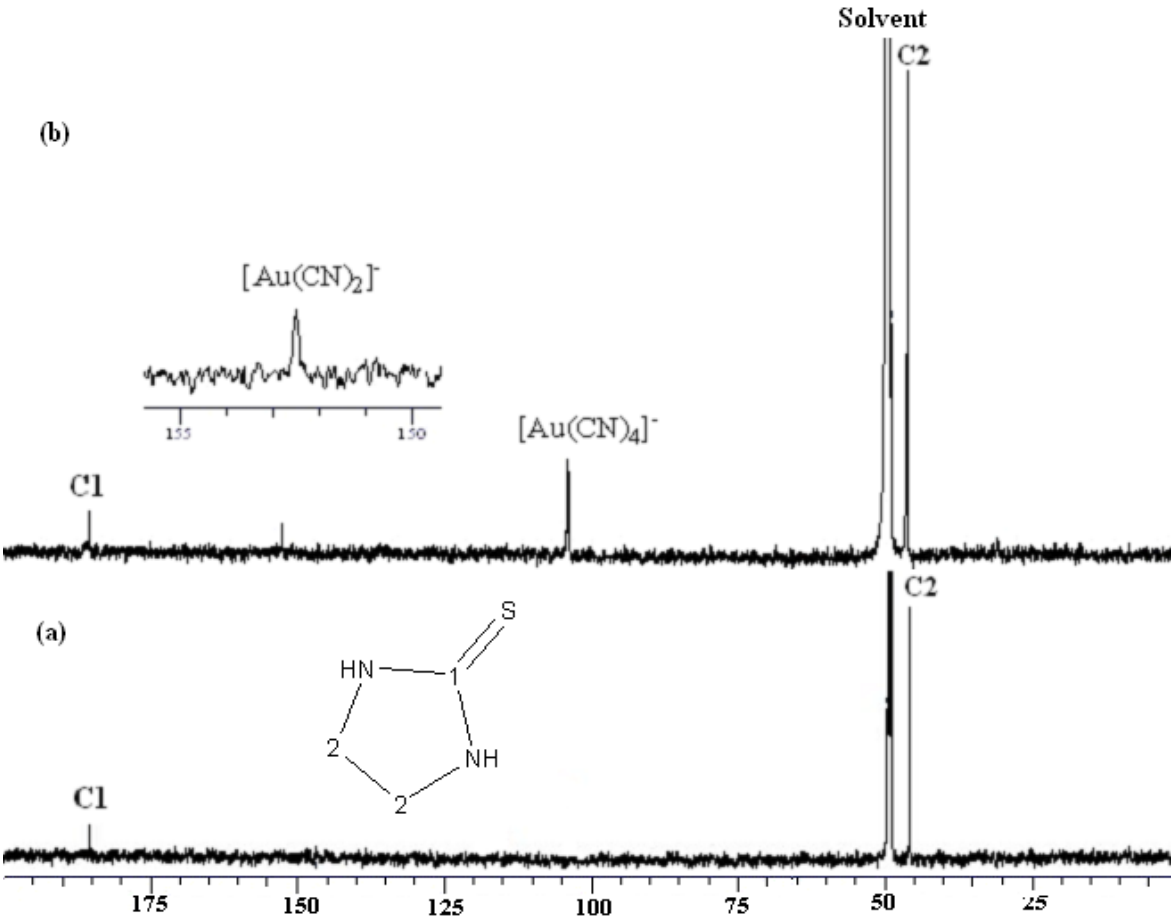

Figure 4.40: ^{13}C NMR spectrum for (a) Imt before reaction, (b) after reaction with $[Au(CN)_4]^-$, at 25 ^oC.

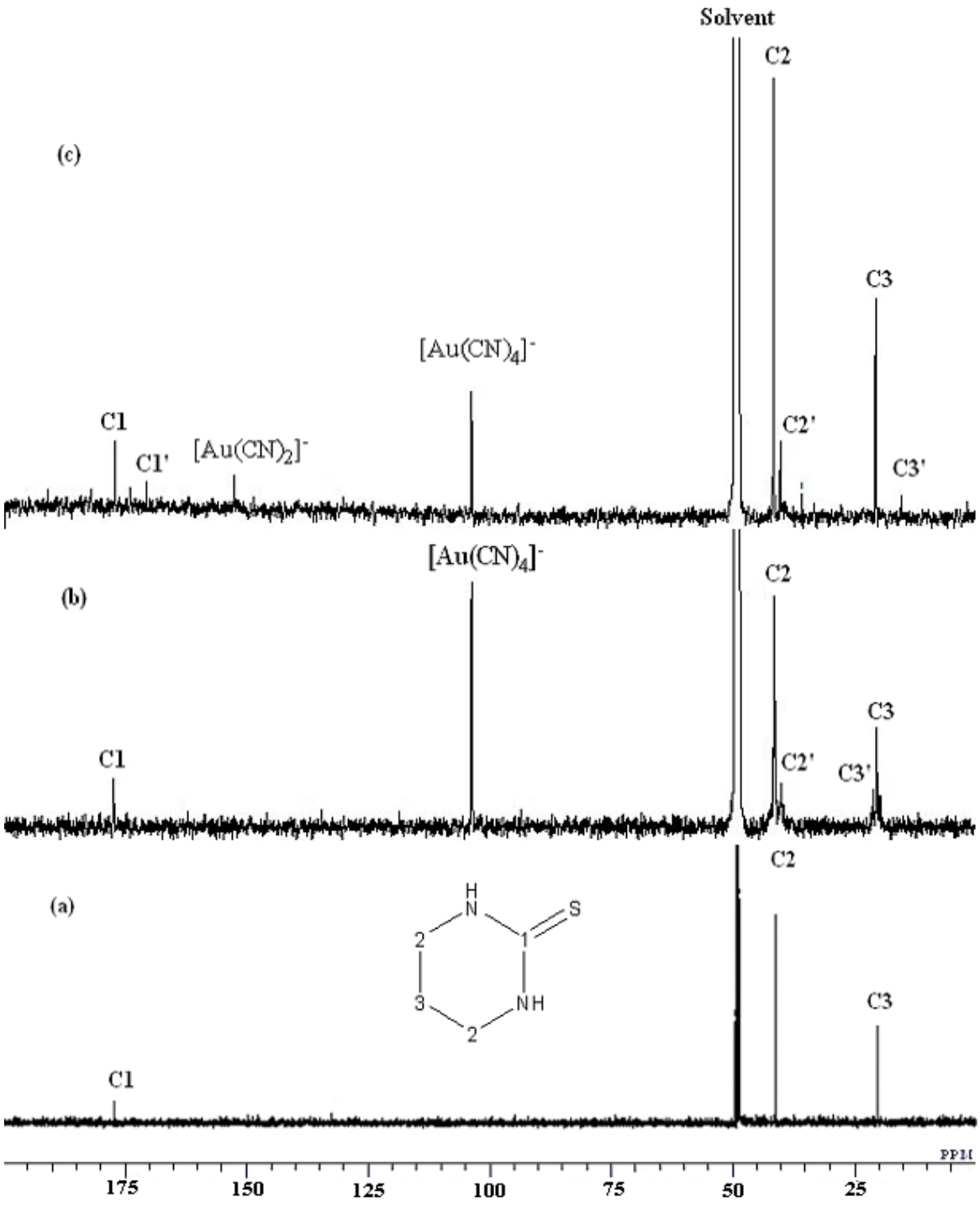

Figure 4.41: ^{13}C NMR spectra of (a) Diaz before reaction, (b) 20 hours after reaction with $K[Au(CN)_4]$ and (c) after 2 day and after heated for overnight at 45 ^{o}C in CD_3OD, at 25 ^{o}C.

Diaz was reacted with $[Au(CN)_4]^-$ in D_2O and in CD_3OD solution at 2:1 ratios. In both solvents no reaction was observed only after heating overnight at 45^oC indication of low reactivity of Diaz against $[Au(CN)_4]^-$. However, after heated redox reaction was observed that produce $[Au(CN)_2]^-$, (152 ppm) while oxidation of Diaz ligand is expected. Diaz-C1 signal shifted ~ 7 ppm up-field after reaction indication of more shielding of thione carbon.

Reaction of Diaz with $[Au(CN)_4]^-$ was repeated in D_2O at 2:1 ratios. Signals at 118 ppm was detected by ^{13}C NMR for cyanide, this was corresponding to $[(Diaz)_2Au(CN)_2]^+$, while C1 signal was shifted ~ 4 ppm downfield after reaction (δ = 178 ppm), corresponding chemical shifts are given in table 4.32.

Diaz reaction with H_2O_2 was carried out in D_2O, produced spectra are given in figure 4.41. Up-field shift of C1 signal is observed in figure 4.41b after reaction with H_2O_2, indication of more shielding on C1. This could be interpreted by the partial positive charge formed at C1 carbon after the formation of disulphide. Electron resonance from neighboring nitrogen atoms can increase electron density at C1. Similar trend were found for other thione derivatives after reaction with H_2O_2.

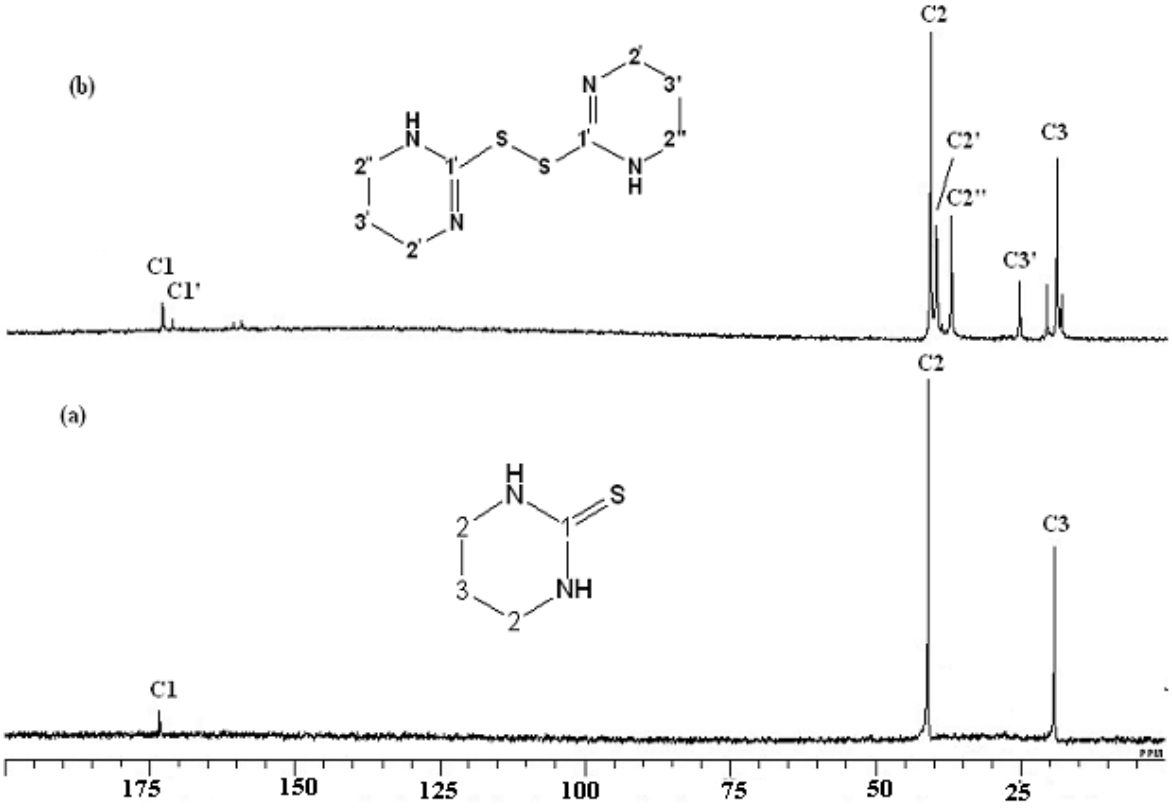

Figure 4.42: ^{13}C NMR spectra of (a) Diaz before reaction, (b) after reaction with H_2O_2, at 25 ^{o}C.

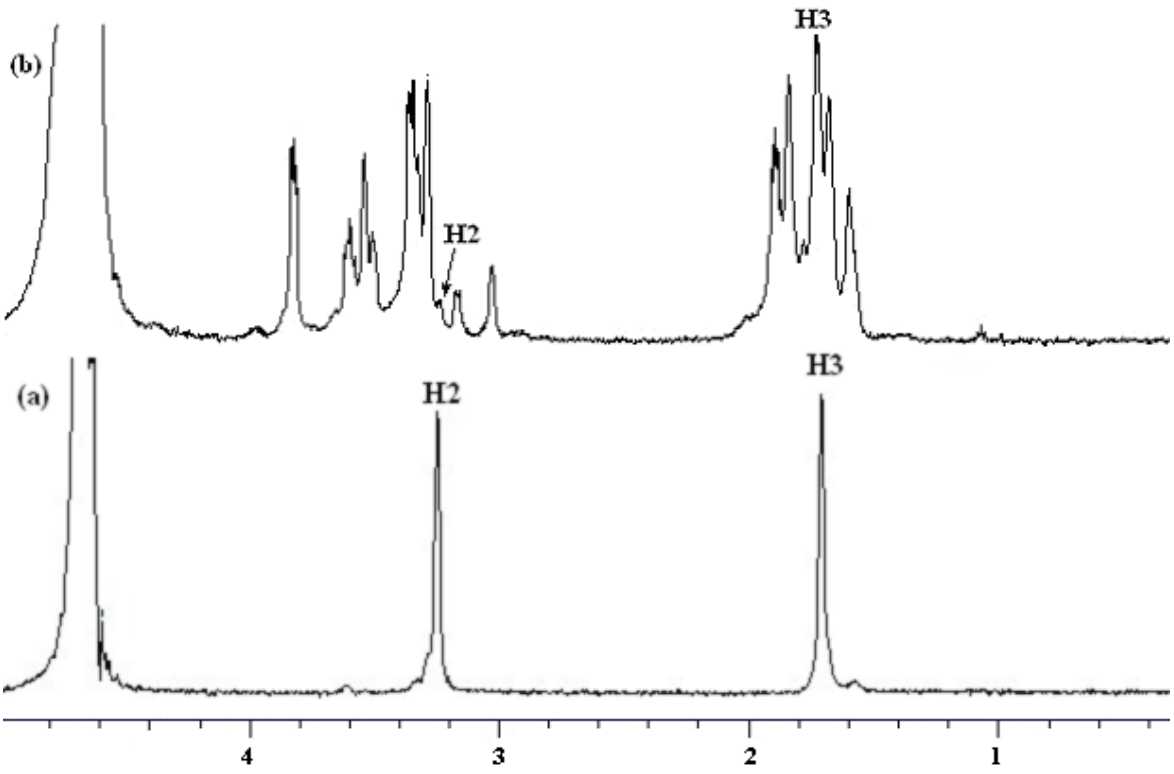

Figure 4.43: ^{1}H NMR spectra for (a) Diap before reaction, (b) after reaction with $K[Au(CN)_4]$ in D_2O, at 25 ^{o}C, pH = 7.4.

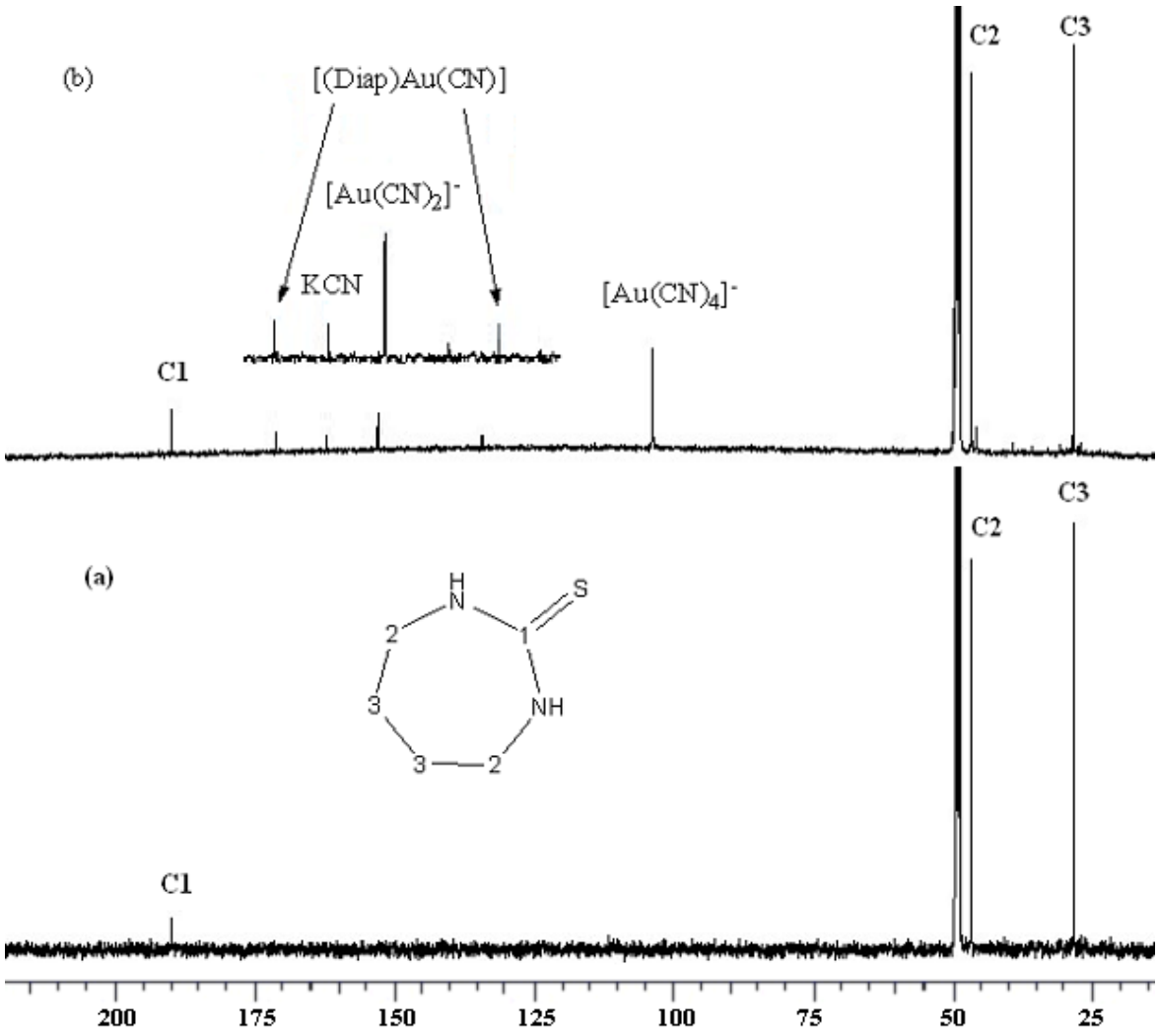

Figure 4.44: ^{13}C NMR spectra of (a) Diap before reaction, (b) after reaction with $K[Au(CN)_4]$ in CD_3OD, at 25 ^{o}C.

Diap was reacted with $[Au(CN)_4]^-$ at 2:1 ratios in both; D_2O and CD_3OD. Resulting ^1H and ^{13}C NMR spectra are presented in Figures 4.42-4. ^1H NMR spectra for diap reaction with $K[Au(CN)_4]$ in D_2O are presented in Figure 4.42. After 9 hours (Figure 4.42b) several species were formed in solution. This indicates that Diap is more reactive than both Diaz and Imt ligand. However, ^{13}C NMR spectra were more informative that showed several intermediates for Diap reaction with $[Au(CN)_4]^-$.

Figure 4.43 shows the spectra of Diap reaction $[Au(CN)_4]^-$ in methanol. In addition to non-reacted Diap, several species was detected by spectrum (Figure 4.43b); $[Au(CN)_2]^-$ (152 ppm), free KCN (164 ppm), [(Diap)Au(CN)] (135 ppm for cyanide signal and at 171 for C1').

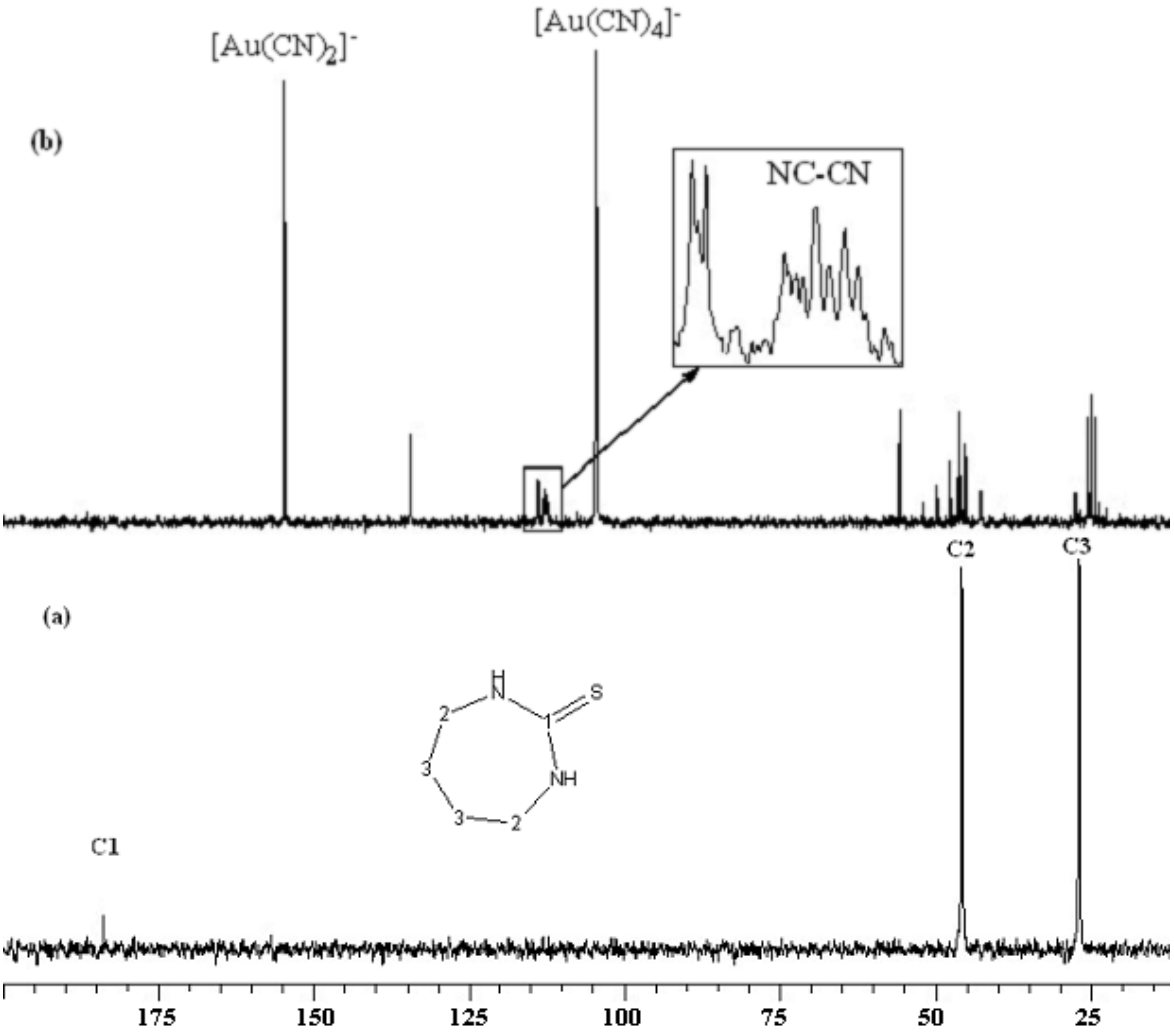

Figure 4.45: ^{13}C NMR spectra, (a) for Diap ligand before reaction, (b) after 9 hours, in D_2O at 25 ^{o}C, pH = 7.4.

Reaction of Diap with $[Au(CN)_4]^-$ was repeated in D_2O at 2:1 ratios. Similar species were obtained in aqueous, like in methanol, in addition to cyanogen at 113 ppm and $[(Diap)Au(CN)_3]$ at 114 ppm.

Diap exchanged cyanide ligand from gold(III)-tetracyanide complex. Multiplet signal at 113 ppm was attributed to cyanogen NCCN, which appear as a deceptive triplet due to fully labeled cyanogen which has a spin system of AA'XX'. The large one bond ^{13}C-^{13}C coupling in the spin system provides a deceptive triplet [43,44,114].

Doublet appear at 114 ppm was attributed to the mono-substituted complex, $[(Diap)Au(CN)_3]$ as shown by Yangyuoru *et al* [41]. Intense signal at ~155 ppm appeared in D_2O and 152 ppm in CD_3OD solution that correspond to $[Au(CN)_2]^-$ that produce after reduction of gold(III) into gold(I).

Diap oxidation by H_2O_2 in D_2O was carried out and corresponding ^{13}C NMR chemical shifts are given in Table 4.33 and reaction is the formation of the bis-diap.

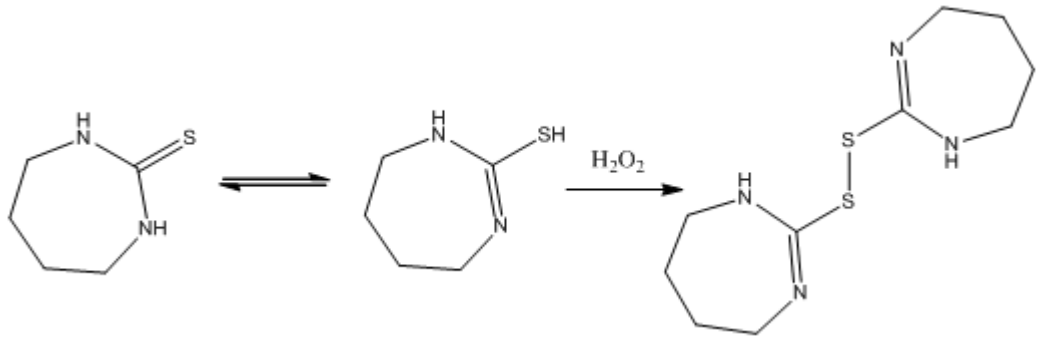

Scheme 4.27: Diap oxidation by H_2O_2.

CHAPTER FIVE

CONCLUSIONS

5.1 Synthesis and characterization of gold(III)-alkyldiamine complexes and their interactions with biologically important ligands.

1. Two series of gold(III) complexes were prepared with alkyldiamine ligands, the first contain various metalacycle rings of five to seven membered rings, the other contain N-mono and N,N'-disubstituted ethylenediamine ligands.
2. Data collected from both solid and solution NMR were complementary, e. g. butylenediamine complex, 1c, showed four signals in both solid and solution ^{13}C NMR, that reveals folded geometry of lower symmetry level for the seven membered rings.
3. ^{15}N NMR showed that seven membered ring has the highest electron donation.
4. Interaction of L-histidine and imidazole with [Au(*en*)Cl_2]Cl complex in solution at different pD's show [Au(*en*)Cl_2]$^+$ to be very stable at pD > 7.0 because of better donation through *en* ligand.
5. Reaction of L-histidine with [Au(*en*)Cl_2]$^+$ starts by binding reaction of histidine with Au(III) metal ion, while L-histidine oxidation products was detected after ~ 1 hour.
6. L-histidine binding reaction to [Au(*en*)Cl_2]$^+$ along with redox reaction were found to be directly proportional to solution pH.
7. Gold(III) ion suggested to be encapsulated by L-histidine by legation through imidazole-Ns in η^3 and amine-N as well as carboxylate group as counter ion.

This binding elucidates high gold histidine affinity, gold reduction and L-histidine oxidation at C6 position.

8. Increasing of the chelating alkyldiamine length in Au(III)-alkyldiamine complex, leads to the increase in reaction rate with L-histidine, *i.e. bn* > *pn* >> *en*.
9. Reaction of L-histidine with [Au(*en*)Cl_2]Cl was of first order with respect to each component at pH 2.9 and 25 ^{o}C.
10. Thiols were found to react with [Au(*en*)Cl_2]Cl, first by chloride ligand exchange by thiols then reductive elimination of the di-sulfide dimer, while Au(III) reduced into the Au(I) and *en* ligand dissociate from gold complex.
11. [Au(*en*)Cl_2]Cl reaction with Met and Se-Met was found to proceed through the exchange of chloride ligands, gold(III) reduction then precipitation of polymeric gold(I)-Met and gold(I)-Se-Met along with release of the *en* ligand from the gold complex.
12. Thio- and seleno-ethers react with [Au(*en*)Cl_2]Cl first by hydrolysis step then solvent exchange reaction with the thio or seleno-ether, that followed by another hydrolysis step and reductive elimination of the sulphoxide or seleno-oxide ligand from complex and lead finally to Au(III) reduction.

5.2 Gold(III)-tetracyanide complex and its interactions with biologically important ligands.

1. $[Au(CN)_4]^-$ shows high reactivity toward thiols. At low thiol ratio, the reaction proceeds through exchange of one cyanide ligands followed by reductive elimination of the disulfide from two mono-substituted intermediates produce in

formation of di-sulfide and hexa-cyano-diaurate that disproportionates into auocyanide and auricyanide.

2. At higher thiol ratio, reaction proceeds through two cyanide exchange followed by reductive elimination of the disulfide from *cis*-$[(RS)_2Au(CN)_2]^-$ intermediates along with Au(III) reduction to Au(I) in the form of $[Au(CN)_2]^-$.
3. Met and Se-Met were inert toward auricyanide at pH=7.4 while some reactivity was observed for Se-Met at pH=12.
4. Phosphine ligands can cause the gold(III) reduction into gold(I), while phosphine sulphides and phosphine selenides ligands exchange the cyanide ligands.
5. IR, Far-IR and UV spectroscopy can provide good and complementery data by which gold oxidation state could be characterized.
6. Diap reaction with gold-tetracyanide was faster than Diaz, which was much faster than Imt.
7. Thiones reaction with $[Au(CN)_4]^-$ was dependent on solvent, that redox reaction takes place readily in aqueous solution rather than in methanol.

CHAPTER SIX

REFERENCES

[1] L. Kelland ; Nature Rev.; **7** (2007)**,** 573.

[2] R.A. Alderden, D.H. Matthew and W.H. Trevor, J Chem. Edu, **83** (2006), 728.

[3] B. B. Krajčinović, G. N. Kaluđerović, D. Steinborn, H. Schmidt, C. Wagner, Ž. Žižak, Z. D. Juranić, S. R. Trifunović and T. J. Sabo, J. Inorg. Biochem., **102** (2008), 892.

[4] E. Wong and C.M. Giandomenico, Chem. Rev., **99** (1999) 2451.

[5] S. Zhu, W. Gorski, D. R. Powell, and J. A. Walmsley, Inorg. Chem., **46** (2006), 2688.

[6] K. Nomiya, R. Noguchi, M. Oda, Inorg. Chim. Acta, 298 (2000) 24.

[7] S.P. Fricker, Gold Bull. 29 (1996) 53.

[8] I. Kostova, Anti-cancer agents in medicinal chemistry, 6 (2006) 19.

[9] M. Navarro, Coord. Chem. Rev., 253 (2009) 1619.

[10] A. A. Isab, S. Ahmad, Spectroscopy, 20 (2006) 109.

[11] I. Ott, Coord. Chem. Rev., 253 (2009) 1670.

[12] F. Abbate, P. Orioli, B. Bruni, G. Marcon, L. Messori, Inorg. Chim. Acta, **311**(2000), 1.

[13] C.F. Shaw, Comments Inorg. Chem., 8 (1989) 233.

[14] S.L. Best, P.J. Sadler, Gold Bull., 29 (1996) 87.

[15] G.G. Graham, J.B. Ziegler, G.D. Champion, Agents and Actions Supplements, 44 (1993) 209.

[16] P. M. Yangyuoru, J. W. Webb, C. F. Shaw, J. Inorg. Biochem., 102 (2008) 584.

[17] C. S. Gibson, W. M. Colles, J. Chem. Soc., (1931) 2407.

[18] G. Momekov, D. Ferdinandov, S. Konstantinov, S. Arpadjan, Tsekova, G. Gencheva, P. R. Bontchev and M. Karaivanova, Bioinorg. Chem. Appl., (2008) 1.

[19] E. R. T. Tiekink, Inflammopharmacology, 16 (2008), 138.

[20] C. Gabbiani, A. Casini and L. Messori, Gold Bulletin, **40** (2007), 73.

[21] X. Wang and Z. Guo, J. Chem. Soc. Dalton Trans., (2008) 1521.

[22] S. Carotti, G. Marcon, M. Marussich , T. Mazzei, L. Messori, E. Mini, P. Orioli, Chemico-Biological Interactions, 125 (2000) 29.

[23] U. Sampath, W. C. Putnam, T. A. Osiek, S. Touami, J. Xie, D. Cohen, A. Cagnolini, P. Droege, D. Klug, C. L. Barnes, A. Modak, J. K. Bashkin, and S. S. Jurisson, J. Chem. Soc. Dalton Trans., (1999) 2049.

[24] C. M. Che, R. W. Y. Sun, Z. F. Yang, C. K L. Li, United States, Patent Application Publication, (10th, July 2008) Pub. No. US2008/0166429 A1.

[25] F. K. Keter, S. O. Ojwach, O. A. Oyetunji, I. A. Guzei, J Darkwa, Inorg. Chim. Acta, 362 (2009) 2595.

[26] M. El-Khateeb, T.G. Appleton, L.R. Gahan, B.G. Charles, S.J. Berners-Price, A.J. Bolton, Inorg. Biochem., 77 (1999) 13.

[27] G. Marcon, S. Carotti, M. Coronnello, L. Messori, E. Mini, P. Orioli, T. Mazzei, M.A. Cinellu, G. Minghetti, J. Med. Chem., 45 (2002) 1672.

[28] M. W. Whitehouse, Inflammopharmacology, 16 (2008) 107.

[29] G. G. Graham, M. W. Whitehouse and G. R. Bushell, Inflammopharmacology, 16 (2008) 126.

[30] A. Casini, M. A. Cinellu, G. Minghetti, C. Gabbiani, M. Coronnello, E. Mini and L. Messori, J. Med. Chem., 49 (2006) 5524.

[31] L. Ronconi, L. Giovagnini, C. Marzano, F. Bettı`o, R. Graziani, G. Pilloni, and D. Fregona, Inorg. Chem., 44 (2005) 1867.

[32] G. G. Graham and A. J. Kettle, Biochem. Pharmaco., 56 (1998) 307.

[33] J. Yeh, K. Huang, S. Lin, Y. Wu, C. Huang and S. Liou, J. Nanotech., (2000) 1.

[34] T. Shoeib, D. W. Atkinson, B. L. Sharp, Inorg. Chim. Acta, 363 (2010) 184.

[35] A. Molter, F. Mohr, Coord. Chem. Rev., 254 (2010) 19.

[36] D.W. James, N.W. Ludvigsen, L.G. Cleland, J. Rheumatol. 9 (1982) 532.

[37] R. D. Hancock, N.P. Finnkelstein, A. Avers, J. Inorg. Nucl. Chem., 34 (1972) 3747.

[38] R. J. Puddephatt, The Chemistry of Gold, Elsevier, New York, 4 (1978) 45.

[39] S. Ahmad, Coord. Chem. Reviews, 248 (2004) 231.

[40] G.G. Graham, T.M. Haavisto, H.M. Jones, G.D. Champion, Biochem. Pharmacol., 33 (1984) 1257.

[41] P. M. Yangyuoru, J. W. Webb, C.F. Shaw III, J. Inorg. Biochem., 102 (2008) 576.

[42] R. Ettorre, M. Martelli, Inorg. Chim. Acta, 108 (1985) 73.

[43] A. Danoff, M. F. Sieveking, R. L. Lichter , S. N. Y. Fanso-Free, Org. Mag. Res.,12 (2005) 83.

[44] Staszewska-Krajewska, J. Mol. Str., 269 (2002) 602.

[45] O.M. Ni Dhubhghaill, P.J. Sadler and A. Tucker, J. Am. Chem. Soc., 114 (1992) 1118.

[46] C. F. Shaw, Chem. Rev., 99 (1999) 2589.

[47] E. M. Shoukry, Bioinorg. Chem. and Appl., (2009) 1.

[48] M. S. Masoud and O. M. A. El-Hamid, Trans. Met. Chem., 21 (1994) 19.

[49] D. J. Willimas, D. Van Derveer, L. N. Lipscomb and R. L. Jones, Inorg. Chim. Acta, 51 (1992) 192.

[50] M. T. Räisänen, N. Runeberg, M. Klinga, M. Nieger, M. Bolte, P. Pyykkö,M. Leskelä, and T. Repo, Inorg. Chem., 46 (2007) 9954.

[51] Isab ,M. N. Akhtar, J. Coord. Chem., 39 (1996) 21.

[52] Isab , S. Ahmad , J. Inorg. Biochem., 88 (2002) 53.

[53] S. P. Fricker, Gold Bulletin, 29 (1996) 53.

[54] G. G. Graham, G. D. Champion and J. B. Ziegler, Inflammopharmacology, 1 (1991) 99.

[55] G. Lewis, C. F. Shaw III, Inorg. Chem., 25 (1986) 58.

[56] H. Schmidbaur, Gold Bulletin, 33 (2000) 3.

[57] C. F. Shaw III, M. P. Cancro, P. L. Witkiewicz and J. E. Eldridge, Inorg. Chem., 19 (1980) 3198.

[58] P. L. Witkiewicz and C. F. Shaw III, J. Chem. Soc., Chem. Commun., (1981) 1111.

[59] J. Kasparkova, O. Novakova, N. Farrell and V. Brabec, Biochem., 42 (2003) 792.

[60] P. J. Sadler, Struct. Bonding (Berlin), 171 (1976) 29.

[61] D. H. Brown and W.E. Smith, Chem. Soc. Rev., 217(1980) 9.

[62] R. F. Uson, L. Laguna, J. Jimenez, M. P. Gomez and A. Sainz, J. Chem Soc., Dalton Trans., (1989) 3457.

[63] A. A. Isab, H. Perzanowski and A. Al-Arfaj, Trans. Met. Chem., 17 (1992) 557.

[64] (a)- S. Hayashi and K. Hayamizu, Bull. Chem. Soc. Jpn. 64 (1991), 688.

(b)- K. Eichele, R.E. Wasylischen, WSolid1 NMR Simulation Package, Version 1.4.4, Dalhousie University and University of Tübingen, Canada and Germany, 2001.

[65] M. Maricq, J. Waugh, J. Chem. Soc. 70 (1979) 3300.

[66] N. Zhanpeisov, M. Matsuoka, H. Yamashita, M. Anpo, J. Phys. Chem. B**,** **102** (1998) 6915.

[67] A. Nicklass, M. Dolg, H. Stoll, H. Preuss, J. Chem. Phys., **102** (1995)8942.

[68] Gaussian 03, Revision B.04, M. J. Frisch, G. W. Trucks, H. B. Schlegel, G. E. Scuseria, M. A. Robb, J. R. Cheeseman, J. A. Montgomery, Jr., T. Vreven, K. N. Kudin, J. C. Burant, J. M. Millam, S. S. Iyengar, J. Tomasi, V. Barone, B. Mennucci, M. Cossi, G. Scalmani, N. Rega, G. A. Petersson, H. Nakatsuji, M. Hada, M. Ehara, K. Toyota, R. Fukuda, J. Hasegawa, M. Ishida, T. Nakajima, Y. Honda, O. Kitao, H. Nakai, M. Klene, X. Li, J. E. Knox, H. P. Hratchian, J. B. Cross, C. Adamo, J. Jaramillo, R. Gomperts, R. E. Stratmann, O. Yazyev, A. J. Austin, R. Cammi, C. Pomelli, J. W. Ochterski, P. Y. Ayala, K. Morokuma, G. A. Voth, P. Salvador, J. J. Dannenberg, V. G. Zakrzewski, S. Dapprich, A. D. Daniels, M. C. Strain, O. Farkas, D. K. Malick, A. D. Rabuck, K. Raghavachari, J. B. Foresman, J. V. Ortiz, Q. Cui, A. G. Baboul, S. Clifford, J. Cioslowski, B. B. Stefanov, G. Liu, A. Liashenko, P. Piskorz, I. Komaromi, R. L. Martin, D. J. Fox, T. Keith, M. A. Al-Laham, C. Y. Peng, A. Nanayakkara, M. Challacombe, P. M. W. Gill, B. Johnson, W. Chen, M. W. Wong, C. Gonzalez, and J. A. Pople, Gaussian, Inc., Pittsburgh PA, 2003.

[69] K. Esumi, M. Nawa, N. Aihara and K. Usui, New J. Chem., (1998), 719.

[70] Haruko Ito, Junnosuke Fujita and Kazuo Saito, Bulletin of the Chemical Society of Japan, **40** (1967), 2584.

[71] R.V. Parish , J. P. Wright and R. G. Pritchard, Journal of Organometallic Chemistry, **596** (2000) 165.

[72] P. A. Bonnardel, R .V. Parish and R. G. Pritchard; J. Chem. Soc., Dalton Trans., (1996) 3185.

[73] (a)- W. Beck, W. P. Fehlhammer, P. Pollmann, E. Schuierer, and K. Feldl, Chem. Ber.100 (1967), 2335.

(b)- H. Silva, C. V. Barra, C. F. Costa, M. V. Almeida, E. T. César, J. N. Silveira, A. Garnier-Suillerot, F. C. Paula, E. C. Pereira-Maia and A. P. S. Fontes, J. Inorg. Biochem., 102 (2008) 767.

[74] L. Messori, G. Marcon, and P. Orioli, J Med Chem, **43** (2000), 3541.

[75] L. Messori, G. Marcon, and P. Orioli, Bioinorg Chem Appl, **1**(2003), 177.

[76] F. Zhao, E. G. Schöneich, G. I. Aced, J. Hong, T. Milby, C. Schöneich, J. Biol. Chem., 272 (1997) 9019.

[77] P. Y. Bruice, Organic Chemistry, Pearson Education, Inc., fifth edition (2007) 1025.

[78] G. T. Appleton, F. J. Pesch, M. Wienken, S. Menzer, B. Lippert, Inorg. Chem., 31 (1992) 4410.

[79] F. Iori, S. Corni, and R. D. Felice, J. Phys. Chem. C, 112 (2008) 13540.

[80] A. C. Andrews and E. W. Grundemeier, J. Inorg. Nuc. Chem., 28 (1966) 455.

[81] Y. Zasshi, The Pharma. Soc. Jap., 97 (1977), 76.

[82] M. Y. Combariza and R. W. Vachet, J Am Soc Mass Spectrom, 15 (2004) 1128.

[83] D. J. Radanovic, Z. D. Matovic, G. Ponticelli, P. Scano, I. A. Efimenko, Trans. Met. Chem., 19 (1994) 646.

[84] V. Soni, R. S. Sindal, R. N. Mehrotra, Polyhedron, 24 (2005) 1167.

[85] M. J. Carter, J. K. Beattie, Inorg. Chem., 9 (1970) 1233.

[86] M. Iwaoka, R. Ooka, T. Nakazato, S. Yoshida, and S. Oishi, Chem. & Biodiversity, 5 (2008) 359.

[87] A. A. Isab, Inorg. Chim. Acta, 80 (1983) 3.

[88] A.V. Vujačić, J.Z. Savić, S.P. Sovilj, K. M. Szécsényi, N. Todorović, M.Ž. Petković and V.M. Vasić, Polyhedron, 28 (2009) 593.

[89] M. Salzmann, E. M. Stocking, L. A. Silks (III) and H. Senn, Magn. Reson. Chem., 37 (1999) 672.

[90] A. A. Isab, Transition Met. Chem., 14 (1989) 235.

[91] C. M. T. Mangold, F. Unckell, M. Werr and R. E. Streeck, Archives of Virology, 142 (1997) 2257.

[92] T. Soldatovic, Z. D. Bugarcic and R. V. Eldik, Dalton Trans., (2009) 4526.

[93] D.H. Brown, W.E Smith, Proceedings of the Royal Society of Medicine, 70 (1977) 41.

[94] J. A. Reynaud, B. Malfoy and P. Canesson, J. Electroanalytical Chem., 114 (1980) 195.

[95] T. Suzuki, S. Shishido and N. Ishihara, Br. J. Ind. Med., 33 (1976) 88.

[96] M. H. Pritchard and G. Nuki, Annals of the Rheumatic Diseases, 37 (1978) 493.

[97] L. H. Marcolino-Junior, V. G. Bonifácio, F. C. Vicentini, B. C. Janegitz and O. Fatibello-Filho, Canadian J.Anal. Sci. Spectro., 54 (2009) 45.

[98] M. N. Akhtar, A. A. Isab, and A.l R. Al-Arfaj , J. Inorg. Biochem., 66 (1997) 197.

[99] A. A Isab, J. Chem. Soc., Dalton Trans., 3 (1991) 449.

[100] (a)- A.A. Isab, J. Inorg. Biochem., 30 (1987) 69.

(b)- M. A. Hughes, G. L. Smith, and D. R. Williams, Inorg. Chim. Acta, 107 (1985) 247.

(c)- G. L. Christie, M. A. Hughes, S. B. Rees, and D. R.Williams, Inorg. Chim. Acta, 15 (1988) 215.

(d)- D. L. Rabenstein, A. A. Isab, Anal. Chem., 54 (1982) 526.

[101] S. Hillaert and W. V. Bossche, J. Pharm. Biomed. Anal., 21 (1999) 65.

[102] S. Chavan, L. Sava, V. Saxena, S Pillai, A. Sontakke and D. Ingole, Ind. J. Clin. Biochem., 20 (2005) 150.

[103] A. J. Canumalla, N. Al-Zamil , M. Phillips , A. A. Isab , C. F. Shaw III, J. Inorg. Biochem. 85 (2001) 67.

[104] S. Ahmad, A. A. Isab, Inorg. Chem. Commun., 4 (2001) 362.

[105] A.A. Isab, J. Inorg. Biochem., 45 (1992) 261.

[106] J. Xu, J.C. Yadan, J. Org. Chem., 60 (1995) 6296.

[107] D. J. Willimas, D. Van Derveer, L. N. Lipscomb and R. L. Jones, Inorg. Chim. Acta, 51 (1992) 192.

[108] R. F. Uson, L. Laguna, J. Jimenez, M. P. Gomez and A. Sainz, J. Chem Soc., Dalton Trans., 3457 (1989).

[109] G. Socrates, Infrared Characteristics Group Frequencies, Wiley-Interscience Publication, (1980) 5.

[110] A. Ray and D. N. Sathyanarayana, Bull. Chem. Soc. Japan, 46 (1973) 1969.

[111] R. Ettorre, M. Martelli, Inorg. Chim. Acta, 108 (1985) 73.

[112] A. Danoff, M. F. Sieveking, R. L. Lichter , S. N. Y. Fanso-Free, Org. Mag. Res.,12 (2005) 83.

[113] S. Krajewska, J. Mol. Str., 269 (2002) 602.

[114] G. Jonsall and P. Ahlberg, J. Am. Chem. Soc., 108 (1986) 3819.

[115] S. W. Griffiths, J. King and C. L. Cooney, J. Biol. Chem., 277 (2002) 25486.

[116] L. R. Njaa Brit. J. Nutr., 16 (1962) 571.

[117] T. Wieland, C. Gotzendorfer, J. Dabrowski, W. N. Lipscomb and G. Shoham, Biochemistry, 22 (1983) 1264.

[118] Y. H. Kim, A. H. Berry, D. S. Spencer and W. E. Stites, Protein Engineering, 14 (2001) 343.

[119] M. Seigneuret, J. M. Neumann, D. Levy and J. L. Rigaud, Biochemistry, 30 (1991) 3885.

[120] J. D. Bell, R. E. Norman and P. J. Sadler, J. Inorg. Biochem., 31(1987) 241.

[121] A. A. Isab, M. I.M. Wazeer, Spectroscopy, 19 (2005) 275.

[122] A. Samanta, S. N. Limaye and M. C. Saxena, J. Chem. Sci., 97 (1986) 543.

[123] M. J. Potrzebowski, R. Katarzyński, W. Ciesielski, Mag. Res. in Chem., 37 (1999) 173.

[124] S. Ahmad, A. A. Isab, H. P. Perzanowski, M. S. Hussain and M. N. Akhtar, Trans. Met. Chem., 27 (2002) 177.

[125] E. R. T. Tiekink, J. G. Kang, Coord. Chem. Rev., 253 (2009) 1627

[126] R. V. Parish, Gold Bull., 15 (1982) 51.

[127] G. A. Bowmaker, B. J. Kennedy and J. C. Reid, Inorg. Chem., 37 (1998) 3968.

[128] L. H. Jones, J.Chem. Phys., **27** (1957) 468.

[129] M. H. Ford-Smith, J. J. Habeeb and J. H. Rawsthorne, J. Chem. Soc., Dalton Trans., (1972) 2116.

[130] K. Shobatake, C. Postmus, J. R. Ferraro, and K. Nakamoto, Appl. Spectro., 23 (1969) 12.

[131] J. R. Durig, J. S. Di Yorio and D. W. Wertz , J. Mol. Spectro., 28 (1968) 444.

[132] Y. Yamamoto and Z. Kanda, Bull. Chem. Soc. Jpn., 53 (1980) 3436.

[133] N. D. Draper, R. J. Batchelor, P. M. Aguiar, S. Kroeker, and D. B. Leznoff, Inorg. Chem., 43 (2004) 6557.

[134] M. Fettouhi, M. I.M. Wazeer, A. A. Isab, Inorg. Chem. Commun., 11 (2008) 252.

[135] N. O. Al-Zamil, K. A. Al-Sadhan, A. A. Isab, M. I.M. Wazeer and A. R. A. Al-Arfaj, Spectroscopy, 21 (2007) 61.

[136] M. Hirota, Y. Koike, H. Ishizuka, A. Yamasaki and S. Fujiwara, Chem. Lett., (1973) 853.

[137] A. A. Isab, J. Inorg. Biochem. , 46 (1992) 145.

APPENDIX A - LIST OF ABBREVIATION

2,4-DTU	2,4-dithiouracil
AuSTg	Gold thioglucose
AuSTm	Gold sodium thiomalate
Autm	Aurothiomalate
bn	Butylenediamine
Cap	L-Captopril
Cap-S-S-Cap	Captopril-disulfide
cis-Pt	*Cis*platin
Cys	Cysteine
CyS-SCy	Cystine
Diap	Diazipane-2-thione
Diaz	Diazinane-2-thione
DSS	2,2-Dimethylsilapentane-5-sulphonate
en	Ethylenediamine
ErSH	L-Ergothionene
$Et_3PAuSATg$	Auranofin
Gly	Glycine
GSH	Glutathione
GSSG	Glutathione-S-S- Glutathione
His	L-Histidine
HO-His	2-HO-histidine
HO-Imi	2-Hydroxy-imidazole

Imi	Imidazole
Imt	Imidazolidine-2-thione
Imt-S-S-Imt	Imt-di-sulfide
Met	L-methionine
N,N' –Et_2-*en*	N,N’-di-ethyl-ethylenediamine
N,N'-(2-hydroxy-Et)$_2$-*en*	N,N’-di-2-hydroxy-ethyl Ethylenediamine
N,N'-*i*Pr_2-*en*	N,N’-di-iso-propyl-ethylenediamine
N,N'–Me_2-*en*	N,N’-di-methyl-ethylenediamine
N-Et-*en*	N-ethyl-ethylenediamine
N-hydroxy-Et-*en*	N-hydroxy-ethyl-ethylenediamine
N-*i*Pr-*en*	N-iso-propyl-ethylenediamine
N-Me-*en*	N-methyl-ethylenediamine
PaSH	D-penicillamine
pn	Propylenediamine
PaSH	DL-penicillamine
Se-Met	DL-seleno-methionine
TmSH	Thiomalic acid

APPENDIX B - LIST OF PUBLICATION

1. Bassem A. Al-Maythalony, Anvarhusein A. Isab and Mohammed I. M. Wazeer A study of gold(III)-tetracyanide interaction with imidazolidine-2-thione ligand and its derivatives by NMR spectroscopy, manuscript in preparation.
2. Bassem A. Al-Maythalony, Anvarhusein A. Isab and Mohammed I. M. Wazeer Studies of gold(III)-tetracyanide complex interactions with L-cysteine, glutathione, captopril, L-methionine and DL-Se-methionine by ^{1}H, ^{13}C NMR and UV spectroscopy, submitted.
3. Bassem A. Al-Maythalony, Anvarhusein A. Isab and Mohammed I. M. Wazeer, A study of [Au(ethylenediamine)Cl_2]Cl interaction with L-methionine and DL-Se-methionone by ^{1}H and ^{13}C NMR spectroscopy, submitted.
4. Bassem A. Al-Maythalony, Anvarhusein A. Isab and Mohammed I. M. Wazeer Synthesis and characterization of new cyano-gold(III) and gold(I) complexes of phosphines, phosphine sulphides and phosphine selenides; by UV, IR, Far-IR, solid-state and solution NMR spectroscopy., accepted.
5. Bassem A. Al-Maythalony, Anvarhusein A. Isab, Mohammed I. M. Wazeer and Abdellatif Ibdah, Investigation of the interaction of gold(III)-alkyldiamine complexes with L-histidine and imidazole ligands by ^{1}H and ^{13}C NMR and UV spectrophotometry, accepted.
6. Bassem A. Al-Maythalony, Mohammed Fettouhi, Mohammed I. M. Wazeer and Anvarhusein A. Isab, A novel polymeric Hg[$(CN)_2N_2$] central core four-coordinate complex: Synthesis, X-ray structure and ^{199}Hg, ^{13}C and ^{15}N CP MAS NMR characterization of catena((μ_2-1,4-diaminobutane-

N,N')dicyanomercury(II)), Inorganic Chemistry Communications, 12(6), (2009), 540-543.

7. Bassem A. Al-Maythalony, Mohamed I.M. Wazeer, Anvarhusein A. Isab, Synthesis and characterization of gold(III) complexes with alkyldiamine ligands, Inorganica Chimica Acta, 362, (2009), 3109–3113.
8. Bassem A. Al-Maythalony, Mohammed I. M. Wazeer, Anvarhusein A. Isab, Nael, M. T., Saeed Ahmad, Complexation of $Cd(SeCN)_2$ with imidazolidine-2-thione and its derivatives: Solid state, solution NMR and anti-bacterial studies , Spectroscopy, 22(5), (2008), 361-370.
9. Anvarhusein A. Isab, Mohamed I. M. Wazeer, Mohammed Fettouhi, Bassem A. Al-Maythalony, Abdul Rahman Al-Arfaj, Norah O. Al-Zamil, Solid state and solution NMR, X-ray and antimicrobial studies of 1:1 and 2:1 complexes of silver(I) cyanide with alkanediamine ligands, Inorganica Chimica Acta, 360(12), (2007), 3719-3726.

APPENDIX C - CONFERENCES

- Bassem A. Al-Maythalony, Anvarhusein A. Isab*, Mohammed I. M. Wazeer and Abdellatif Ibdah, Investigation of the interaction of gold(III)-alkyldiamine complexes with L-histidine and imidazole ligands by ^{1}H and ^{13}C NMR and UV spectrophotometry, June 1st (2010), 4th Graduate Seminar Day, KFUPM, Dhahran, Saudi Arabia.
- Bassem A. Al-Maythalony*, Mohamed I. M. Wazeer, Anvarhusein A. Isab, Studies of gold(III)-tetracyanide complex interactions with L-cysteine, glutathione, captopril, L-methionine and DL-Se-methionine by ^{1}H, ^{13}C NMR and UV spectroscopy, March 1-4th, (2010), Riyadh, Saudi Arabia. AWARDED
- Bassem A. Al-Maythalony*, Mohamed I. M. Wazeer, Anvarhusein A. Isab," Synthesis and characterization of gold(III) complexes with alkyldiamine ligands" Gordon Research Conference on Bioinorganic Chemistry (GRS), February 4-7th, (2010), California, Ventura, USA.
- Anvarhusein A. Isab *, Mohamed I. M. Wazeer and Bassem A. Al-Maythalony, "Solution as well as solid NMR studies on 1:1 and 2:1 adducts of silver(I) cyanide with alkanediamine ligands", 233rd ACS National Meeting, March 25-29th, (2007), Chicago, IL, USA.

  * Presented by,,,

APPENDIX D - CURRICULUM VITAE

- **BASSEM ABDULLATIF MAHMOUD AL-MAYTHALONY**

- Date of birth : 19th April, 1975

- Nationality : Jordanian

- Current Address: 4-123, Chemistry Department, King Fahd University of Petroleum and Minerals, Dhahran, Saudi Arabia.
    - Tel.(Work) +966 3860 2886, (Home) +966 3860 6076.
    - Mobile +966 5 6001 0829
    - Email: g200504750@kfupm.edu.sa
- Perminant Address: Hi-Al Qadesieh, Zarqa, Jordan.
    - Mobile 00962 795 191 378, 00962 788 648 311
    - Mail: P. O. Box 737, Al Mafraq, Jordan.
    - Email: bmayth@yahoo.com
    - Email: bmayth@hotmail.com

- PhD of Inorganic Chemistry from King Fahd University of Petroleum and Minerals, [Dhahran, Saudi Arabia], (2006 to 2010).
- MSc in Applied Chemistry, Jordan University of Science and Technology, [Irbid, Jordan], (1997 to 2000).
- BSc in chemistry, Mu'tah University [Al-karak, Jordan], (1993 to 1997).